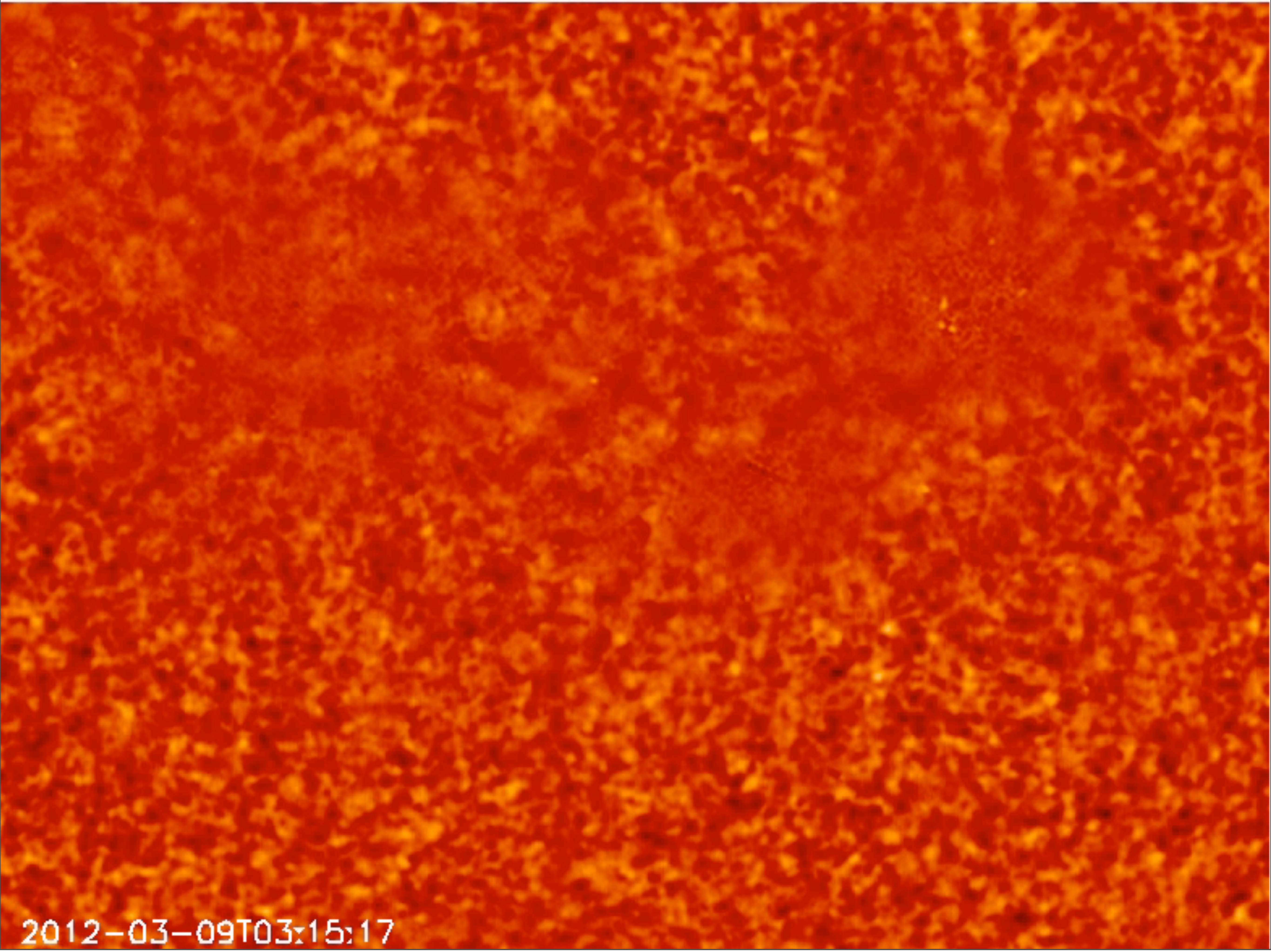
2012-03-09T03:15:17

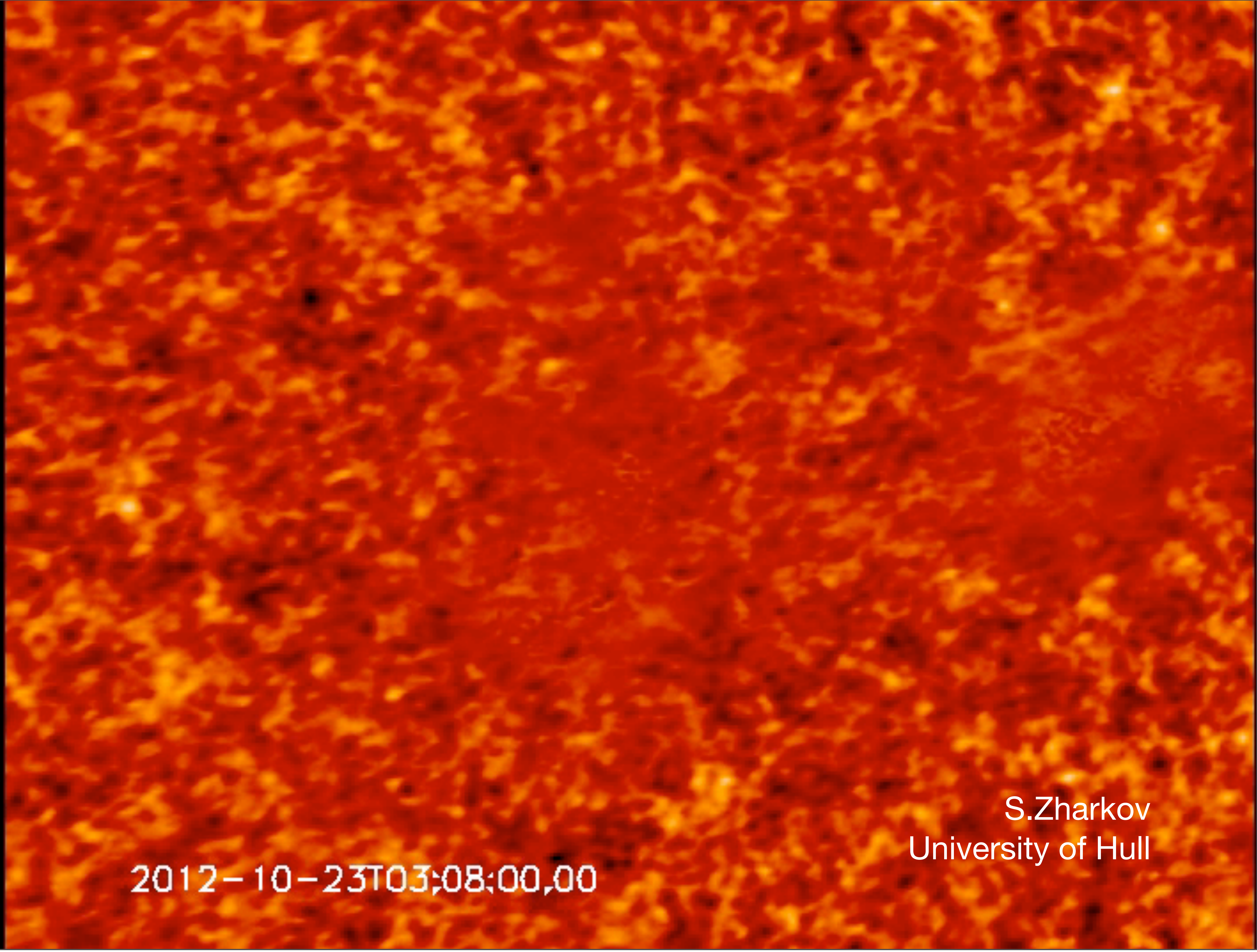
2012-10-23T03:08:00.00
S.Zharkov
University of Hull

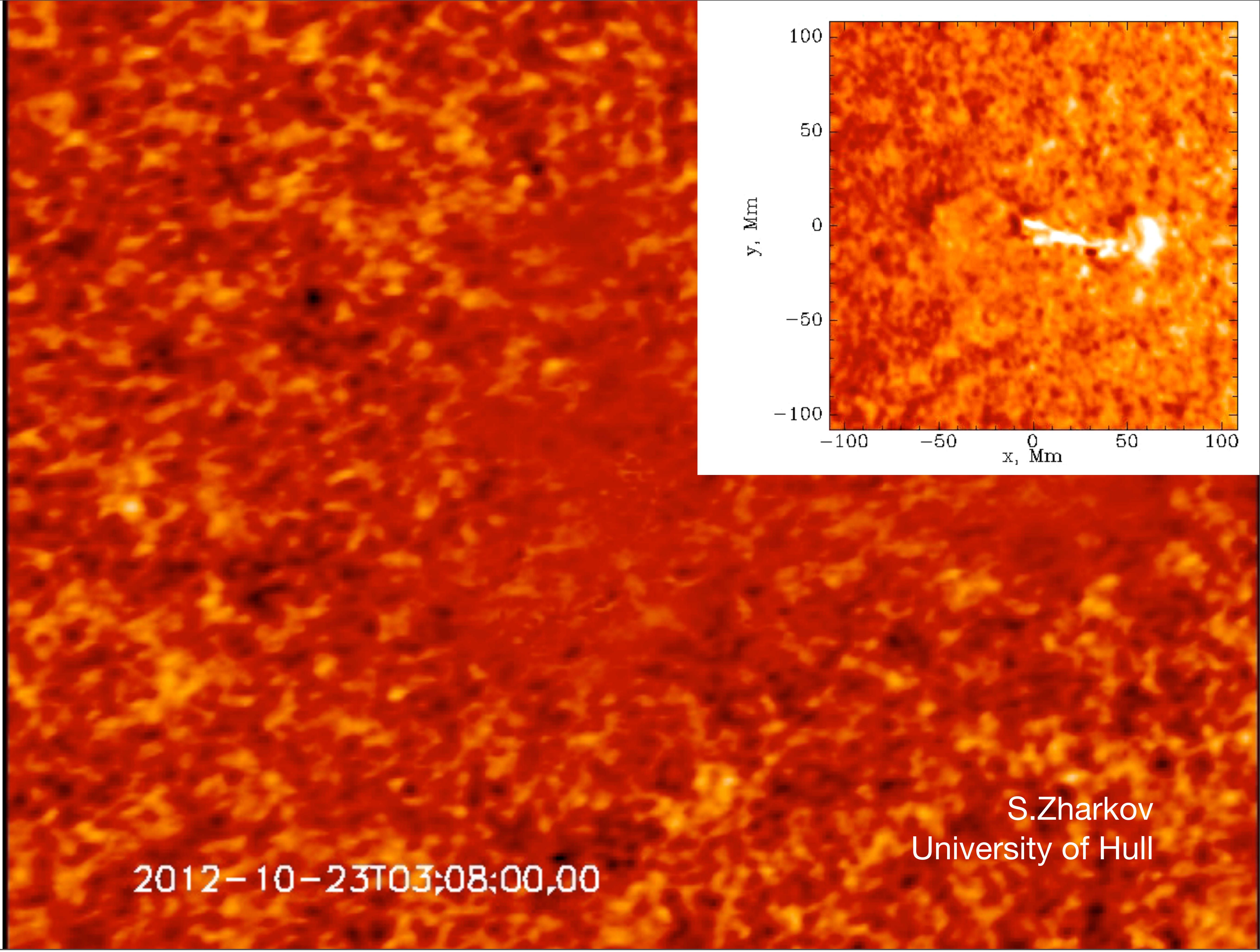
100
50
0
−50
−100
y, Mm
−100
−50
0
50
100
x, Mm
2012-10-23T03:08:00.00
S.Zharkov
University of Hull

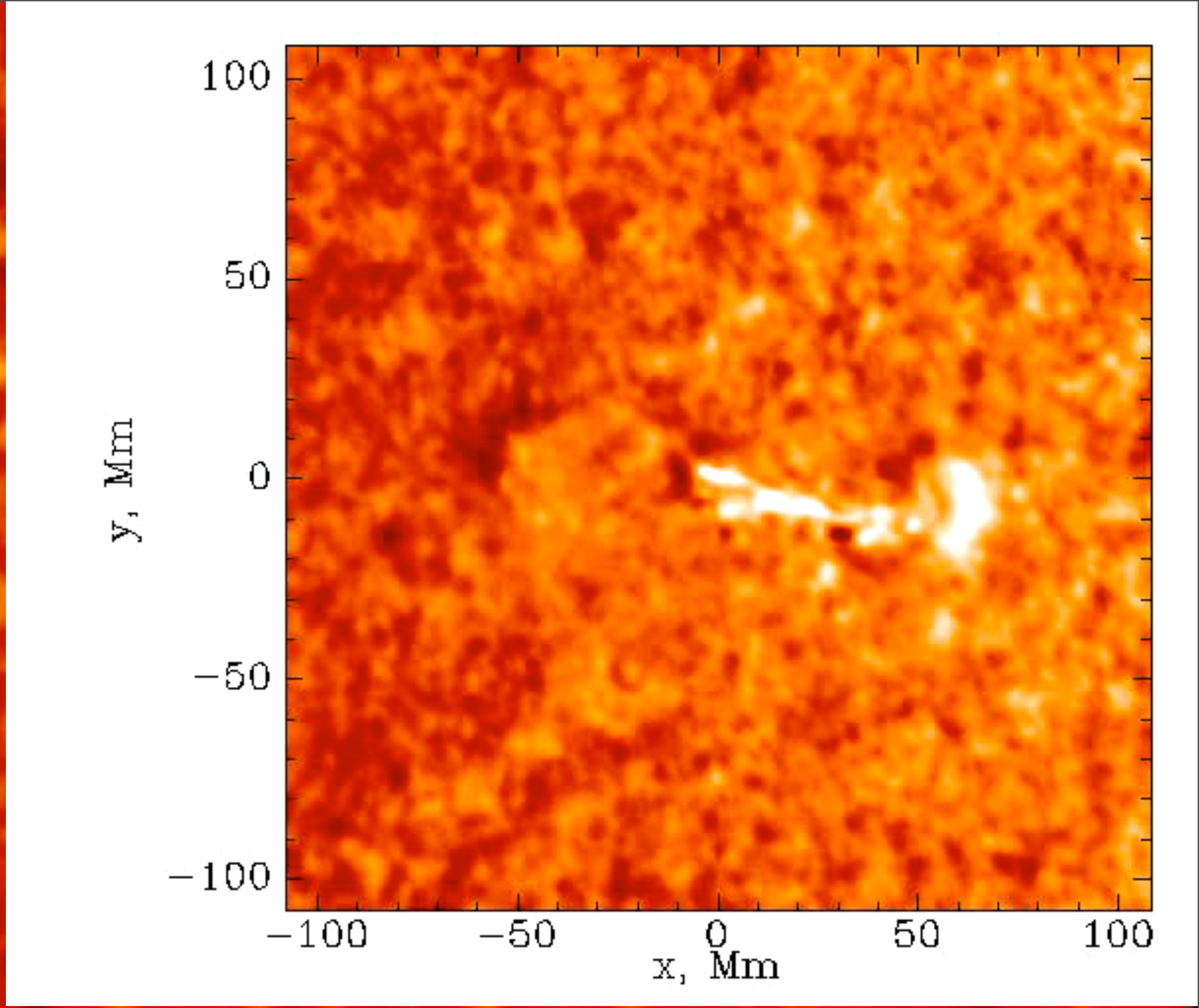

Flare seismology: implications for energy transport in flares

S.Zharkov
University of Hull

2012-10-23T03:08:00.00

Geometric asymptotics

Acoustic wave equation for solar interior:

$$\frac{1}{c^2}\left(\frac{\partial^2}{\partial t^2}+\omega_{ac}^2\right)\Psi-\nabla^2\Psi=0 \qquad \omega_{ac} = \frac{c^2}{4H_\rho^2}\left(1-2\mathbf{n}.\nabla H_\rho\right)$$

$$\Psi(\mathbf{r},t)=\sum_m^{\infty}\frac{A_m(\mathbf{r},t)}{(i\Lambda)^m}e^{i\Lambda\varphi(\mathbf{r},t)}.$$

Guillemin V., Sternberg S., Geometric Asymptotics; Kravtsov, Orlov, Waves in inhomogenous media; Gough D. O., 1993, in Astrophysical Fluid Dynamics - Les Houches 1987, J.-P. Zahn & J. Zinn-Justin, ed., pp. 399-560

Geometric asymptotics

Acoustic wave equation for solar interior:

$$\frac{1}{c^2}\left(\frac{\partial^2}{\partial t^2}+\omega_{ac}^2\right)\Psi-\bigtriangledown^2\Psi=0 \qquad \omega_{ac} = \frac{c^2}{4H_\rho^2}(1-2\mathbf{n}.\bigtriangledown H_\rho)$$

$$\Psi(\mathbf{r},t)=\sum_m^\infty \frac{A_m(\mathbf{r},t)}{(i\Lambda)^m}e^{i\Lambda\varphi(\mathbf{r},t)}.$$

$$|\bigtriangledown\varphi|^2-\frac{1}{c^2}\left|\frac{\partial\varphi}{\partial t}\right|^2+\frac{\omega_{ac}^2}{c^2}=0$$

eikonal equation, find phase function

$$2\bigtriangledown A_0.\bigtriangledown\varphi+A_0\bigtriangledown^2\varphi-$$
$$-\frac{2}{c^2}\frac{\partial\varphi}{\partial t}\frac{\partial A_0}{\partial t}-\frac{1}{c^2}A_0\frac{\partial^2\varphi}{\partial t^2}=0$$

transport equations, find amplitudes

$$2\bigtriangledown A_1.\bigtriangledown\varphi+A_1\bigtriangledown^2\varphi-$$
$$-\frac{2}{c^2}\frac{\partial\varphi}{\partial t}\frac{\partial A_1}{\partial t}-\frac{1}{c^2}A_1\frac{\partial^2\varphi}{\partial t^2}=-\left(\bigtriangledown^2-\frac{1}{c^2}\frac{\partial^2}{\partial t^2}\right)A_0$$

$$\ldots$$

Guillemin V., Sternberg S., Geometric Asymptotics; Kravtsov, Orlov, Waves in inhomogenous media; Gough D. O., 1993, in Astrophysical Fluid Dynamics - Les Houches 1987, J.-P. Zahn & J. Zinn-Justin, ed., pp. 399-560

Initial conditions for monochromatic spherical source

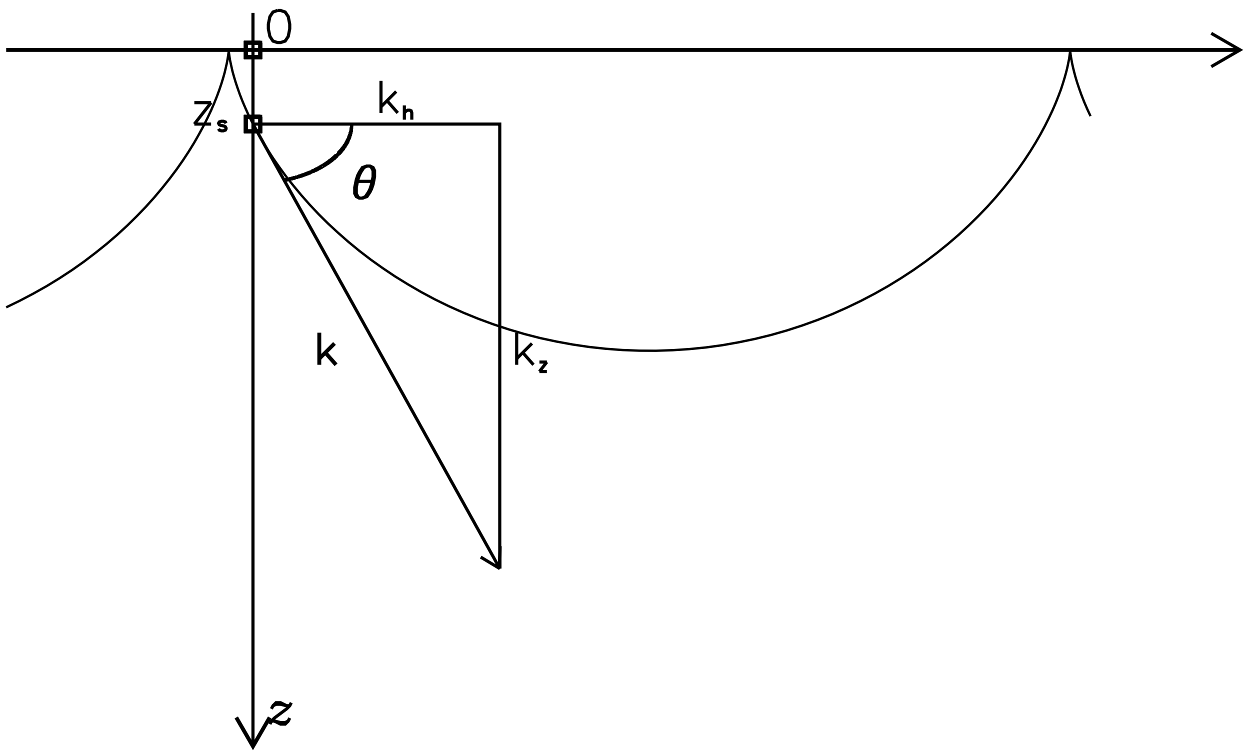

Zharkov 2013

Initial conditions for monochromatic spherical source

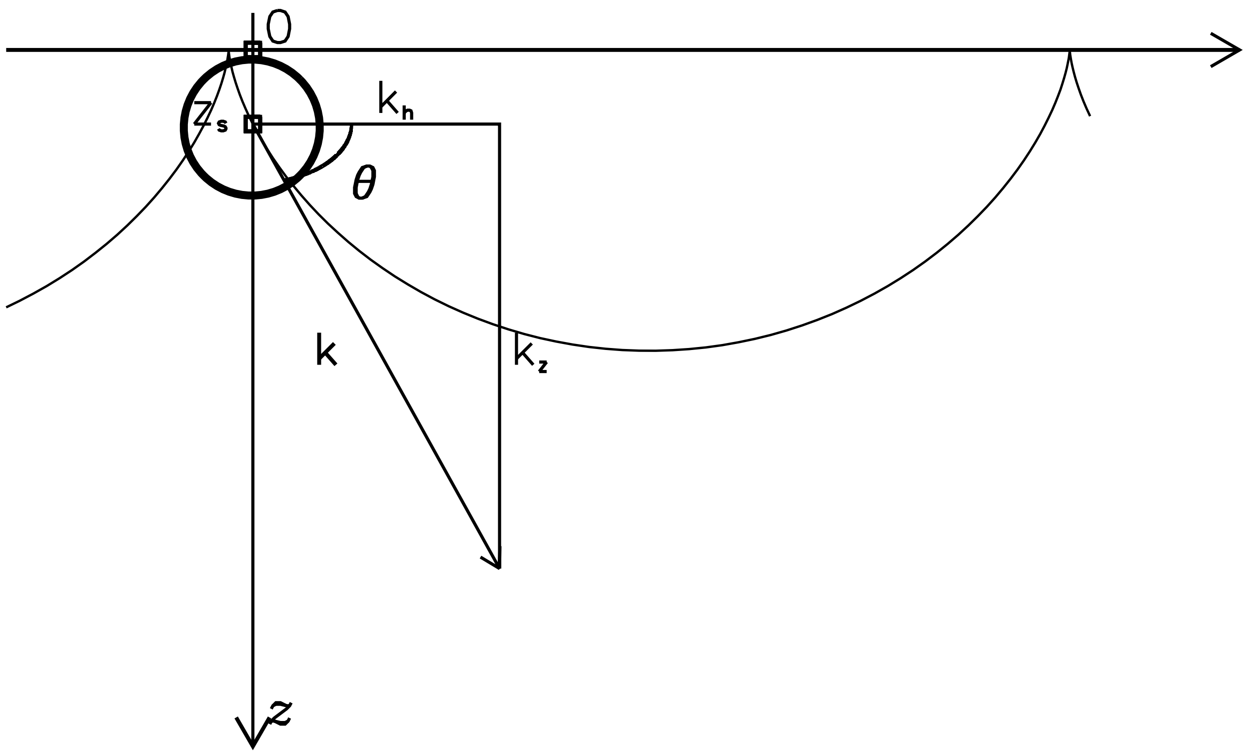

$$\begin{cases} x = x_s + r\cos\theta \\ z = z_s + r\sin\theta \\ t = t_0 \end{cases} \tag{3.9}$$

The initial field on this surface is described as

$$\Psi_0 = A_0(\theta, t_0) e^{i\varphi_0(\theta, t_0)}. \tag{3.10}$$

The unknown initial wavenumbers and frequency, $k_{h0} = \frac{\partial\varphi_0}{\partial x}$, $k_{z0} = \frac{\partial\varphi_0}{\partial z}$ and $\omega_0 = -\frac{\partial\varphi_0}{\partial t}$, are found from the system:

$$\begin{cases} \dfrac{\partial\varphi_0}{\partial t_0} = k_{h0}\dfrac{\partial x}{\partial t_0} + k_{z0}\dfrac{\partial z}{\partial t_0} - \omega_0\dfrac{\partial t}{\partial t_0}, \\ \dfrac{\partial\varphi_0}{\partial \theta} = k_{h0}\dfrac{\partial x}{\partial \theta} + k_{z0}\dfrac{\partial z}{\partial \theta} - \omega_0\dfrac{\partial t}{\partial \theta}, \\ k_{h0}^2 + k_{z0}^2 = \dfrac{\omega_0^2 - \omega_{ac}^2}{c^2}. \end{cases} \tag{3.11}$$

Let us now consider spherical monochromatic homogeneous source of some fixed frequency, ω_f, i.e. $\varphi_0(\theta, t_0) = -\omega_f t_0$. Then from the above $\omega_0 = \omega_f$ and $k_{h0}\sin\theta = k_{z0}\cos\theta$. This implies that in this configuration (see Figure 1) θ can be viewed as ray take-off angle and all rays generated from S are of the same frequency, so frequency subscripts can be dropped. Define $k_s^2(z_s, \omega) = \left.\frac{\omega^2 - \omega_{ac}^2}{c^2}\right|_{z=z_s}$, then horizontal and vertical wavenumbers can be rewritten as $k_{h0} = k_s\cos\theta$, and $k_{z0} = k_s\sin\theta$. Since Hamiltonian is independent of horizontal coordinate and time, ω and k_h are constant on each ray. Then so is the horizontal phasespeed of a ray, $v_{ph}^2 = \frac{\omega^2}{k_h^2} = \frac{c^2}{\cos^2\theta}\frac{1}{1 - \frac{\omega_{ac}^2}{\omega^2}}$.

Zharkov 2013

Acoustic waves in the Sun, geometric optics, 2D

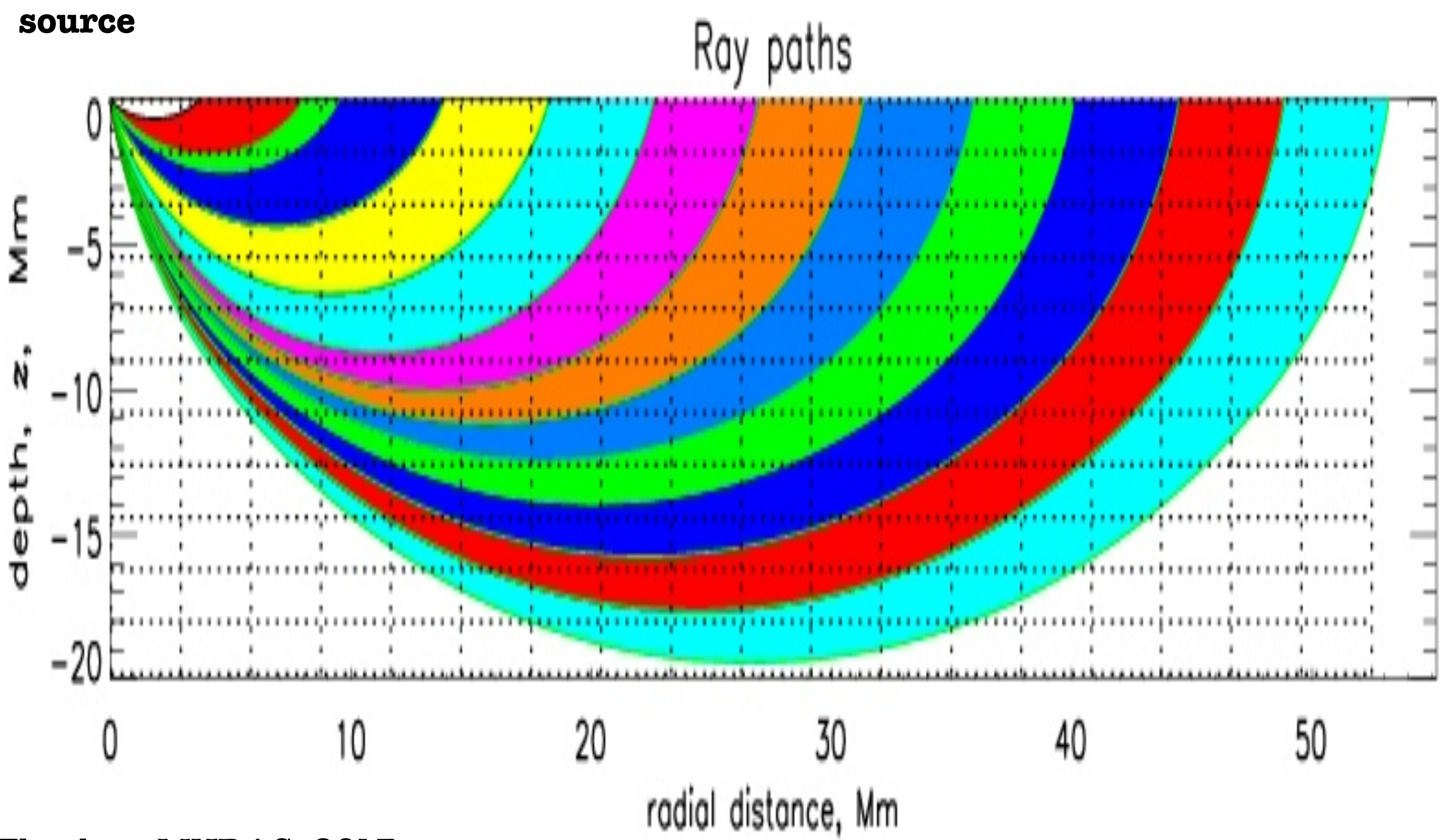

Zharkov, MNRAS, 2013

Acoustic waves in the Sun, geometric optics, 2D

source

Zharkov, MNRAS, 2013

Acoustic waves in the Sun, geometric optics, 2D

source

Zharkov, MNRAS, 2013

Acoustic waves in the Sun, geometric optics, 2D

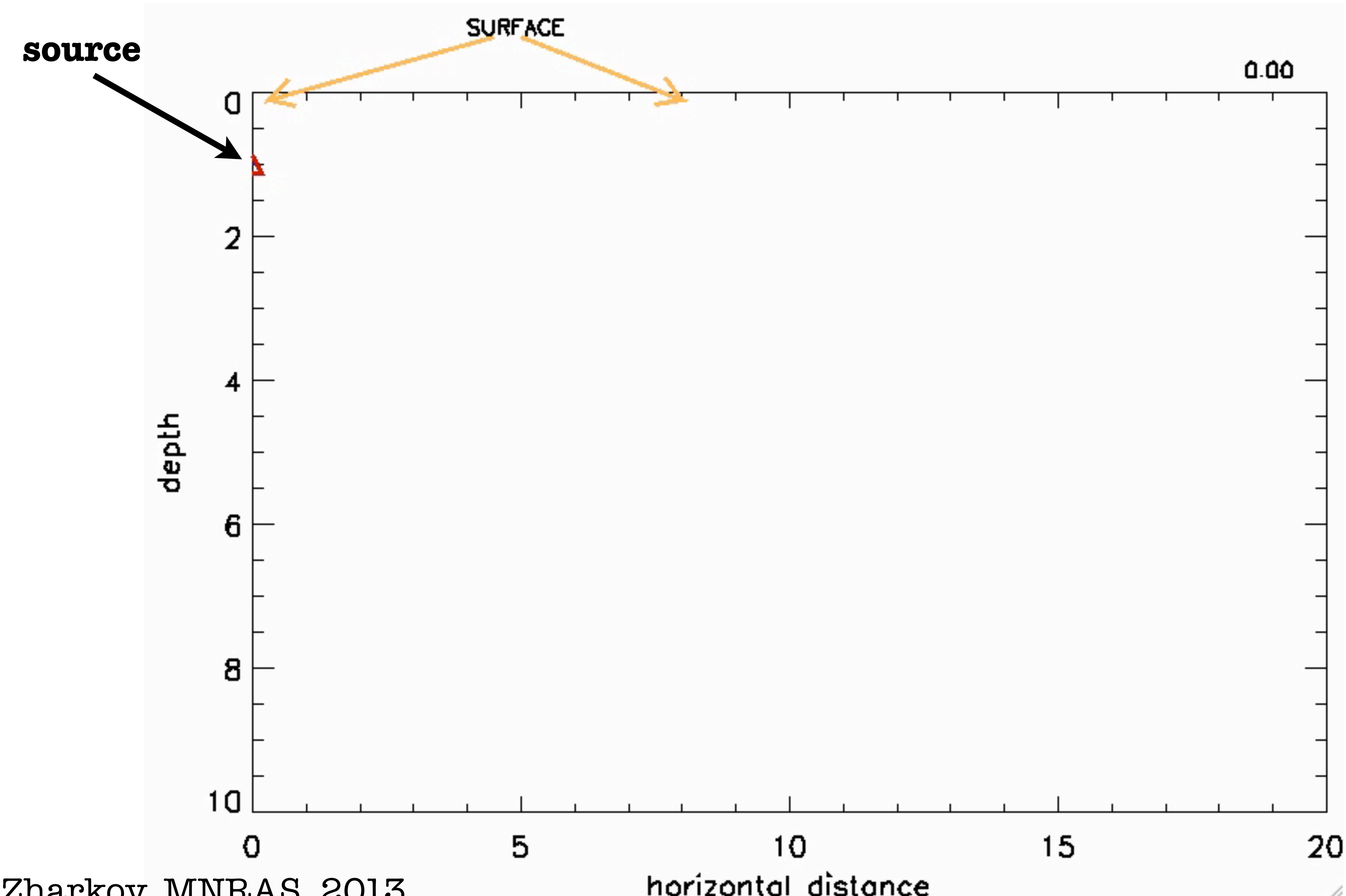

Zharkov, MNRAS, 2013

Surface ripples, geometric optics, 3D

Surface ripples, geometric optics, 3D

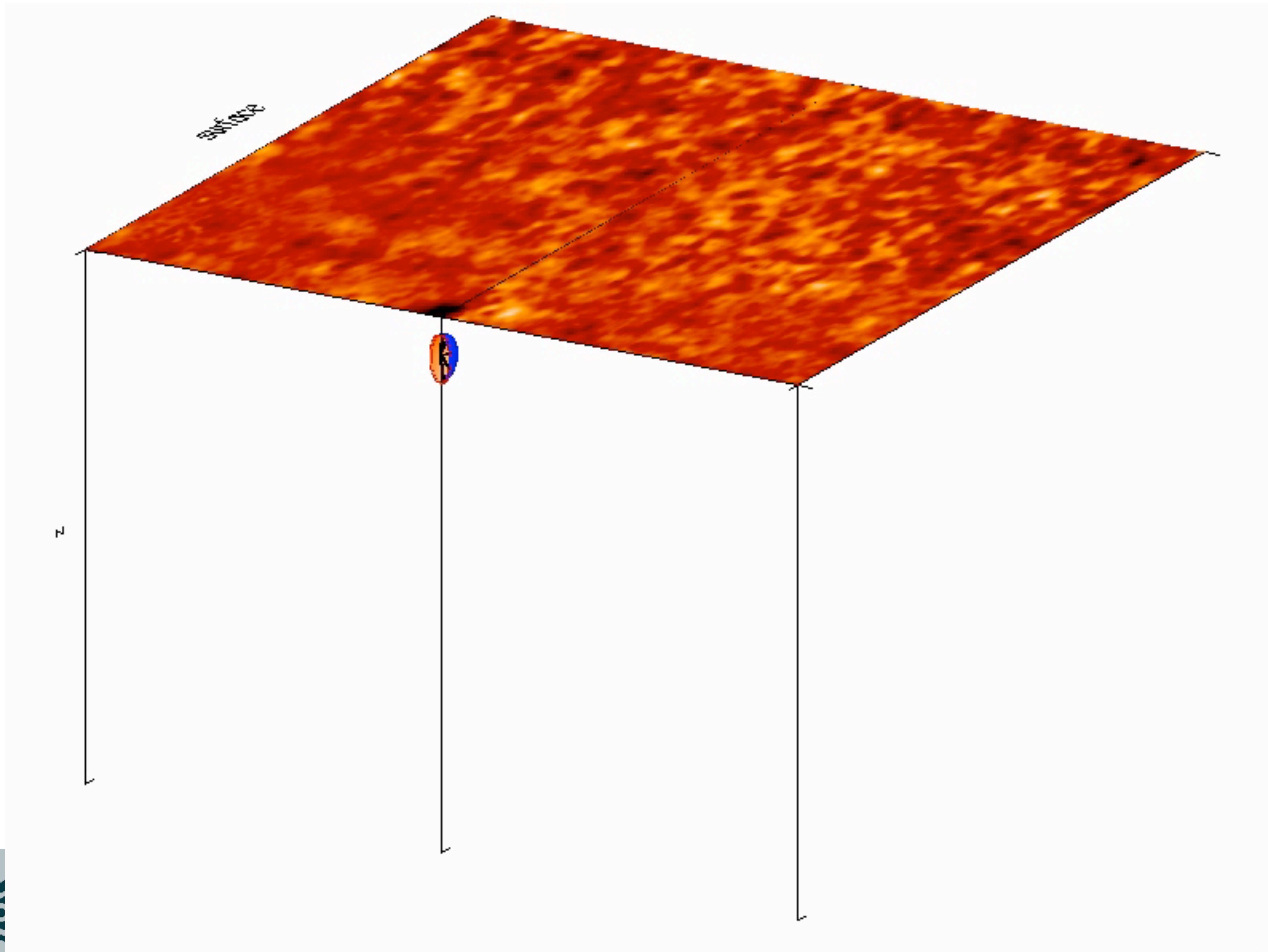

Q: How are the sun-quakes generated?

Q: How are the sun-quakes generated?

- **HD shocks via plasma heating by particle beams**
  - electron, proton or mixed (Zharkova & Zharkov, 2007, ApJ)

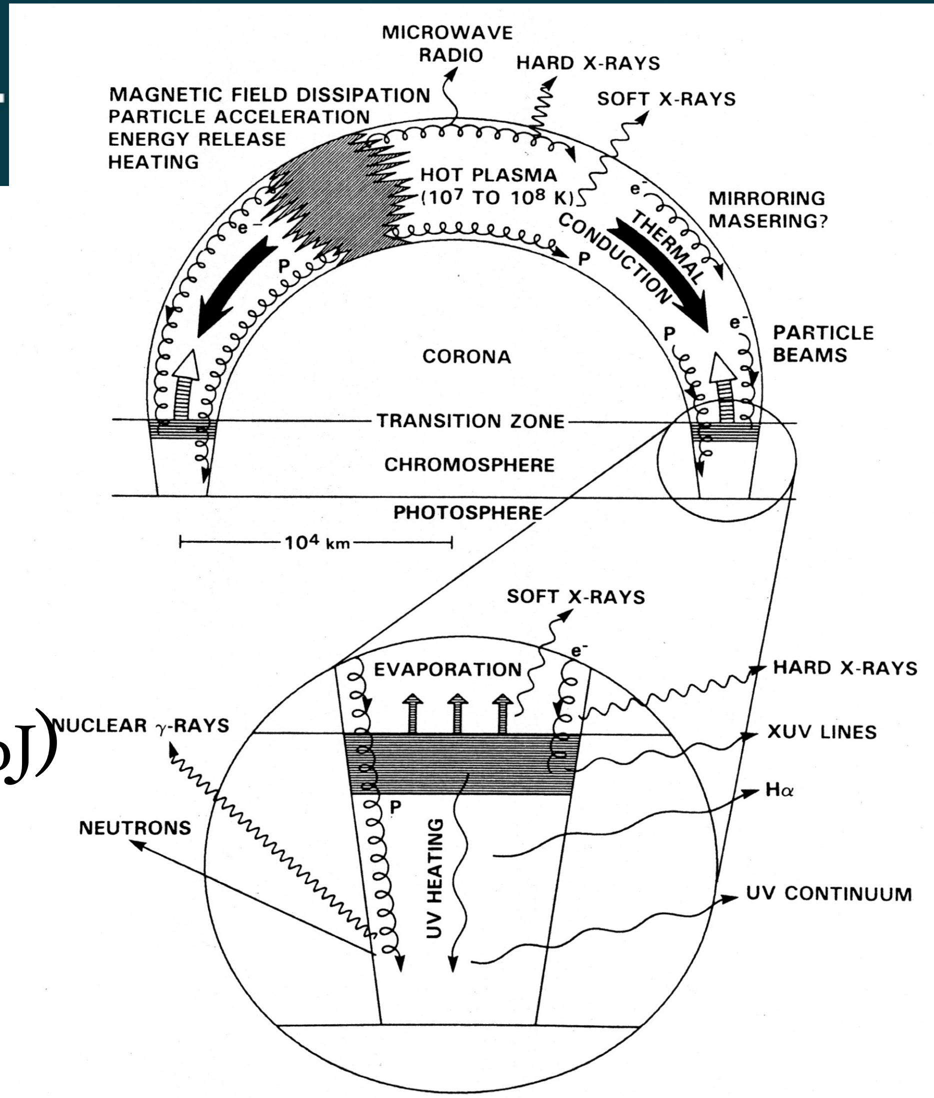

Q: How are the sun-quakes generated?

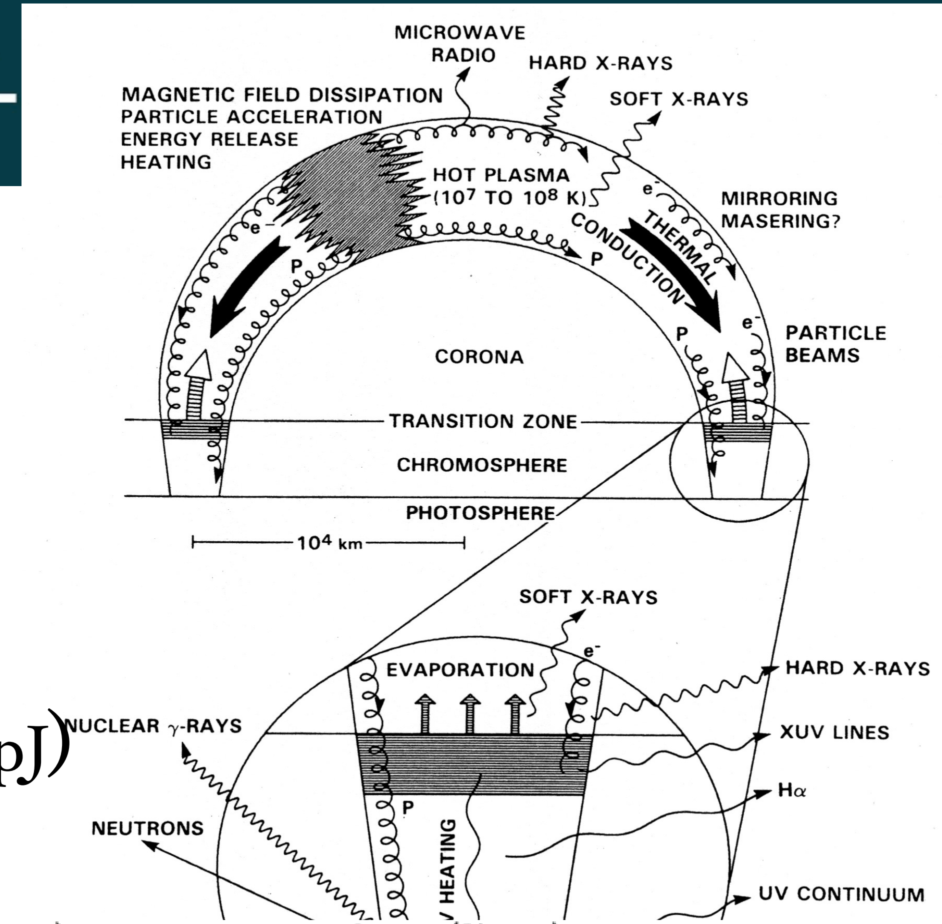

- **HD shocks via plasma heating by particle beams**
  - electron, proton or mixed (Zharkova & Zharkov, 2007, ApJ)

- **Backwarming heating (e.g.Donea et al, 2006)**
  - cospatial with WL & HXR

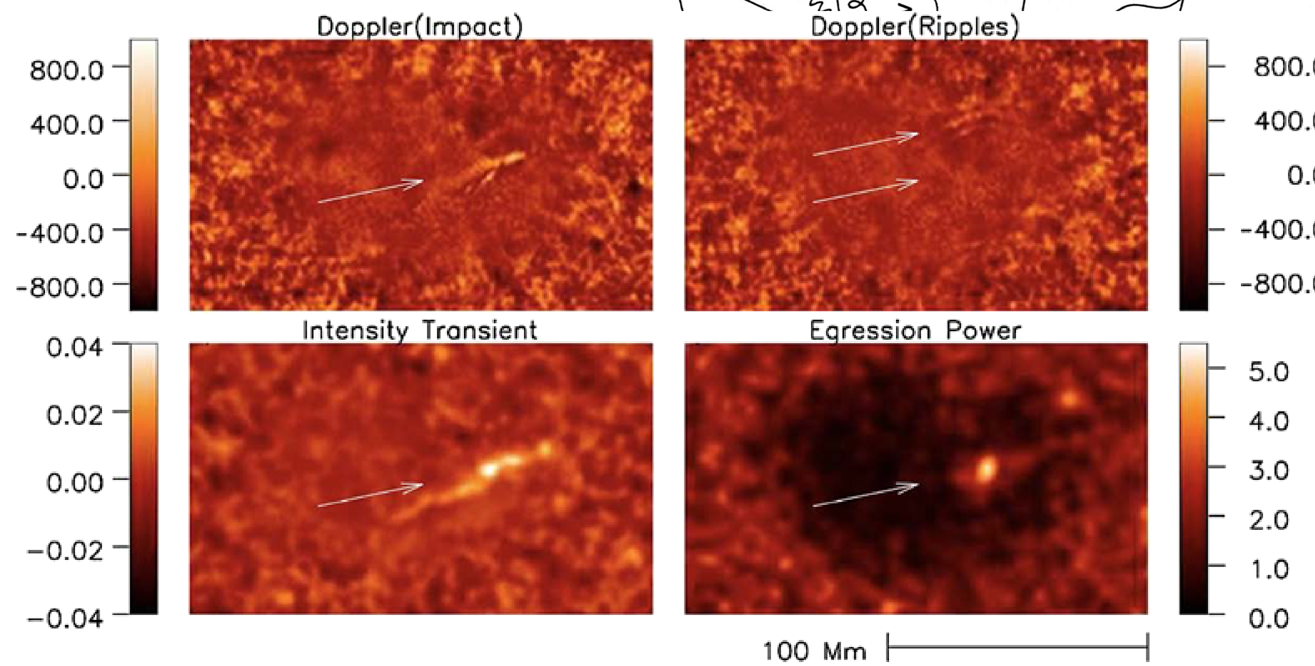

Q: How are the sun-quakes generated?

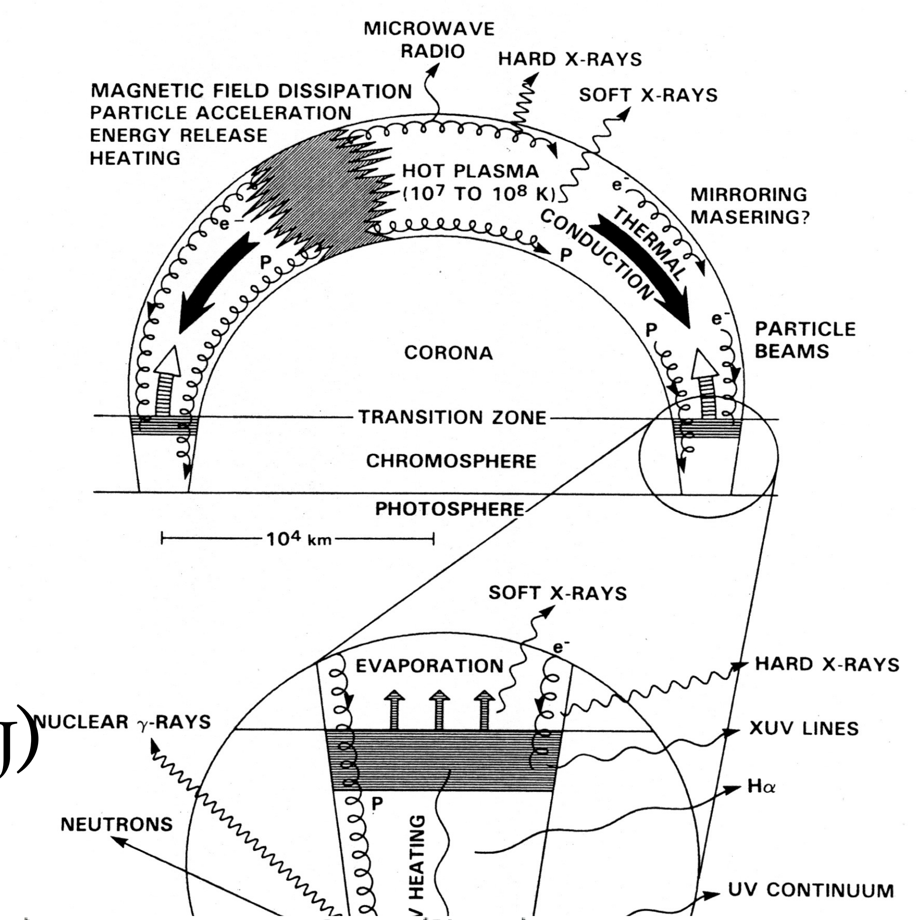

- **HD shocks via plasma heating by particle beams**
  - electron, proton or mixed (Zharkova & Zharkov, 2007, ApJ)

- **Backwarming heating (e.g.Donea et al, 2006)**
  - cospatial with WL & HXR

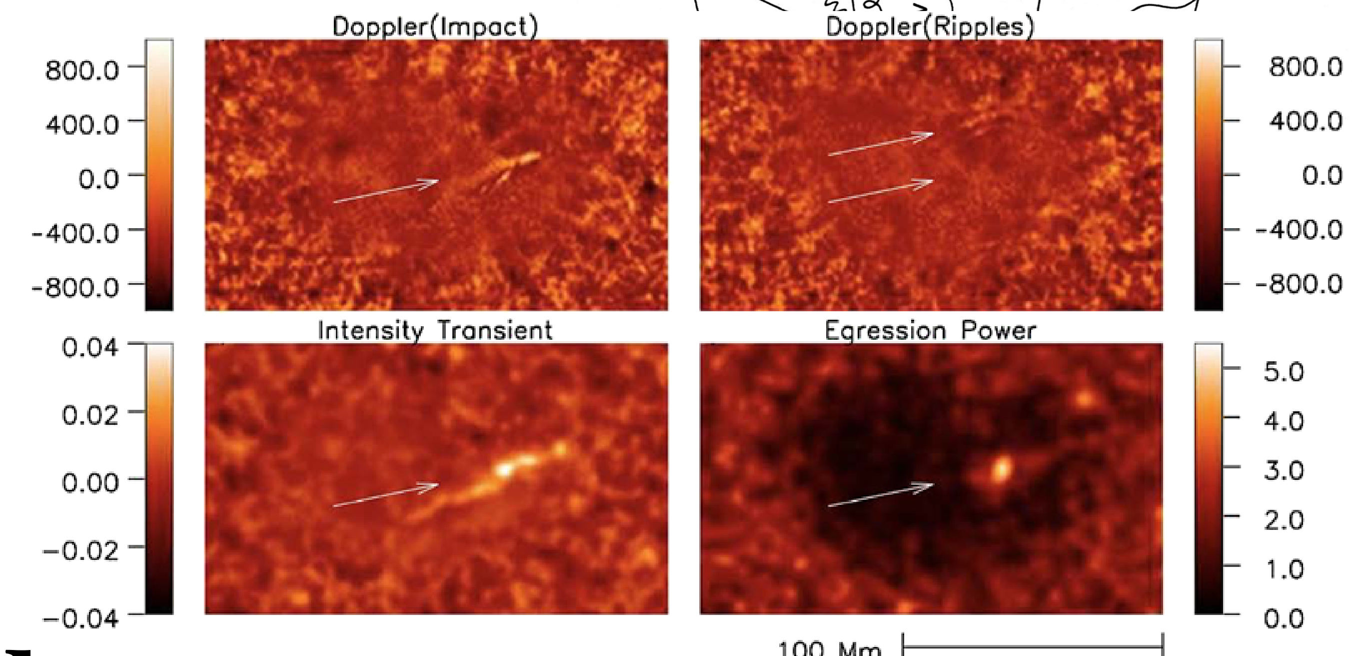

- **Magnetic field restructuring - Lorentz force transients (Hudson et al, 2008, Fisher et al., 2012)**

Q: How are the sun-quakes generated?

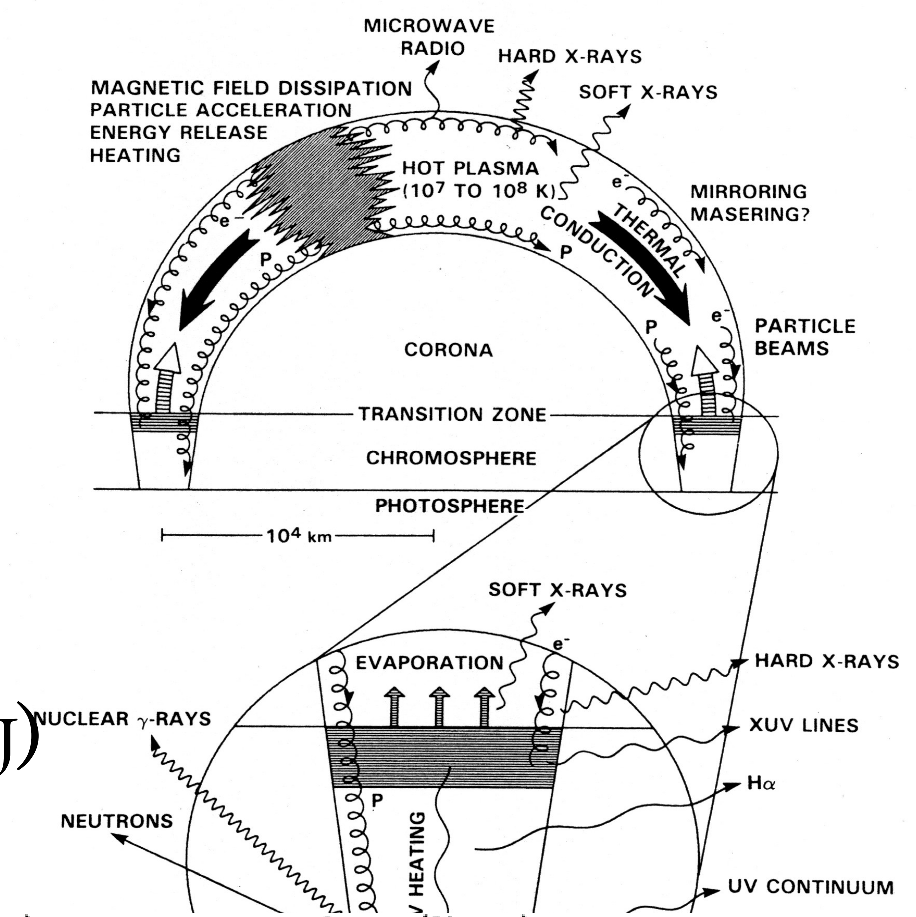

- **HD shocks via plasma heating by particle beams**
  - electron, proton or mixed (Zharkova & Zharkov, 2007, ApJ)

- **Backwarming heating (e.g.Donea et al, 2006)**
  - cospatial with WL & HXR

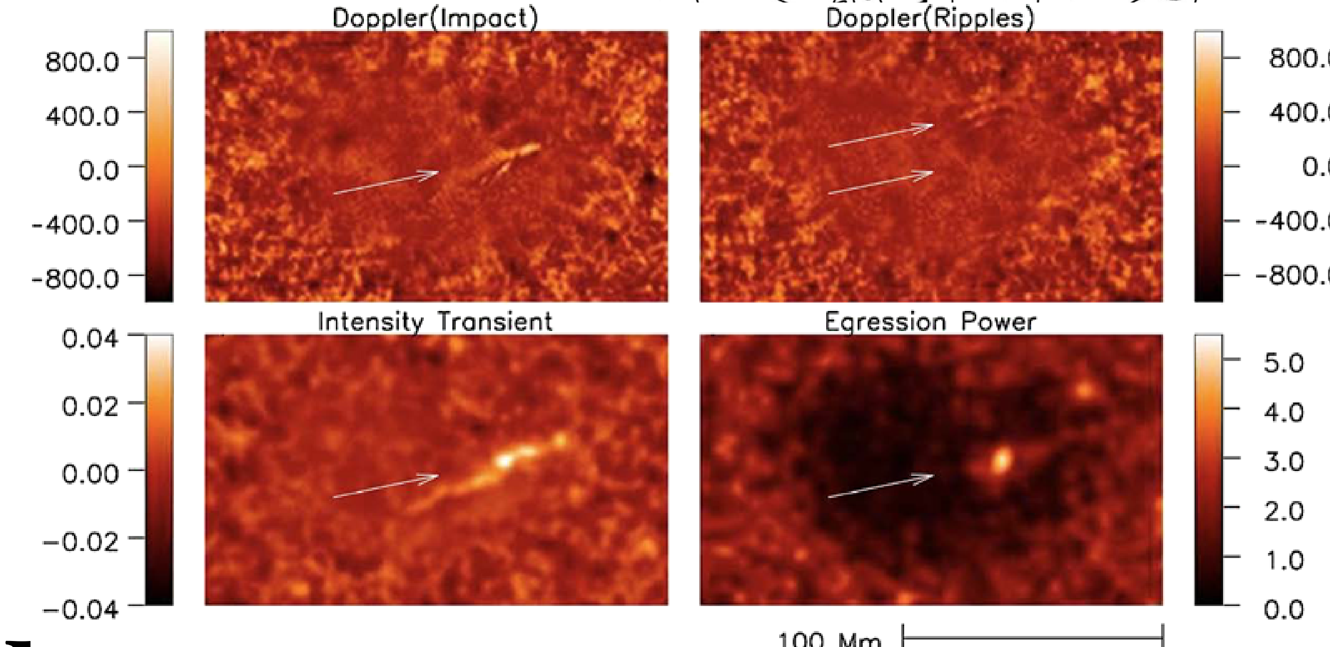

- **Magnetic field restructuring - Lorentz force transients (Hudson et al, 2008, Fisher et al., 2012)**

- **Wave interaction? quasi-periodic pulsations? (Fletcher & Hudson 2008)**

sunquake detection

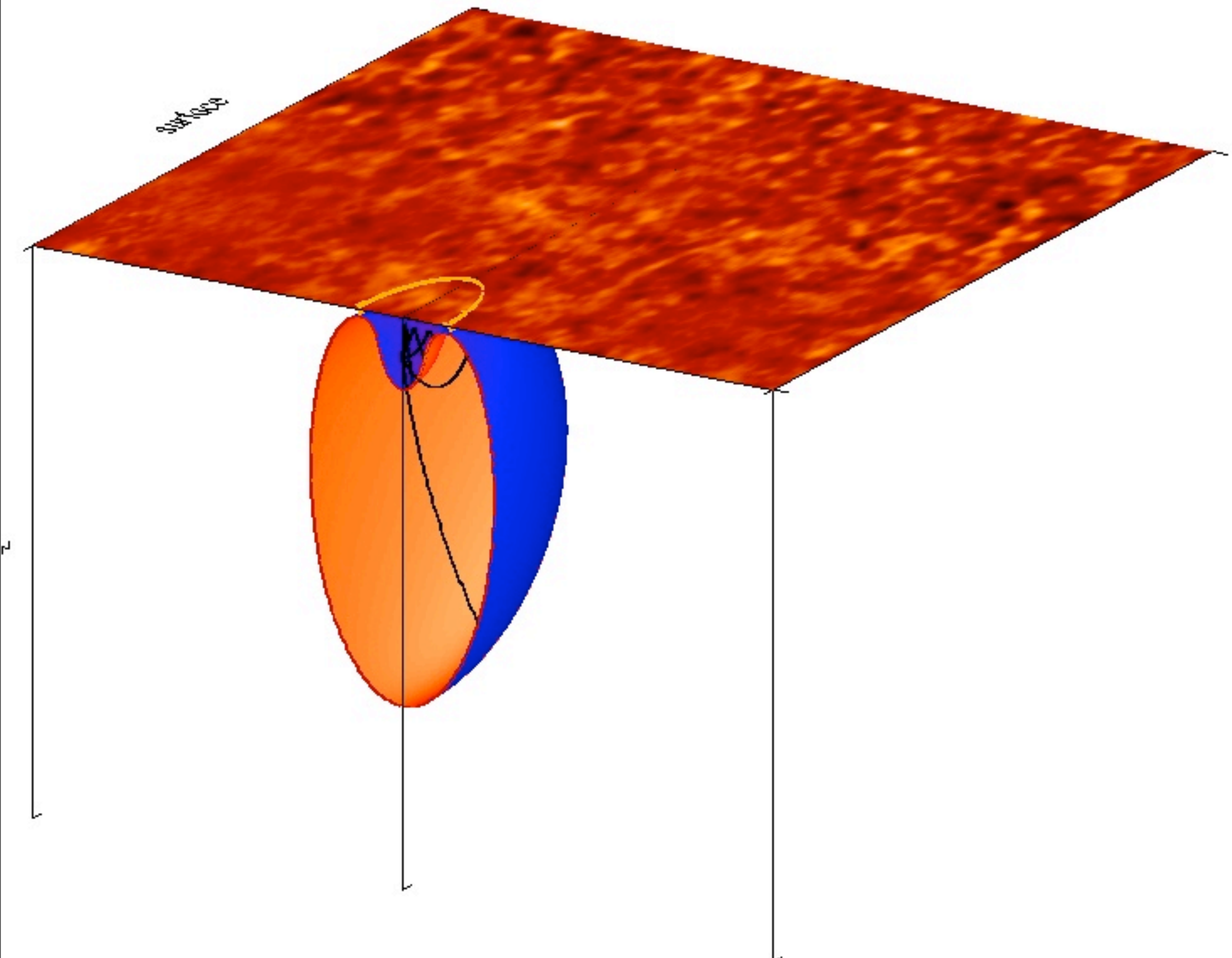

sunquake detection

$$V_m(r,t) = \int_\alpha^\beta v(r,\theta,t) e^{-im\theta} d\theta$$

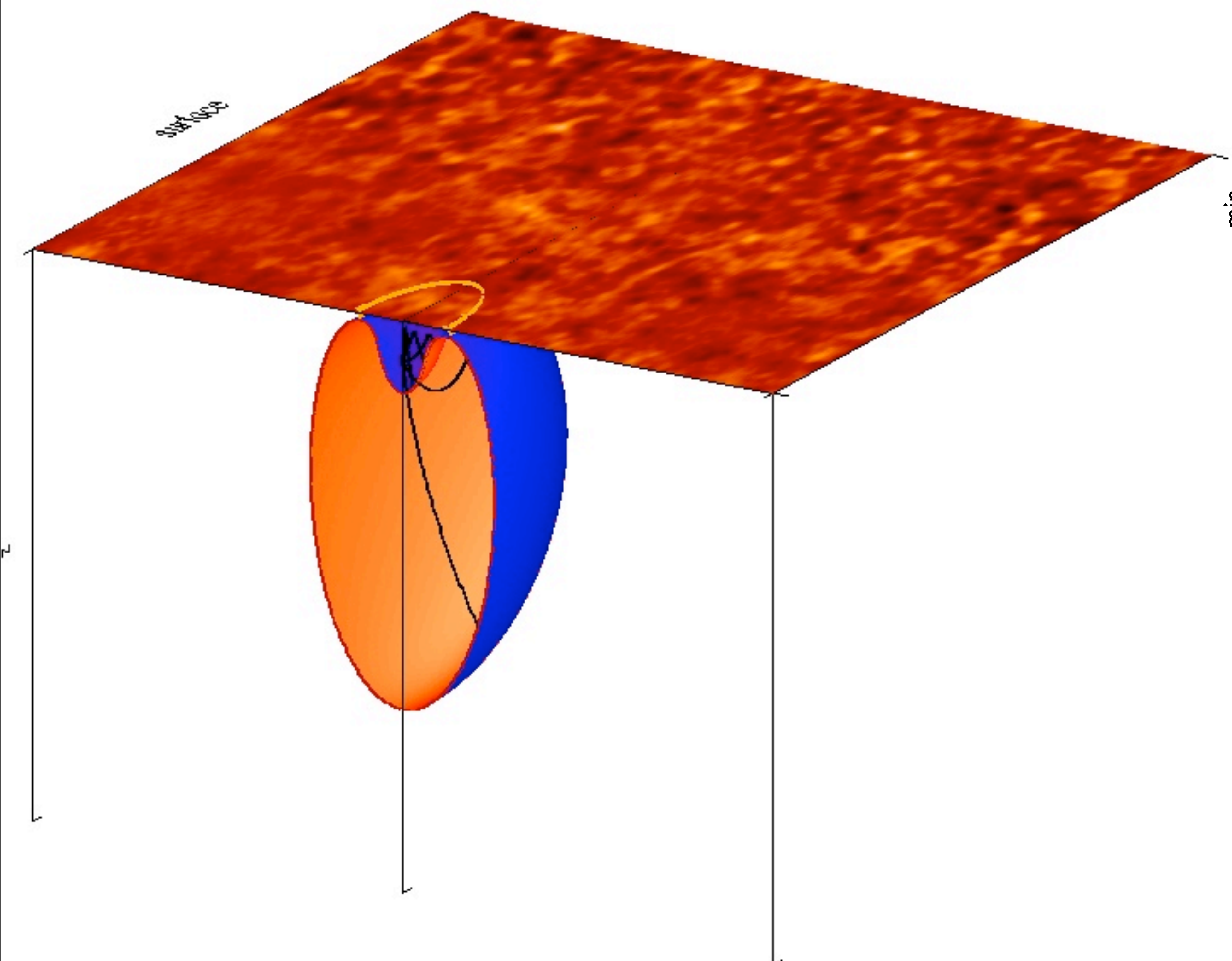

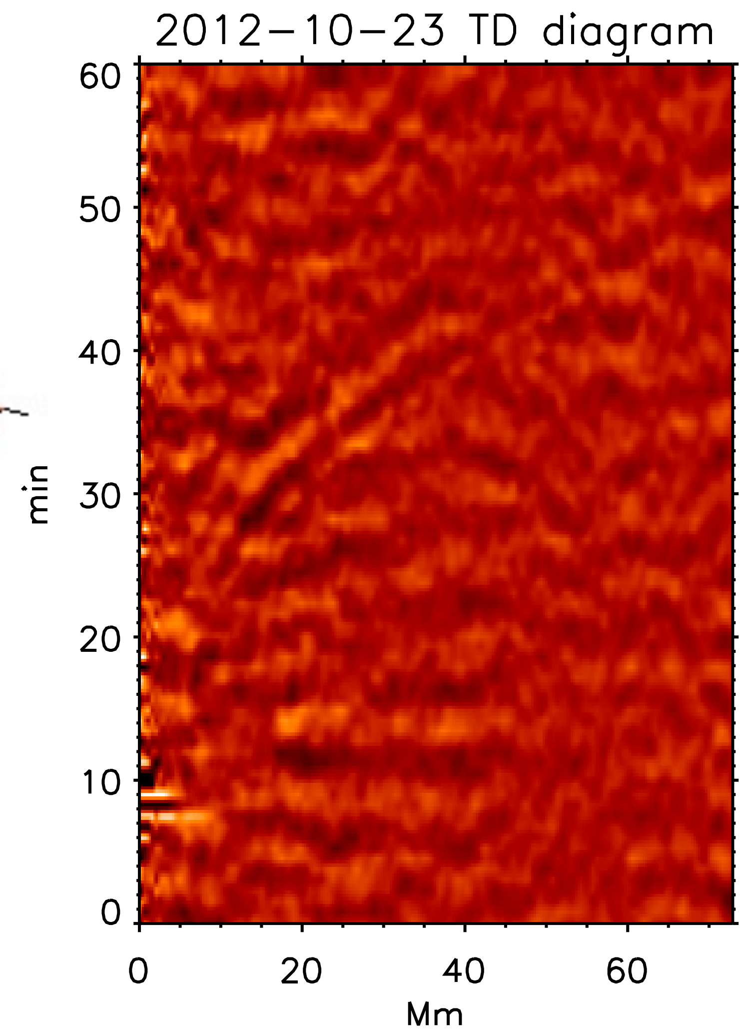

$$V_m(r,t) = \int_{\alpha}^{\beta} v(r,\theta,t) e^{-im\theta} d\theta$$

sunquake detection

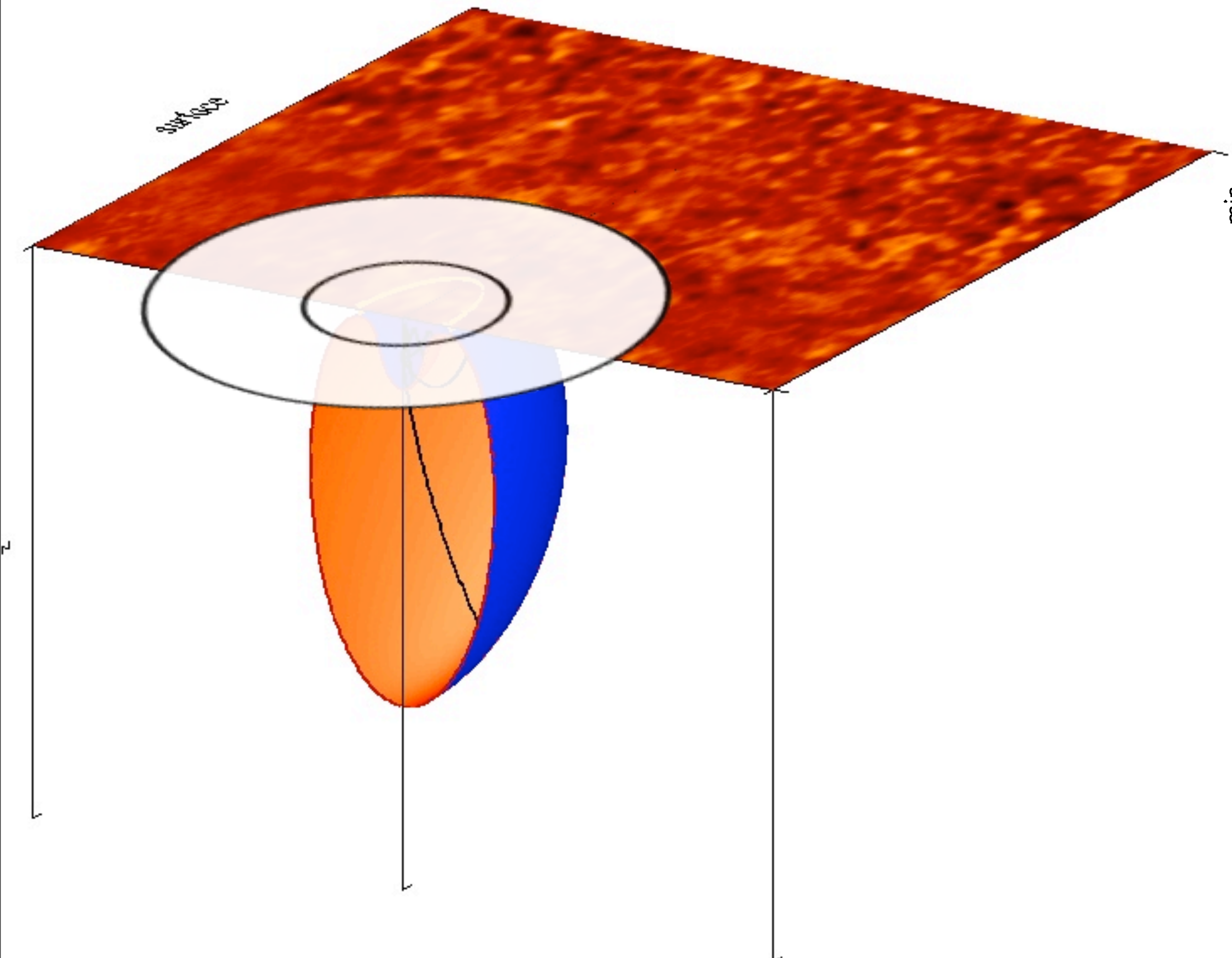

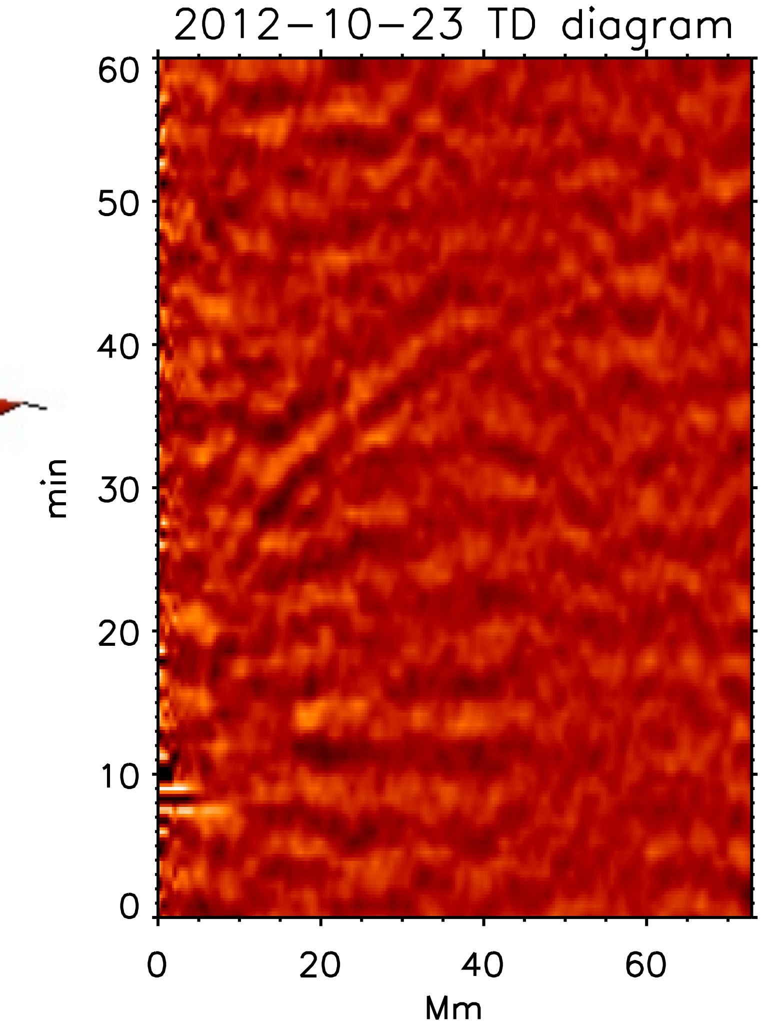

$$V_m(r,t) = \int_{\alpha}^{\beta} v(r,\theta,t)e^{-im\theta}d\theta$$

sunquake detection

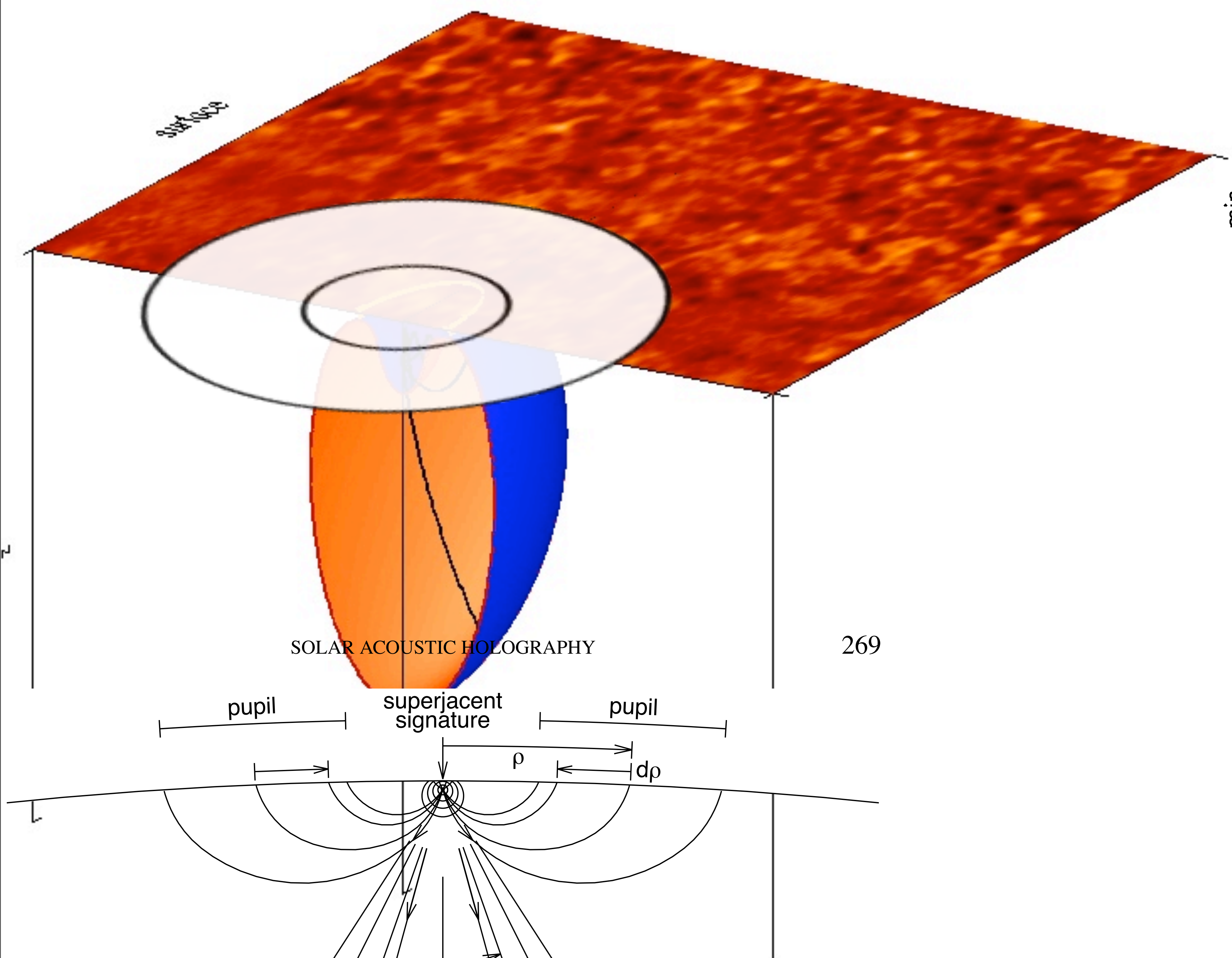

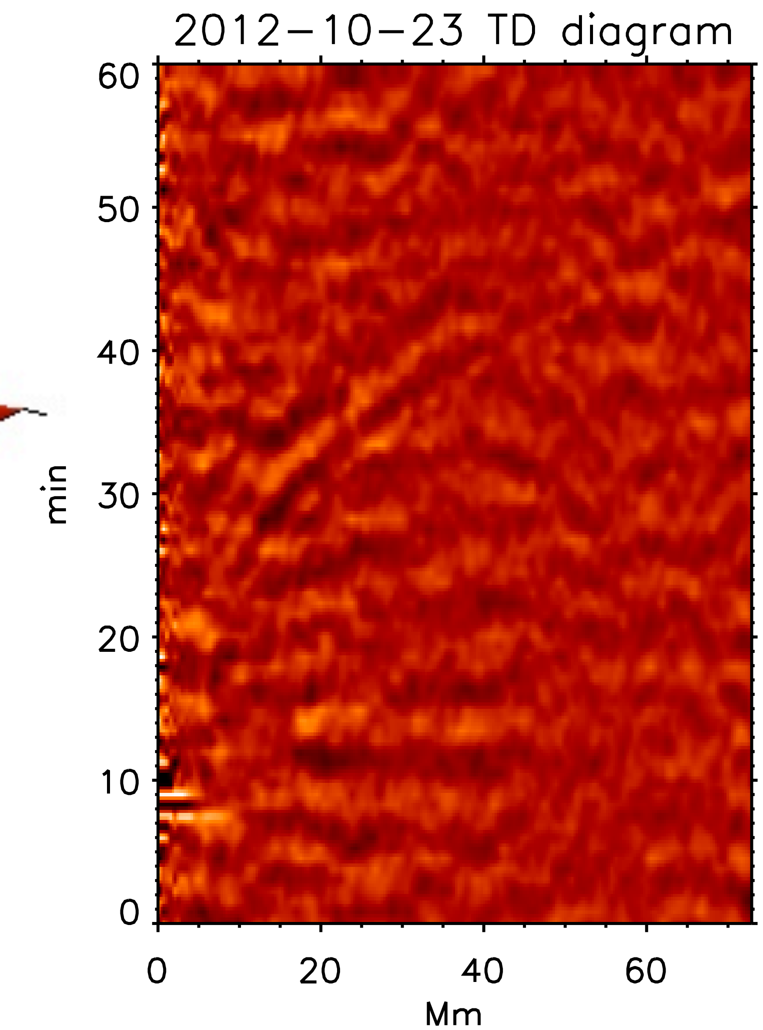

sunquake detection

$$V_m(r,t) = \int_\alpha^\beta v(r,\theta,t)e^{-im\theta}d\theta$$

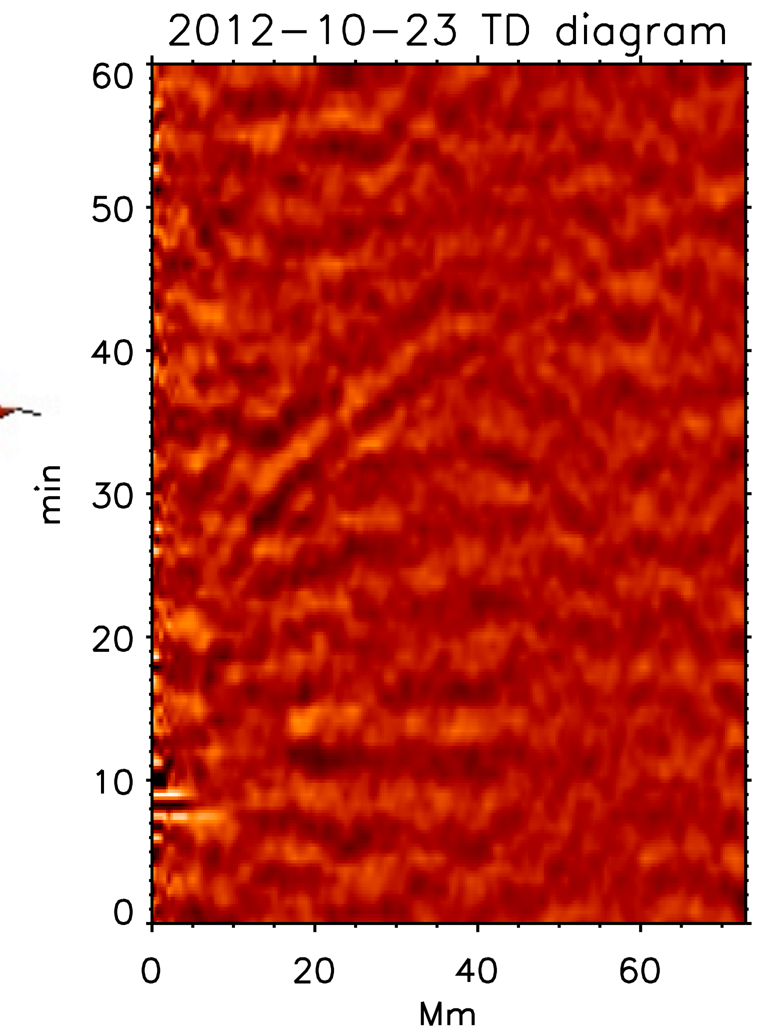

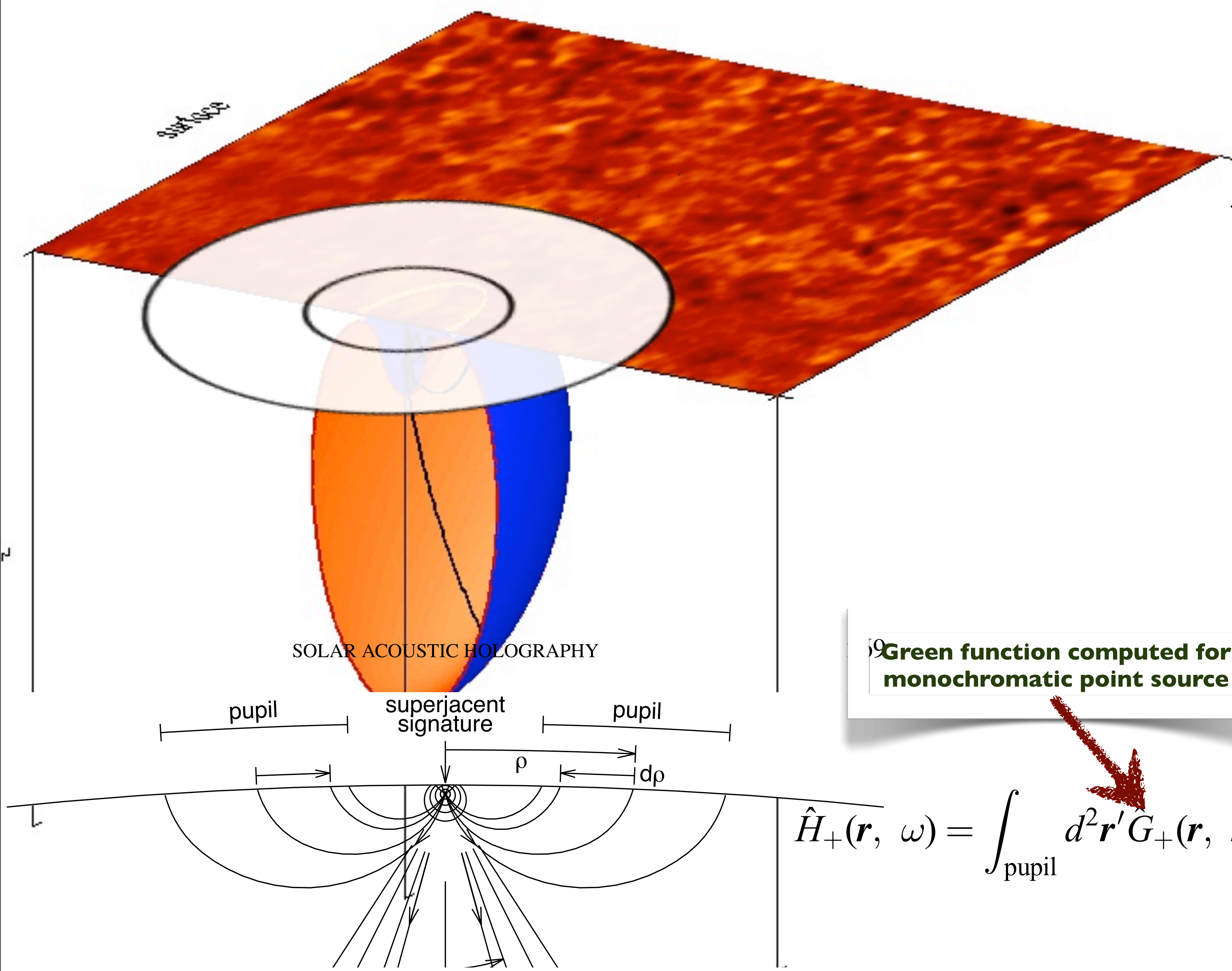

Surface doppergram observations (filtered)

Green function computed for monochromatic point source

$$\hat{H}_+(\mathbf{r},\ \omega) = \int_{\text{pupil}} d^2\mathbf{r}' G_+(\mathbf{r},\ \mathbf{r}',\ \omega)\hat{\psi}(\mathbf{r}',\ \omega).$$

$$V_m(r,t) = \int_\alpha^\beta v(r,\theta,t)e^{-im\theta}d\theta$$

sunquake detection

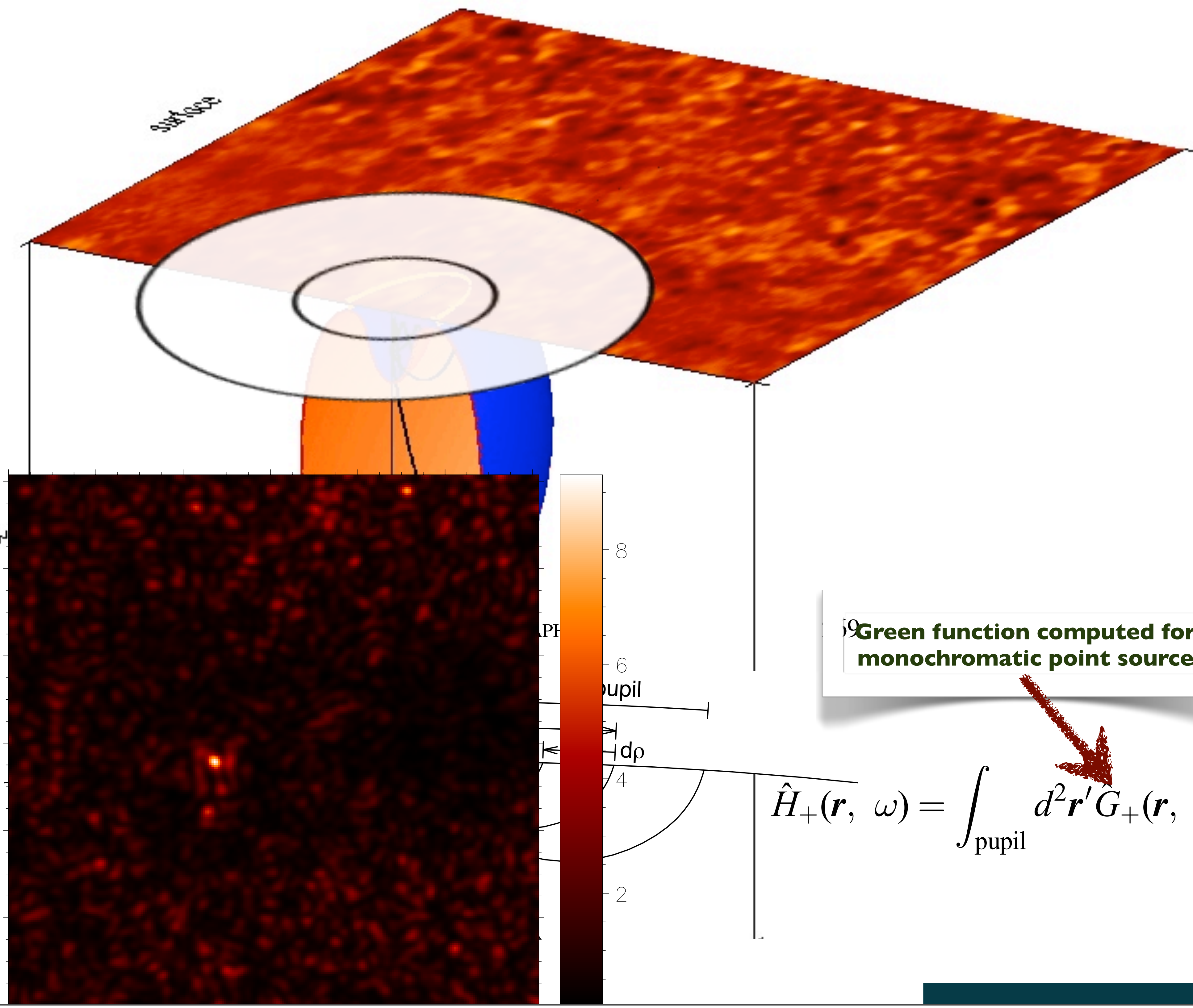

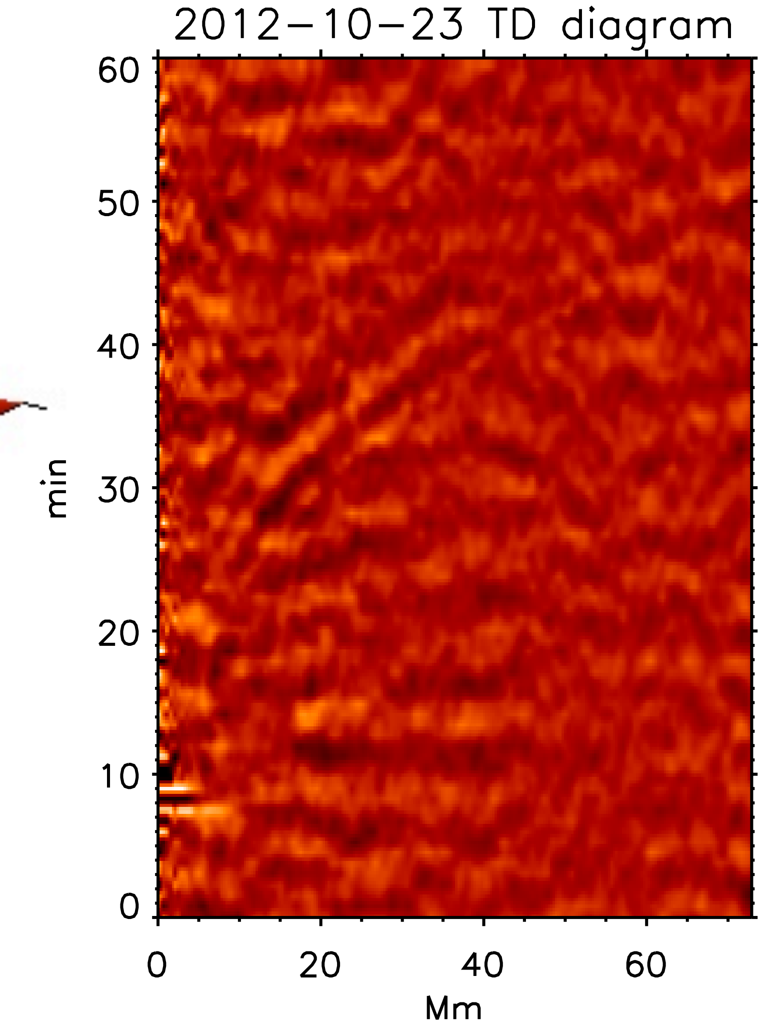

Green function computed for monochromatic point source

Surface doppergram observations (filtered)

$$\hat{H}_+(\mathbf{r},\ \omega) = \int_{\text{pupil}} d^2\mathbf{r}'G_+(\mathbf{r},\ \mathbf{r}',\ \omega)\hat{\psi}(\mathbf{r}',\ \omega).$$

sunquake detection

$$V_m(r,t) = \int_{\alpha}^{\beta} v(r,\theta,t)e^{-im\theta}d\theta$$

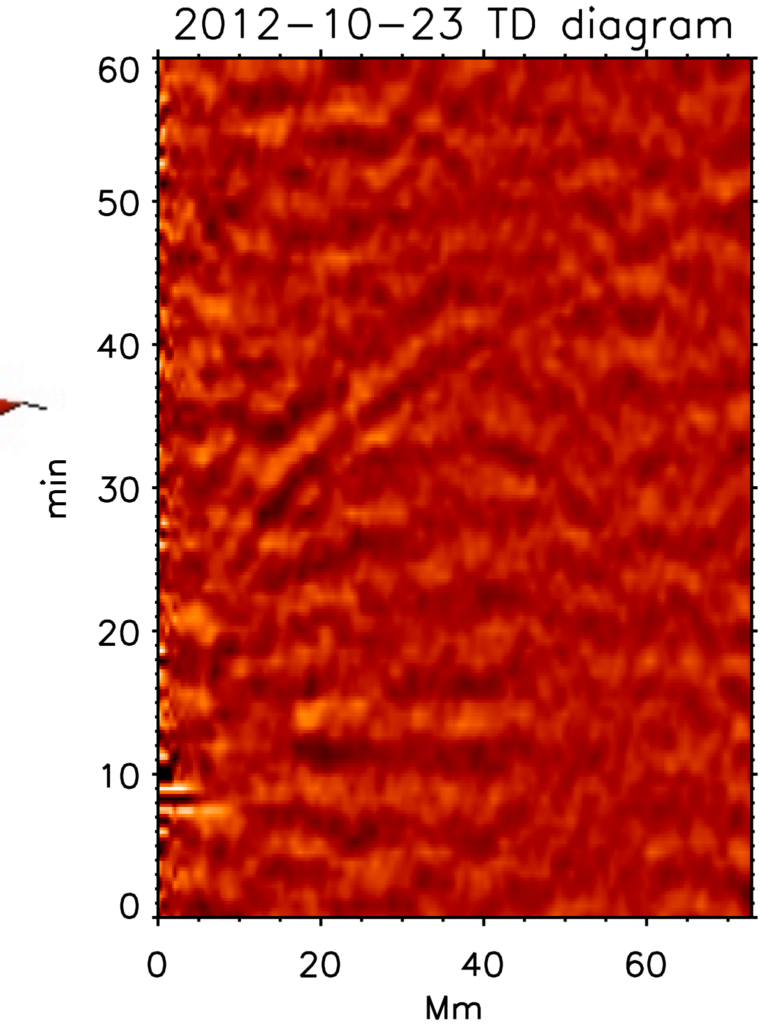

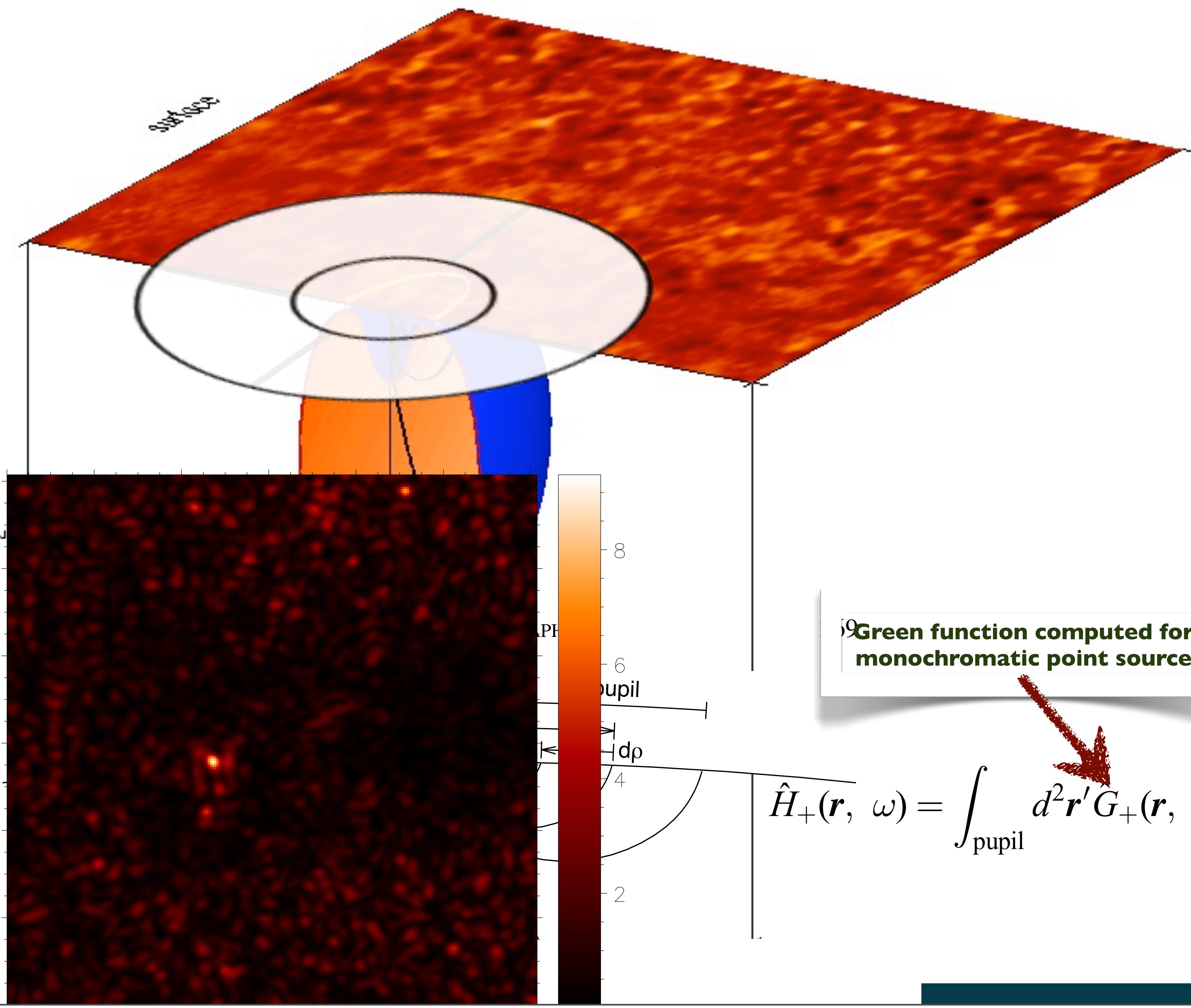

Surface doppergram observations (filtered)

Green function computed for monochromatic point source

$$\hat{H}_+(\mathbf{r},\ \omega) = \int_{\text{pupil}} d^2\mathbf{r}'G_+(\mathbf{r},\ \mathbf{r}',\ \omega)\hat{\psi}(\mathbf{r}',\ \omega).$$

NOAA11158: M2.2 Feb 14, 17:26

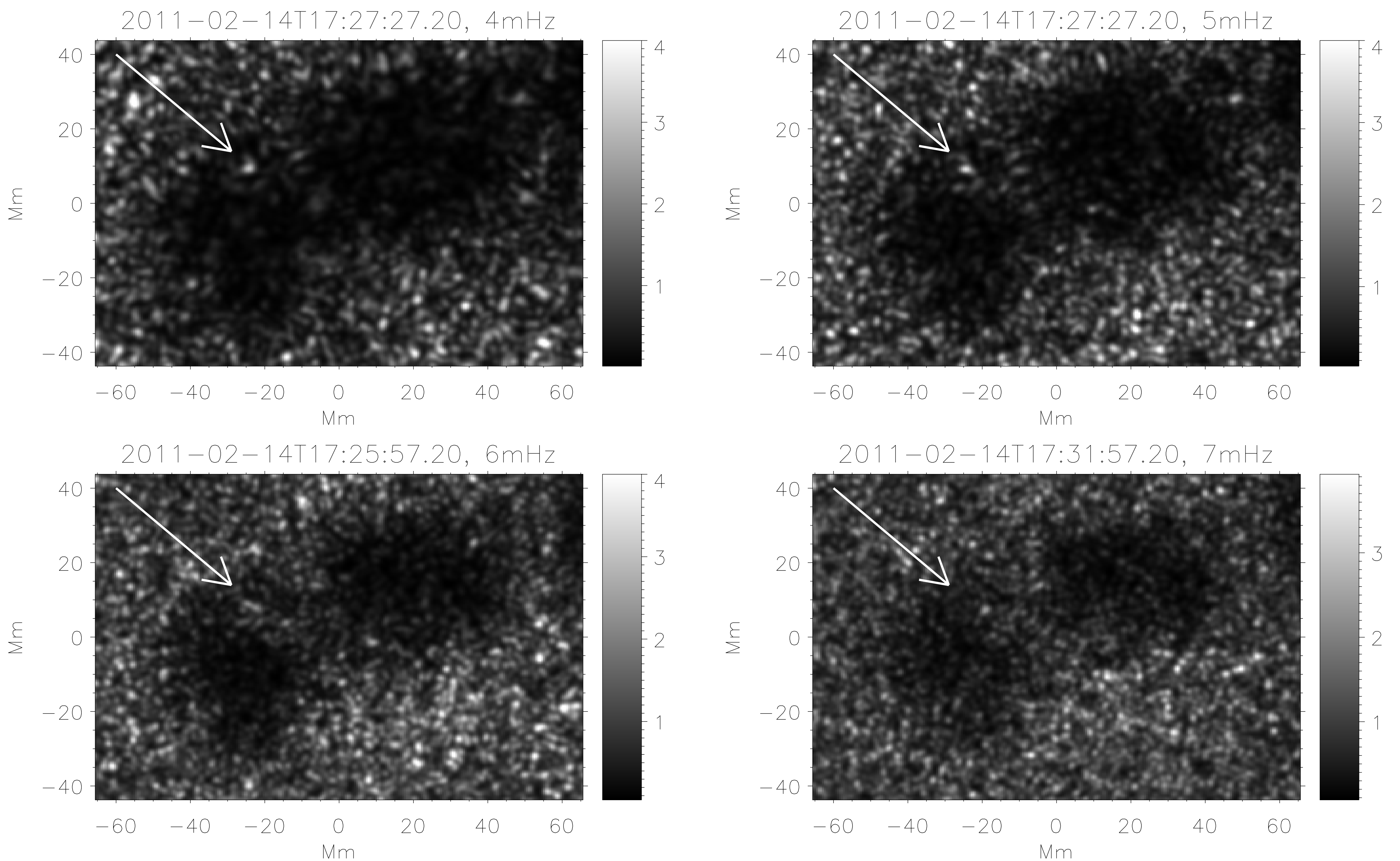

NOAA11158: M2.2 Feb 14, 17:26

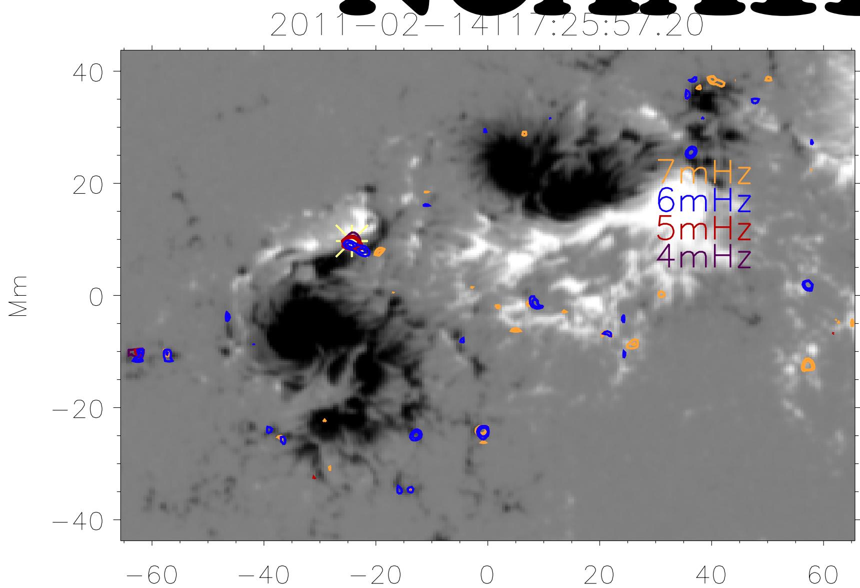

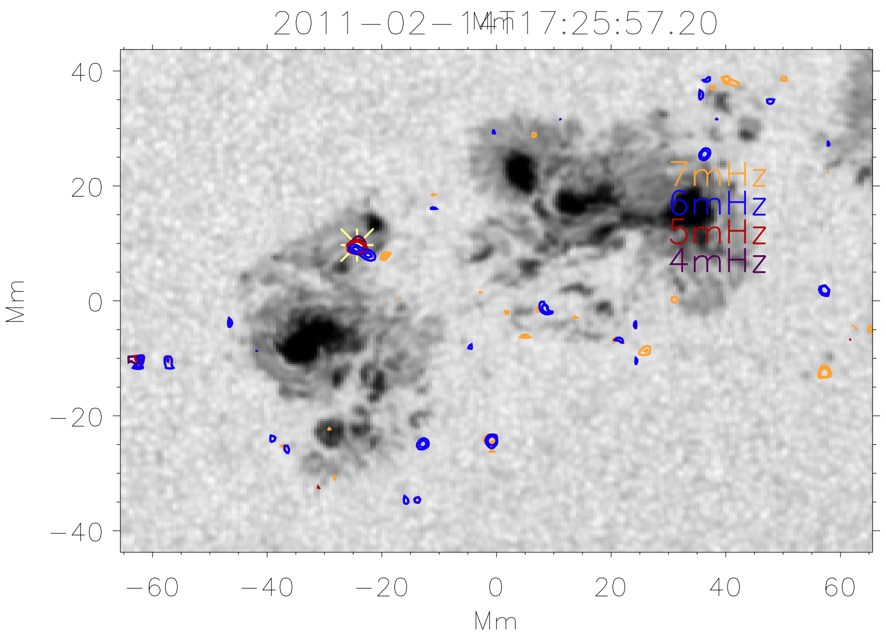

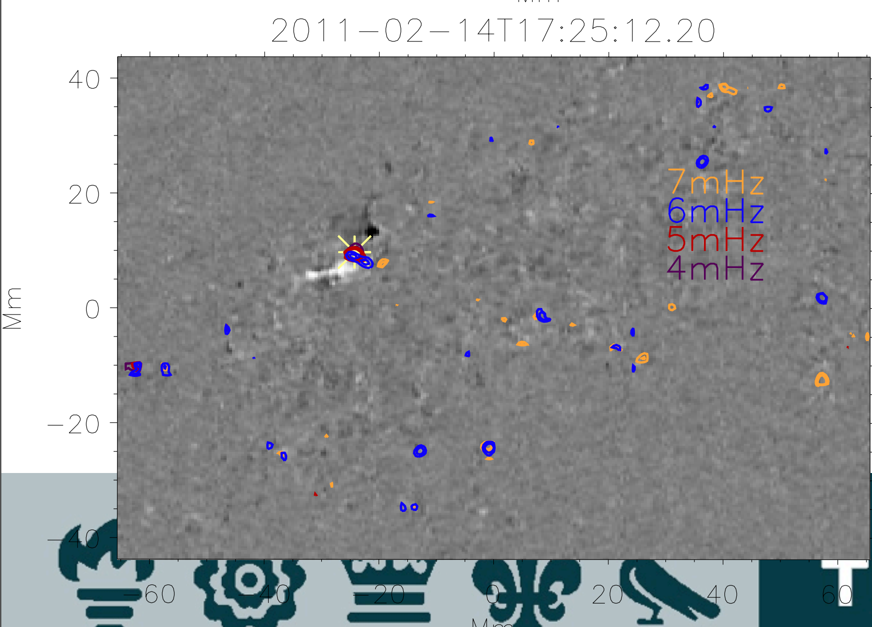

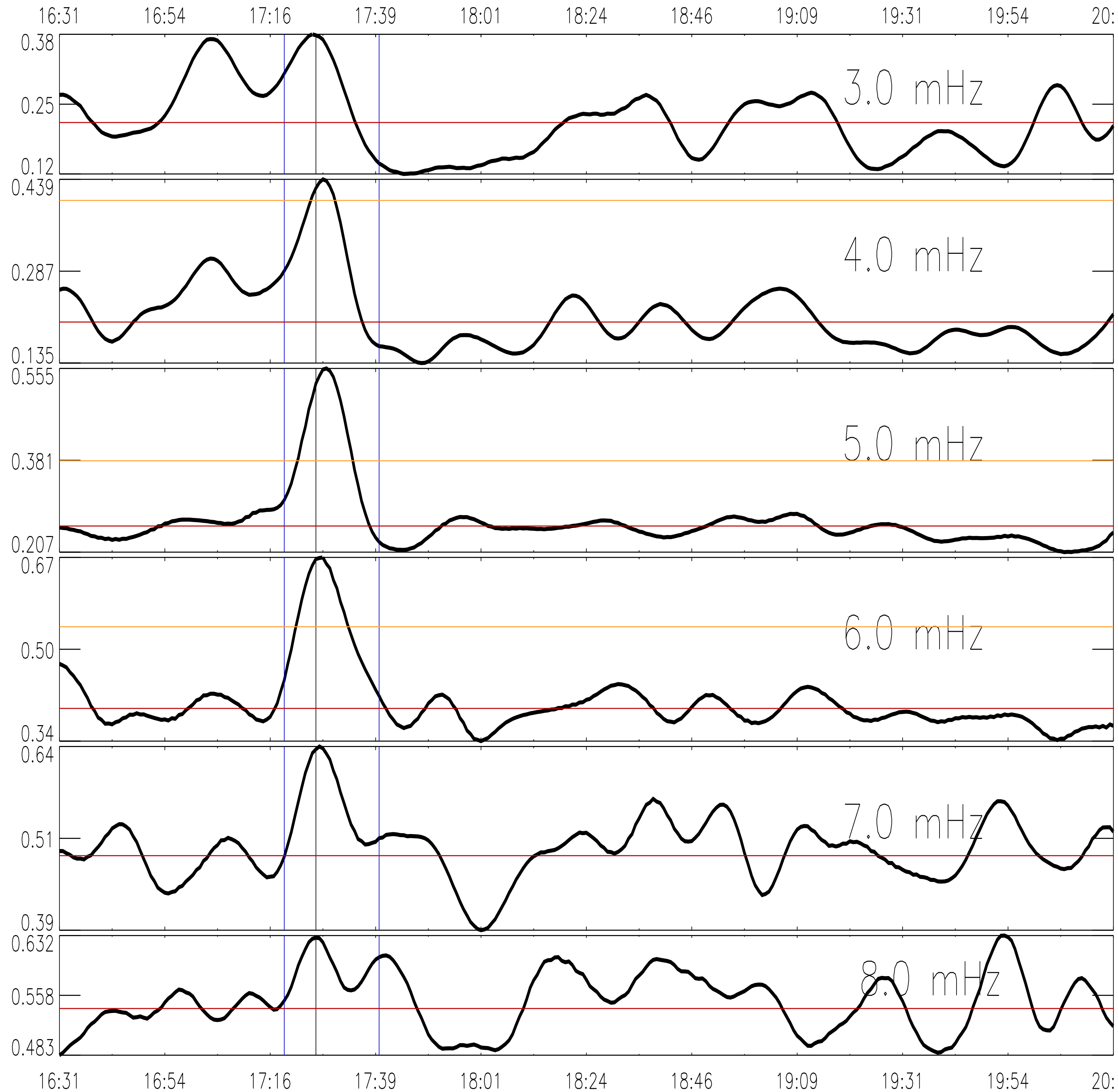

THE UNIVERSITY OF HULL

NOAA11158: M2.2 Feb 14, 17:26

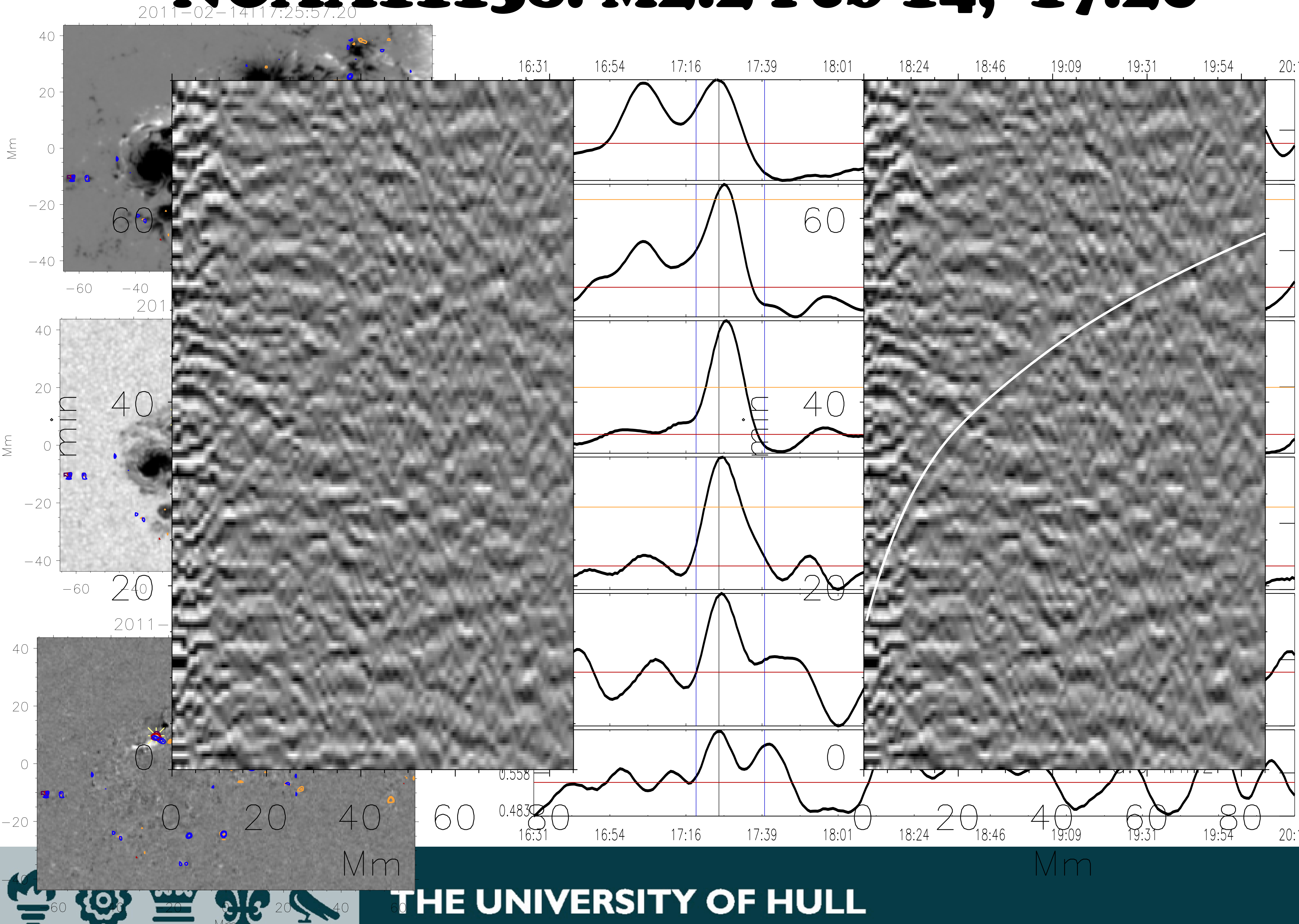

THE UNIVERSITY OF HULL

February 15, 2011 - X2.2 flare

February 15, 2011 - X2.2 flare

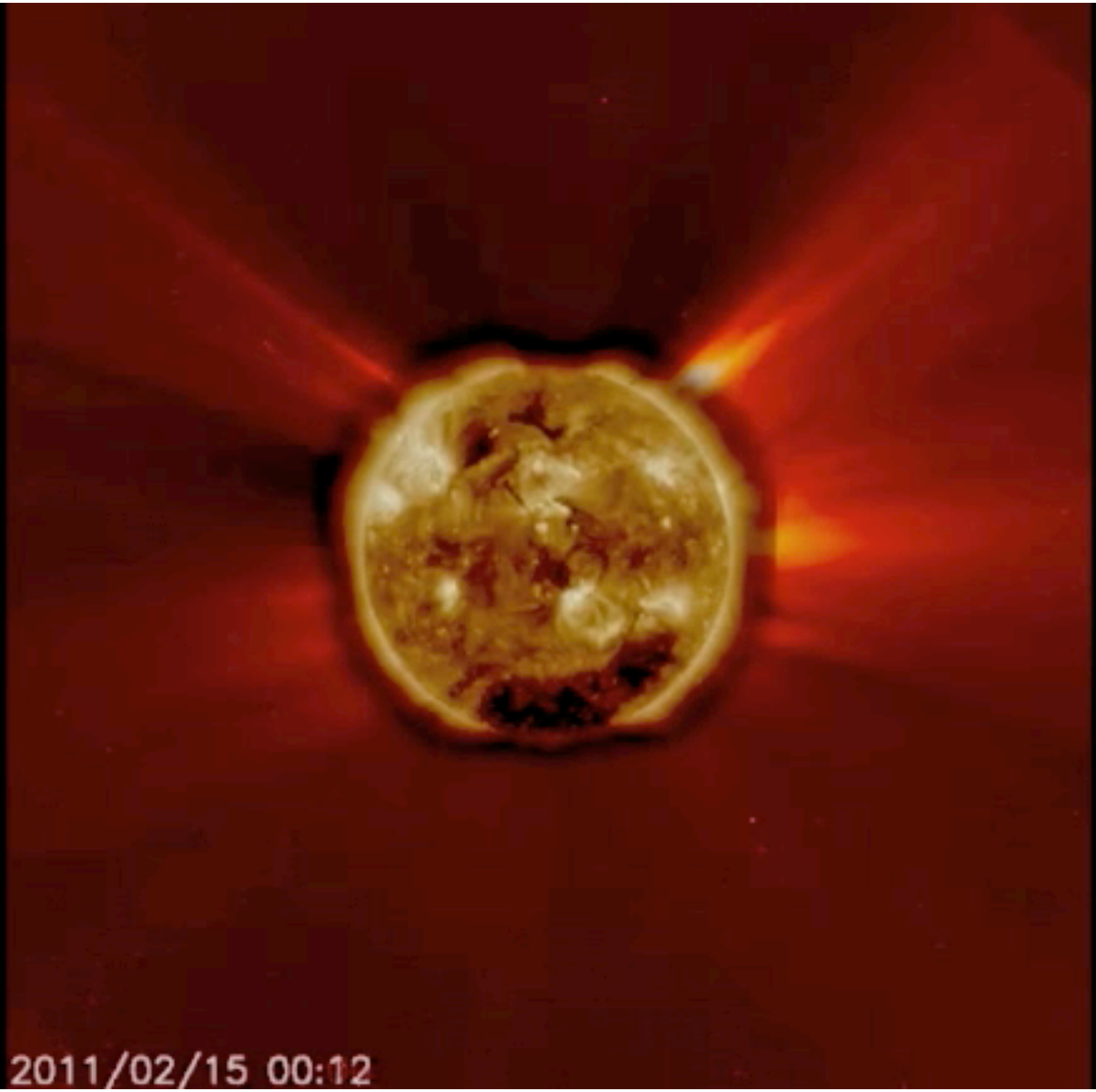

2011-02-15 SQ Sources

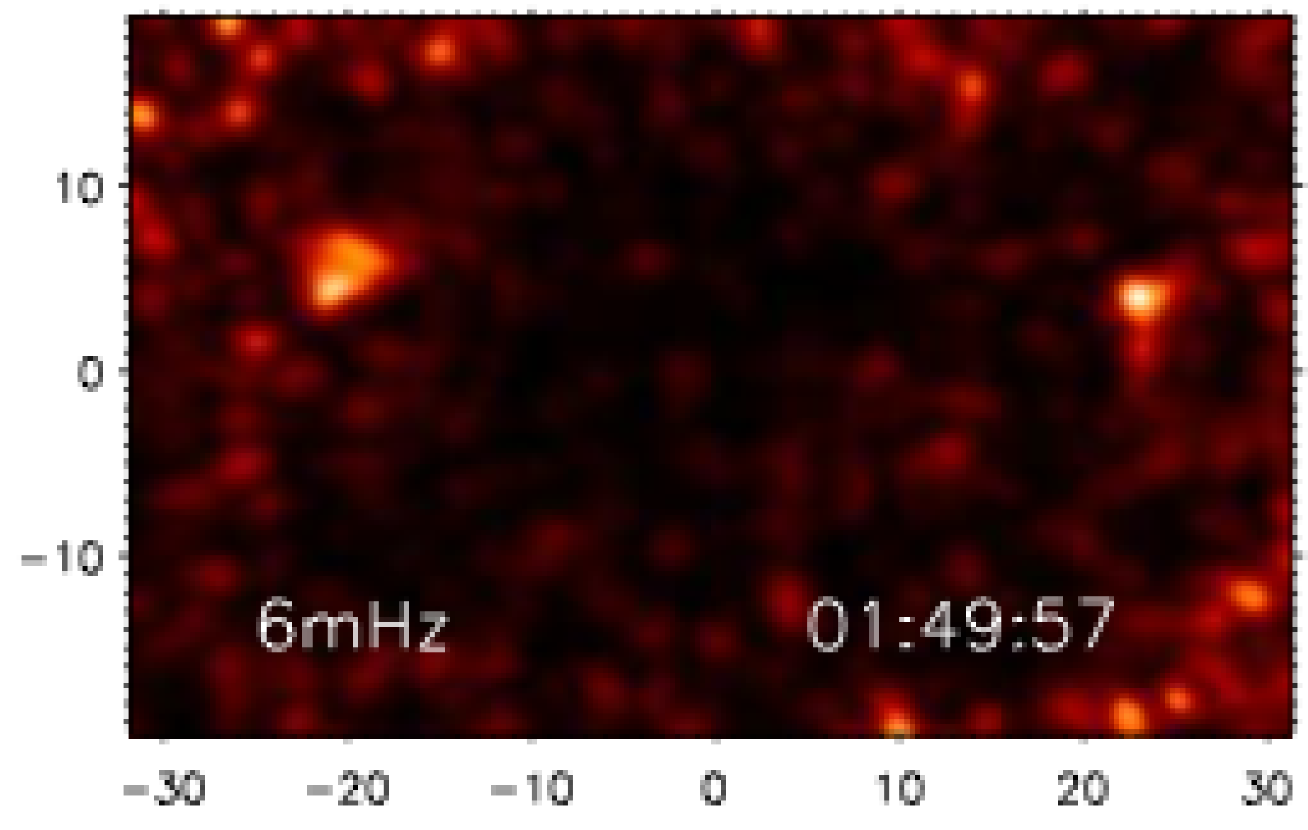

Zharkov et al., ApJL, 2011

2011-02-15 SQ Sources

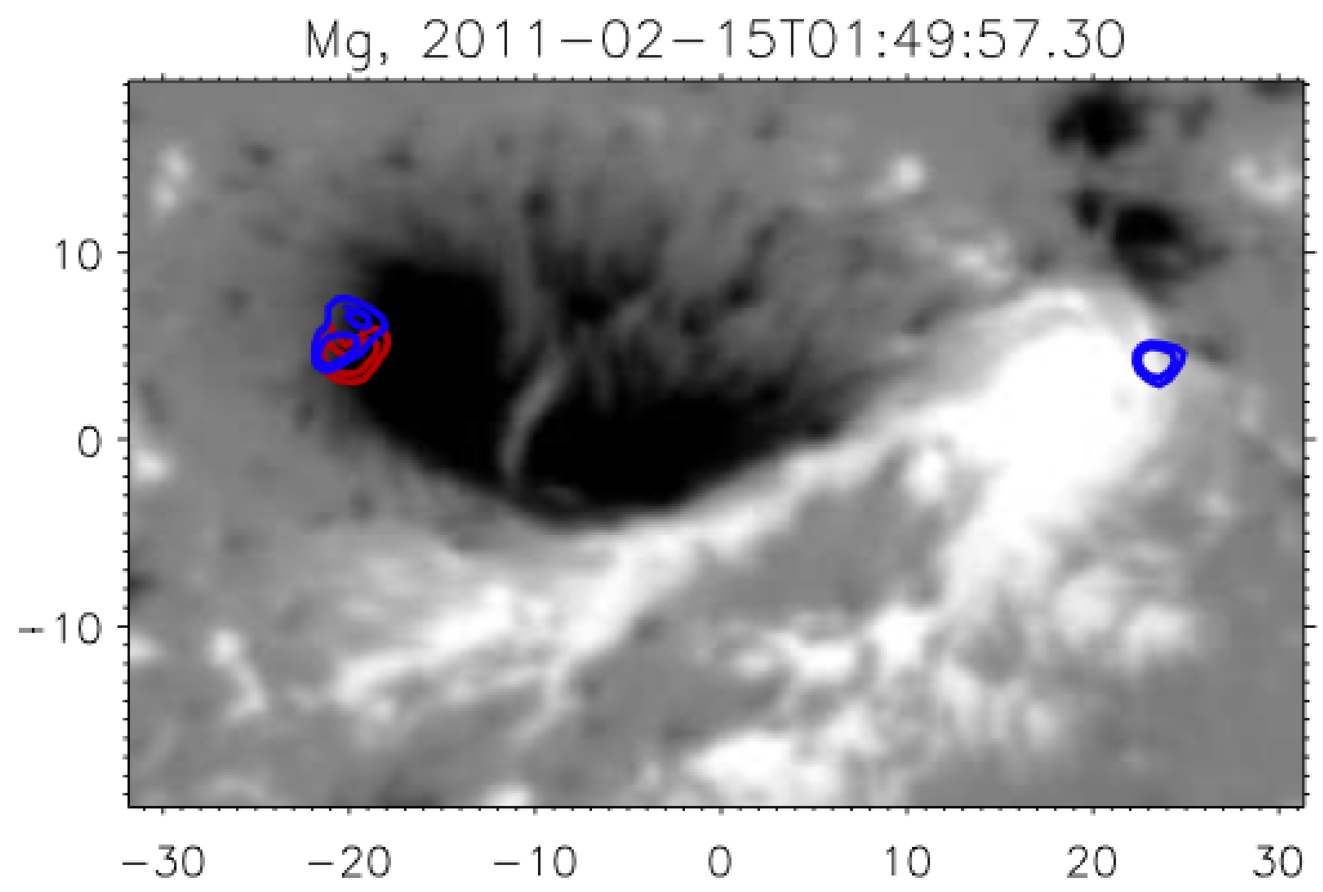

Zharkov et al., ApJL, 2011

2011-02-15 SQ Sources

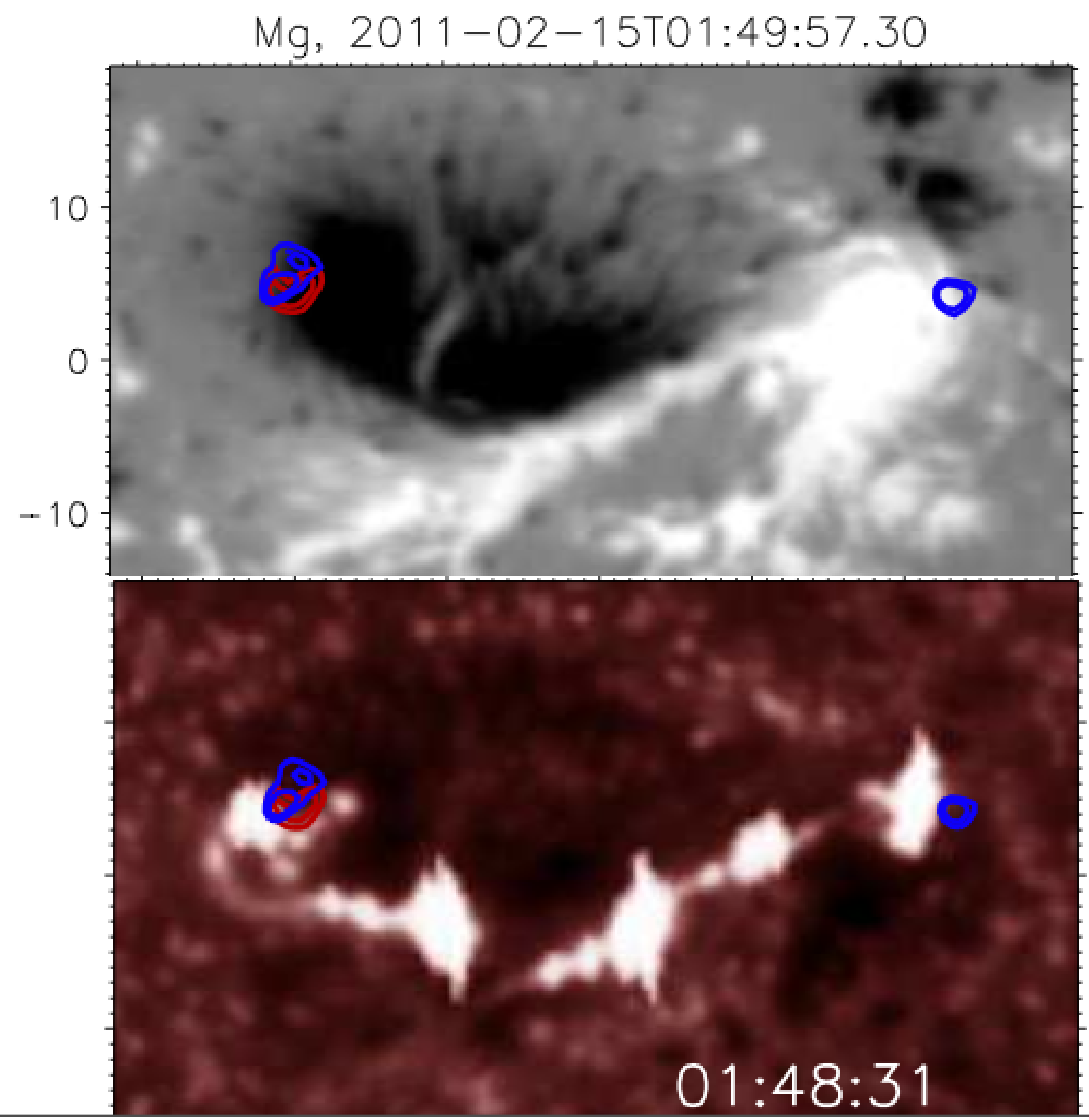

Zharkov et al., ApJL, 2011

2011-02-15 SQ Sources

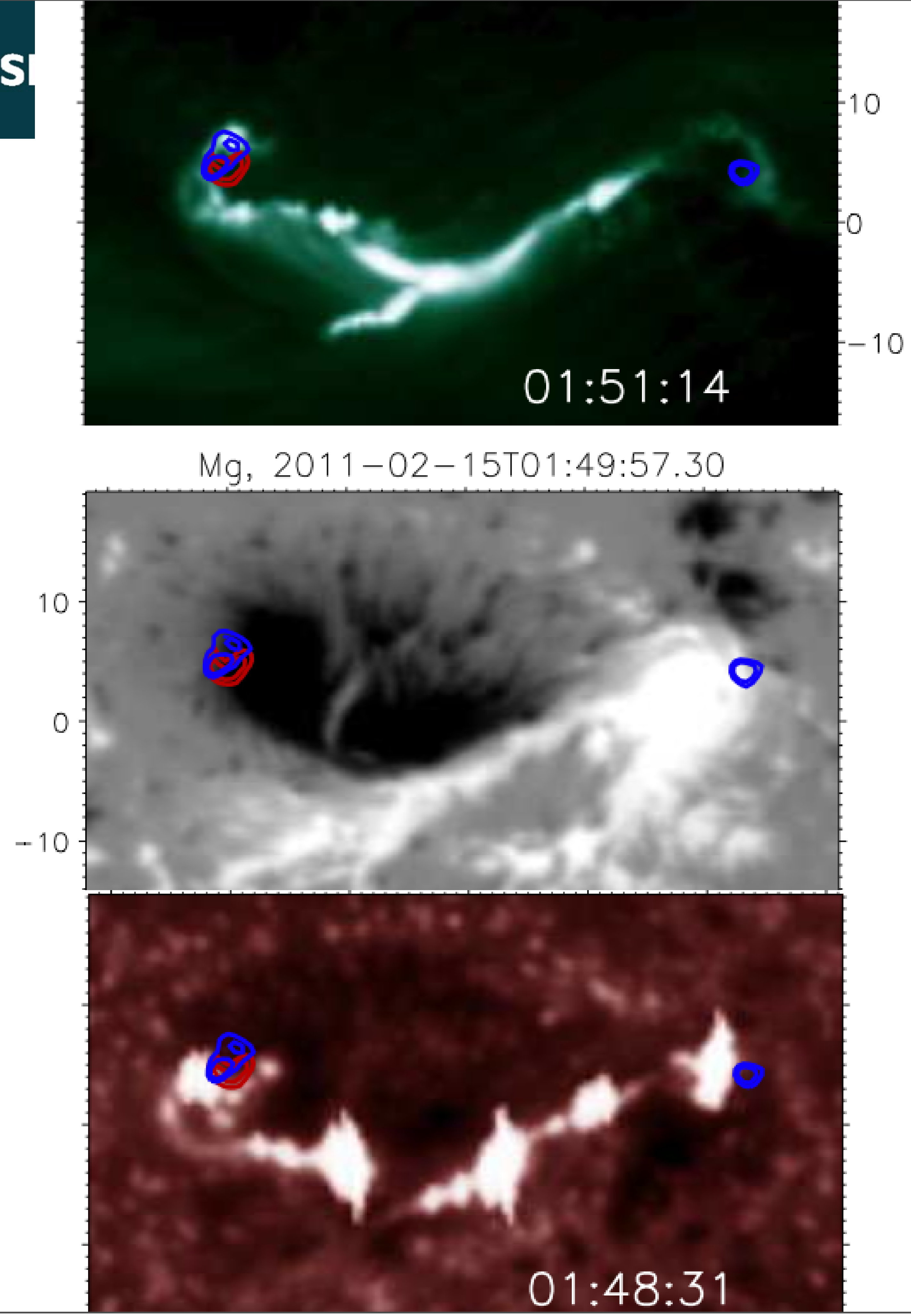

Zharkov et al., ApJL, 2011

2011-02-15 SQ Sources

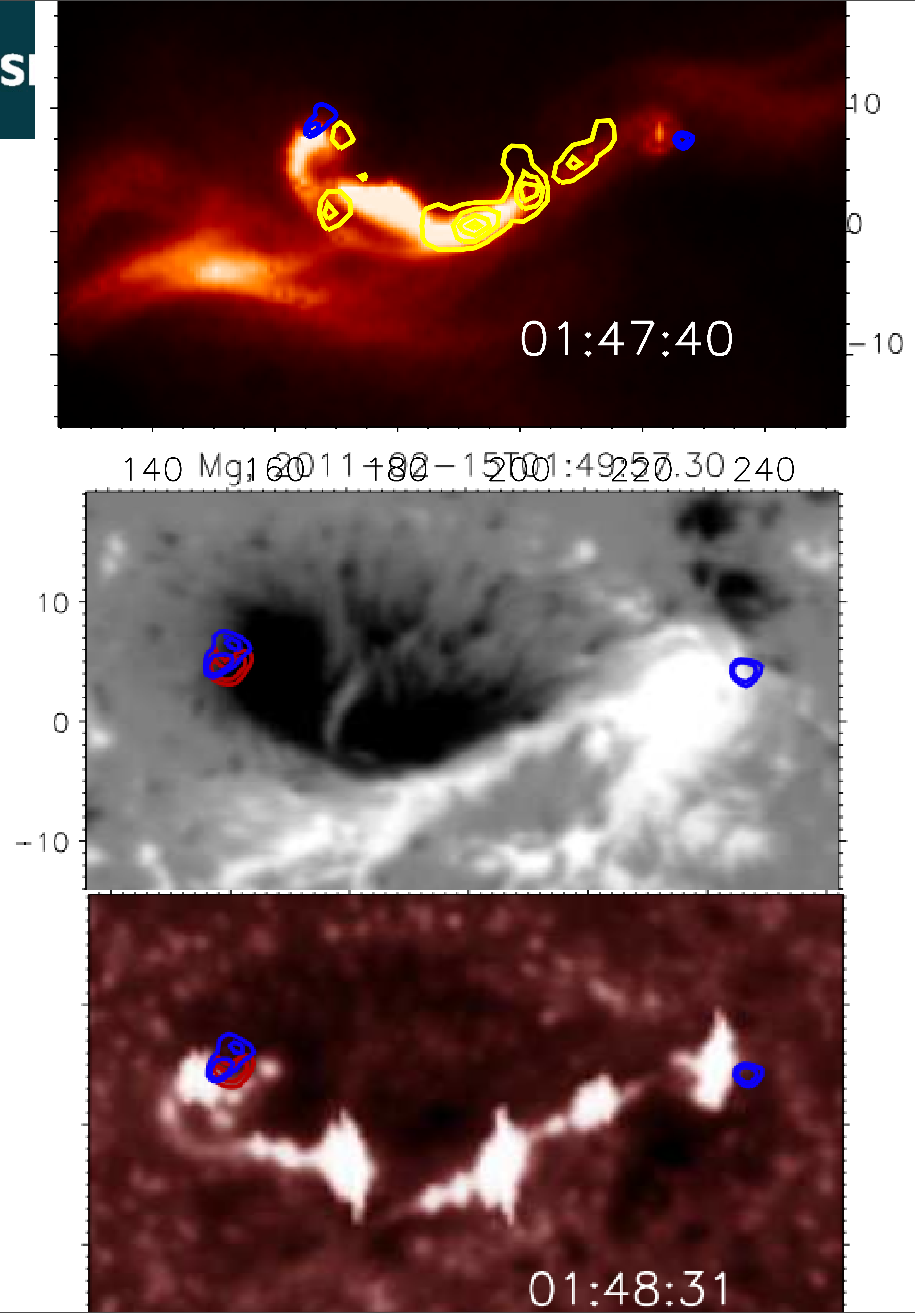

Zharkov et al., ApJL, 2011

THE UNIVERS

2011-02-15 SQ Sources

Shibata et al. 1995

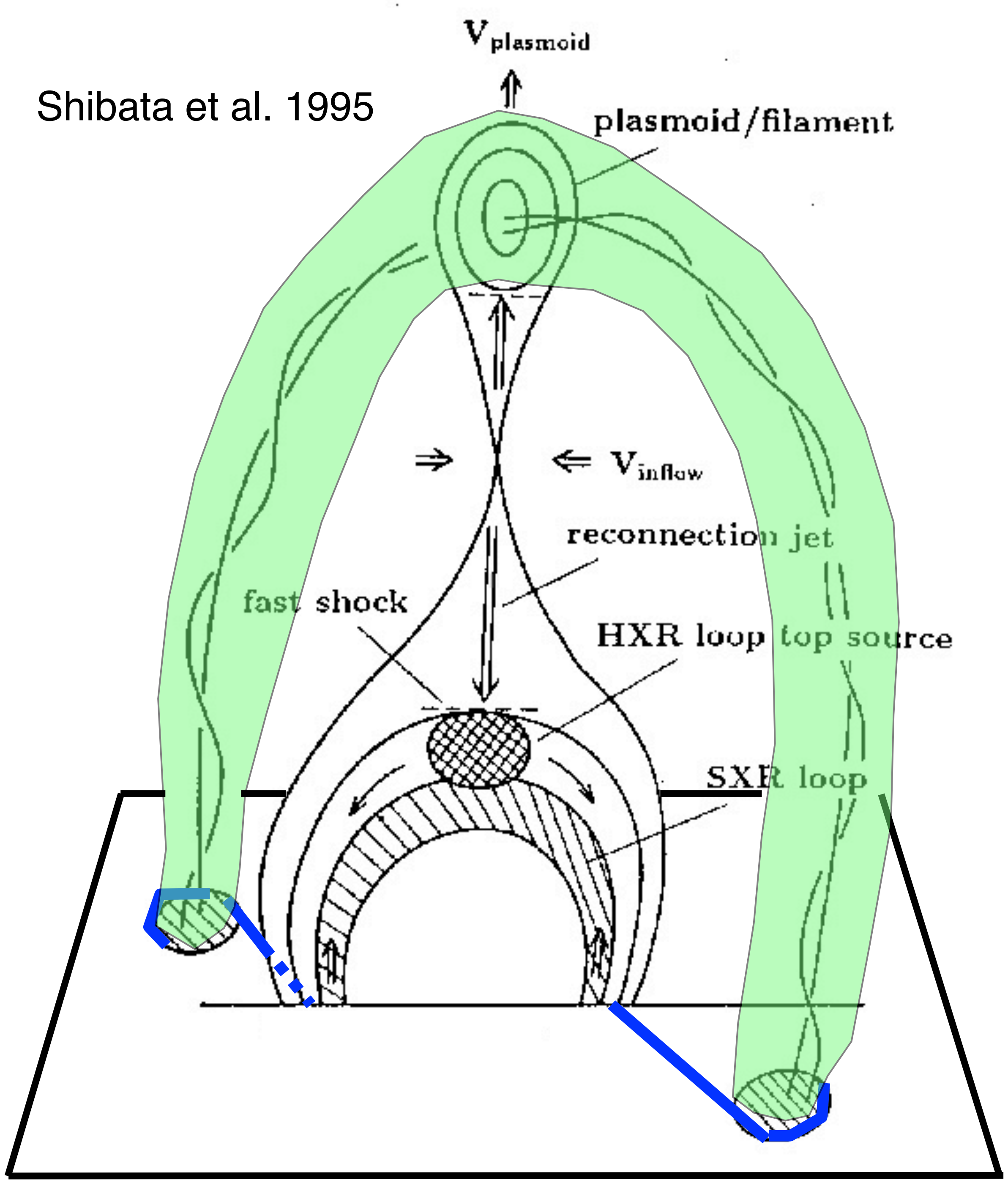

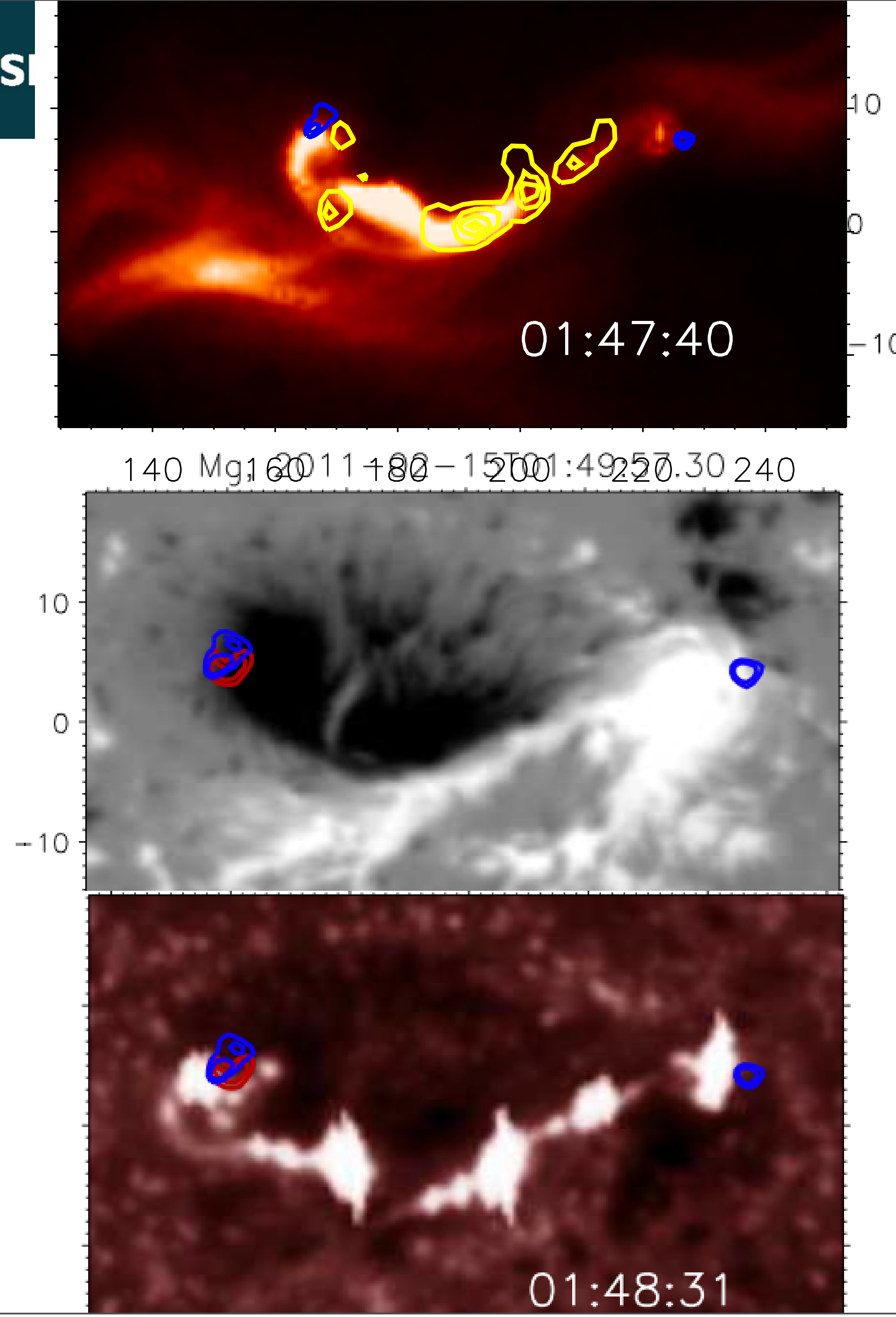

Zharkov et al., ApJL, 2011

Feb15: filament eruption

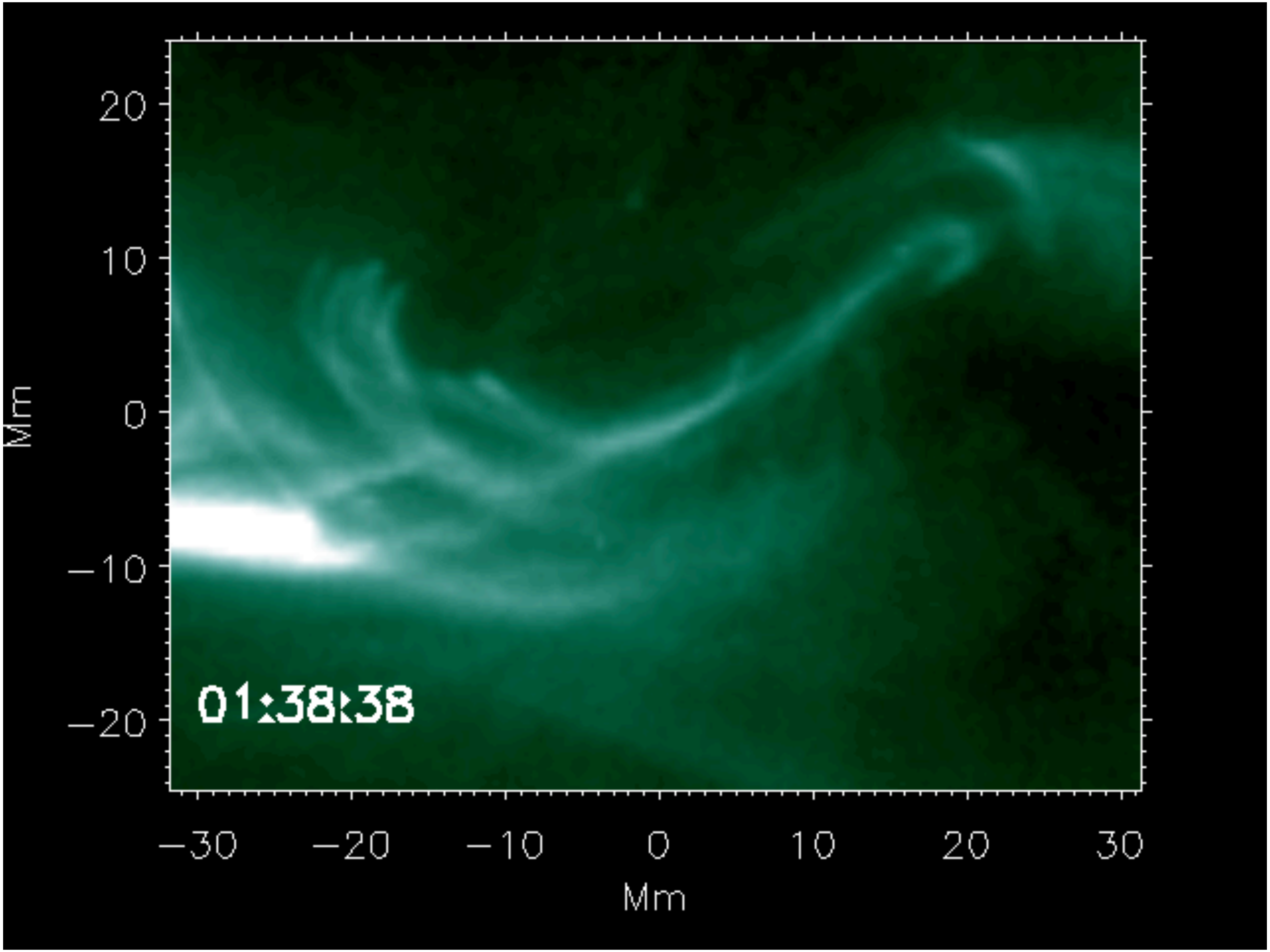

Feb15: filament eruption

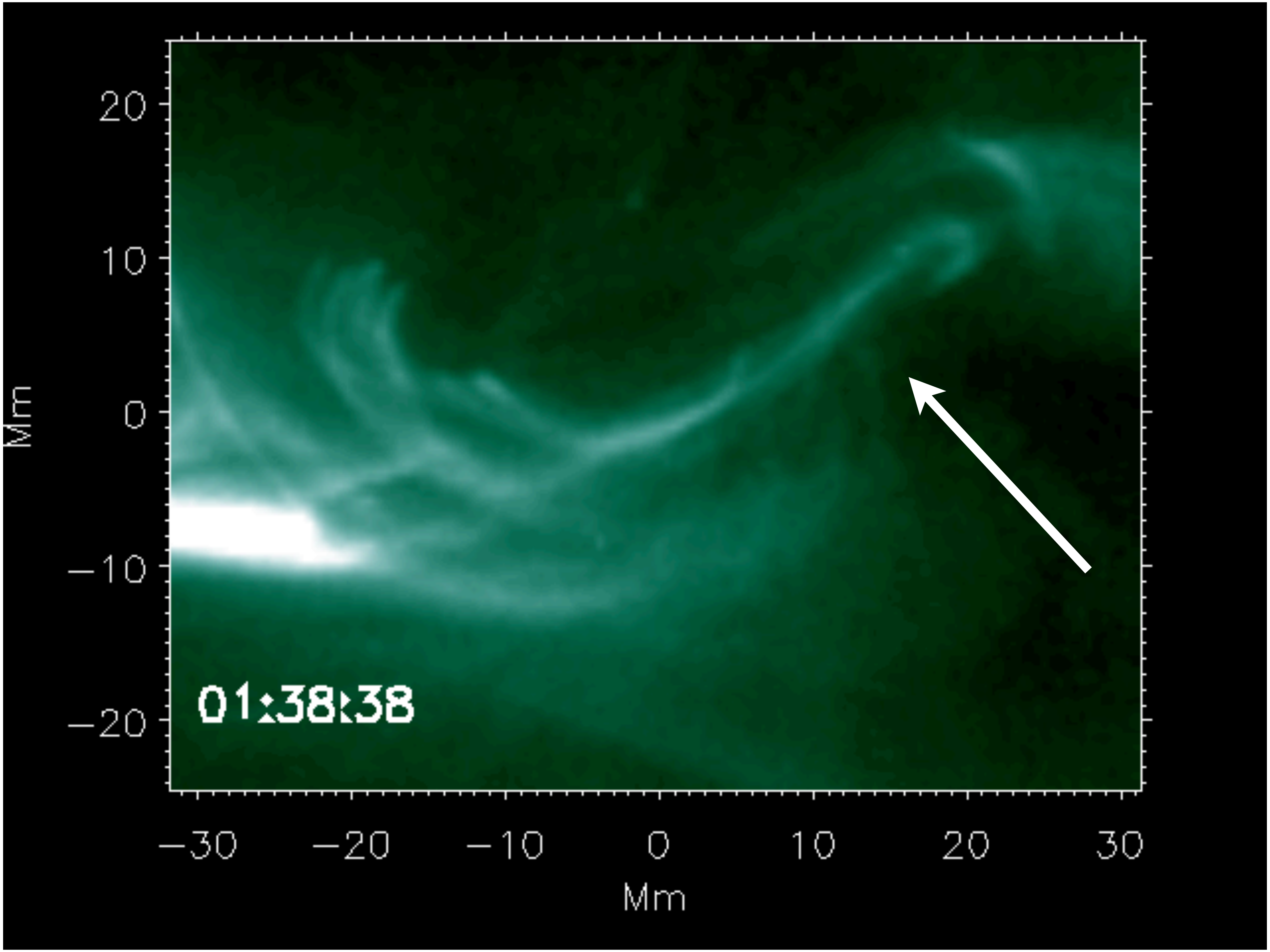

Feb15: filament eruption

Feb15: filament eruption

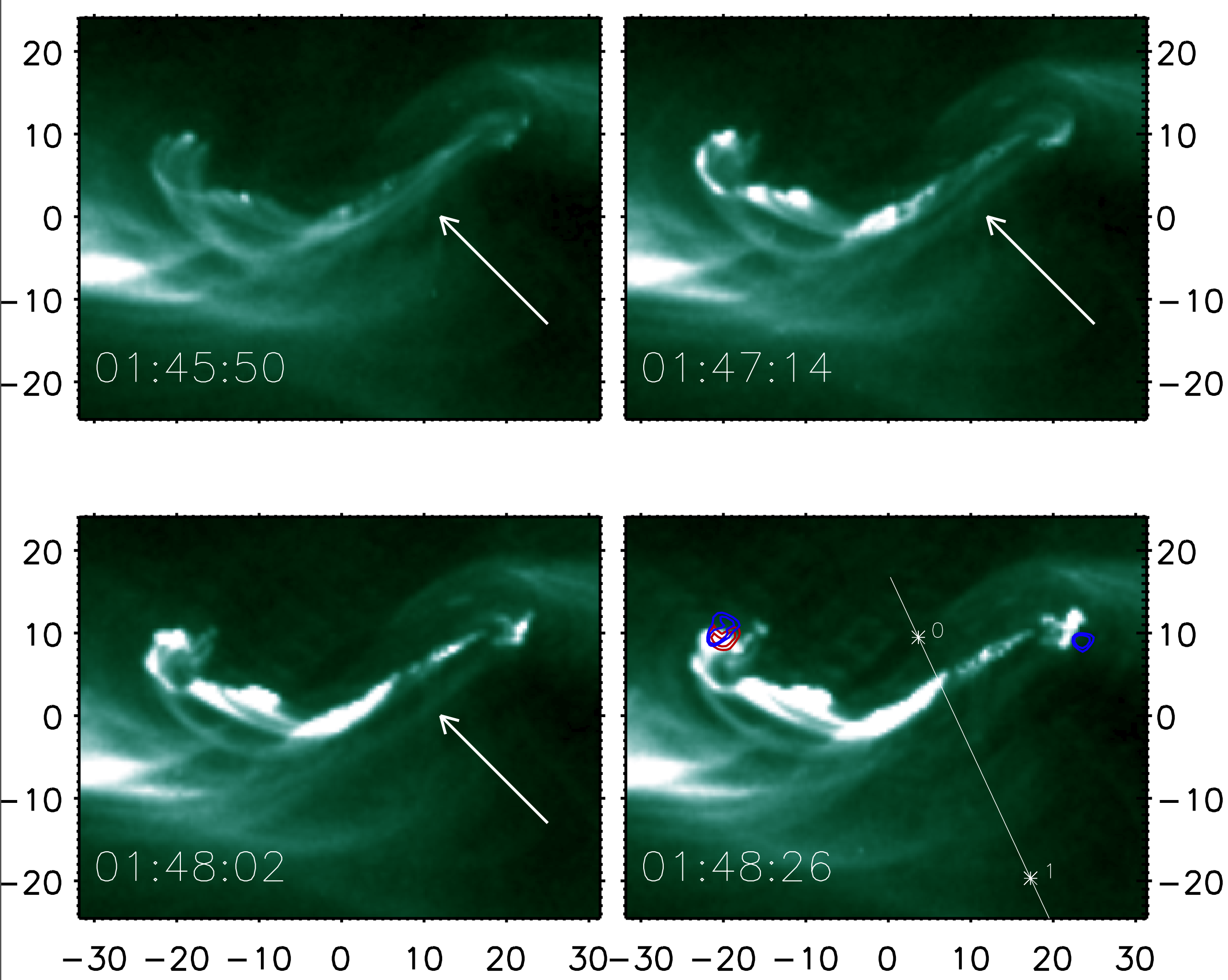

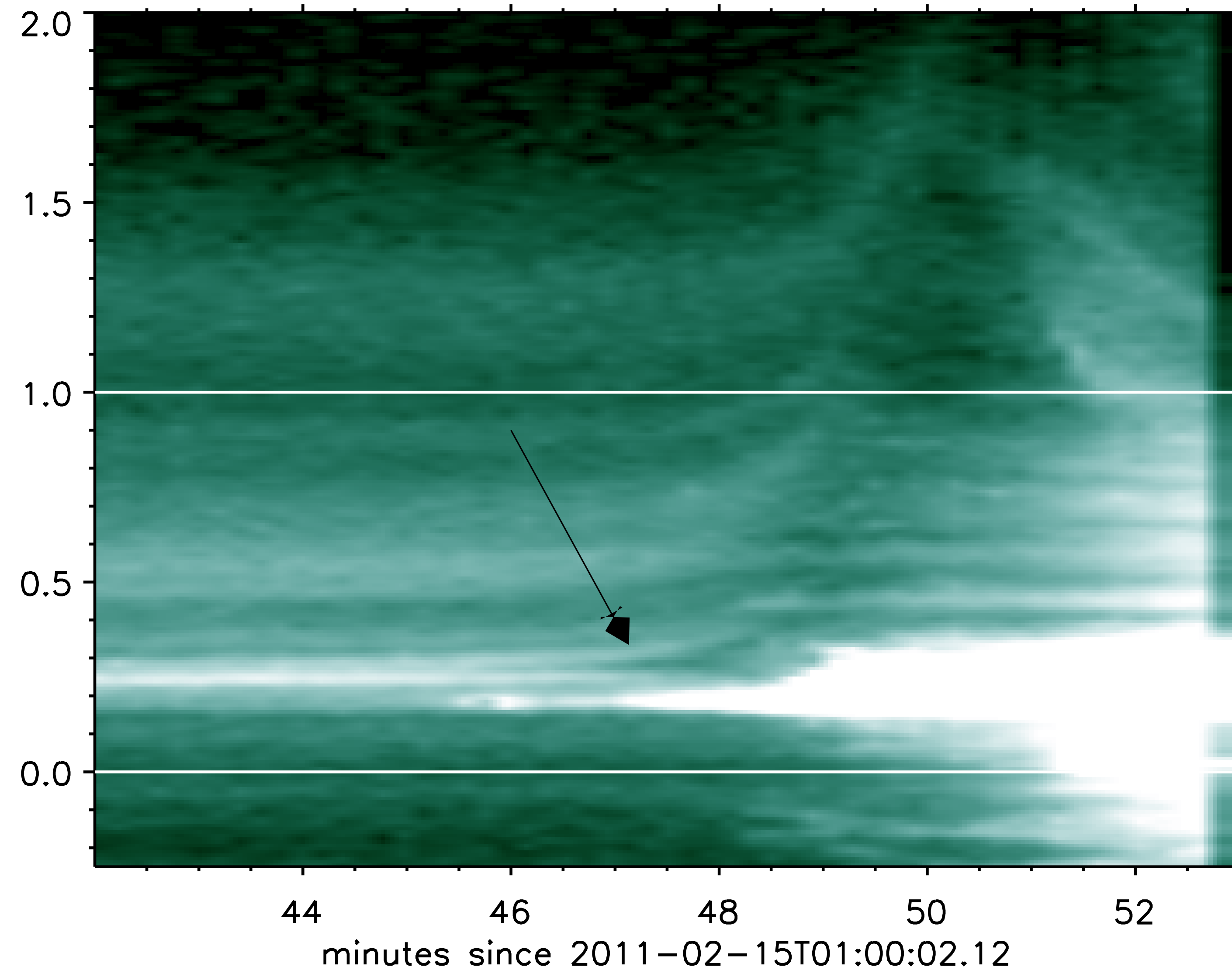

Cartoon description

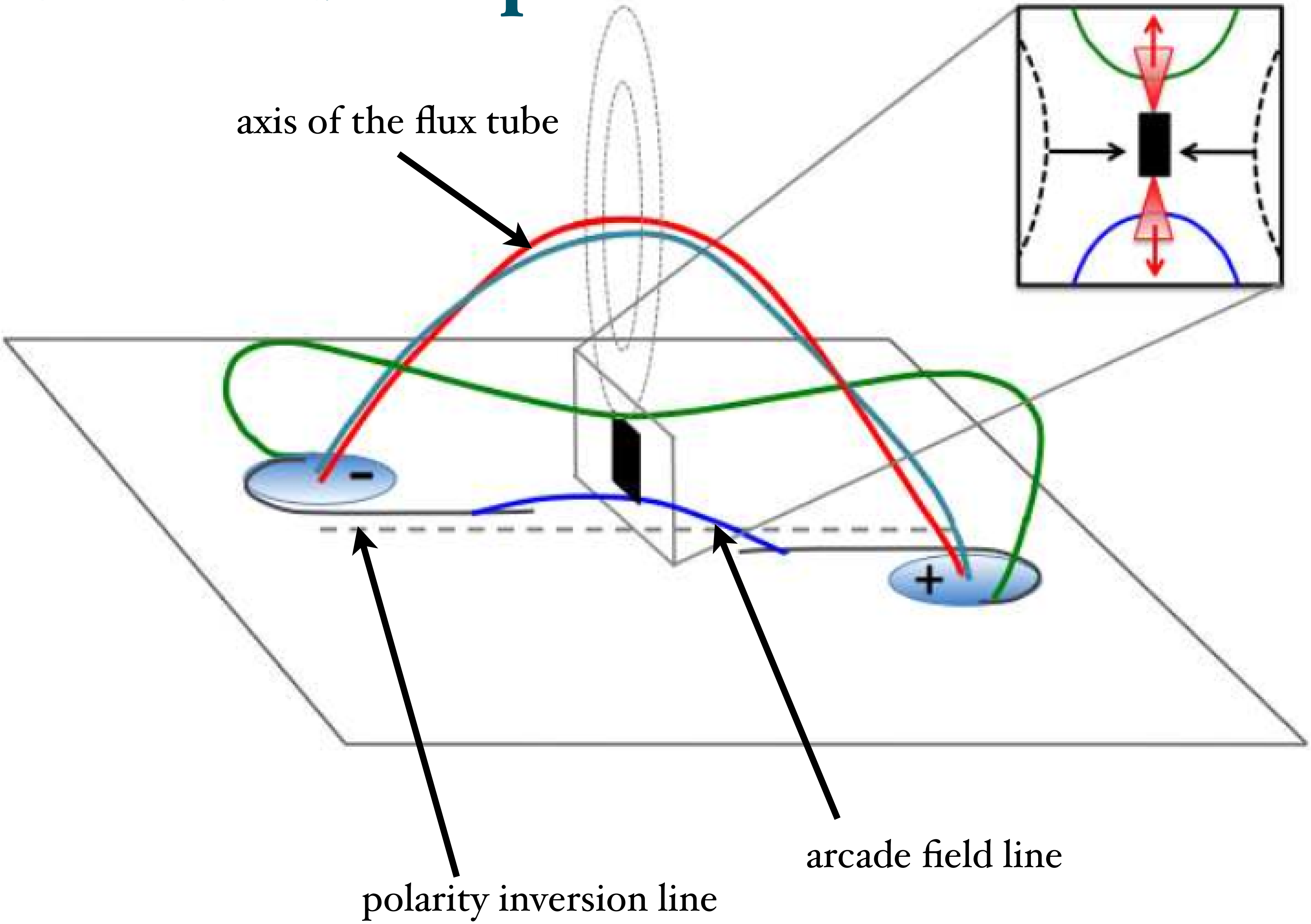

Cartoon description

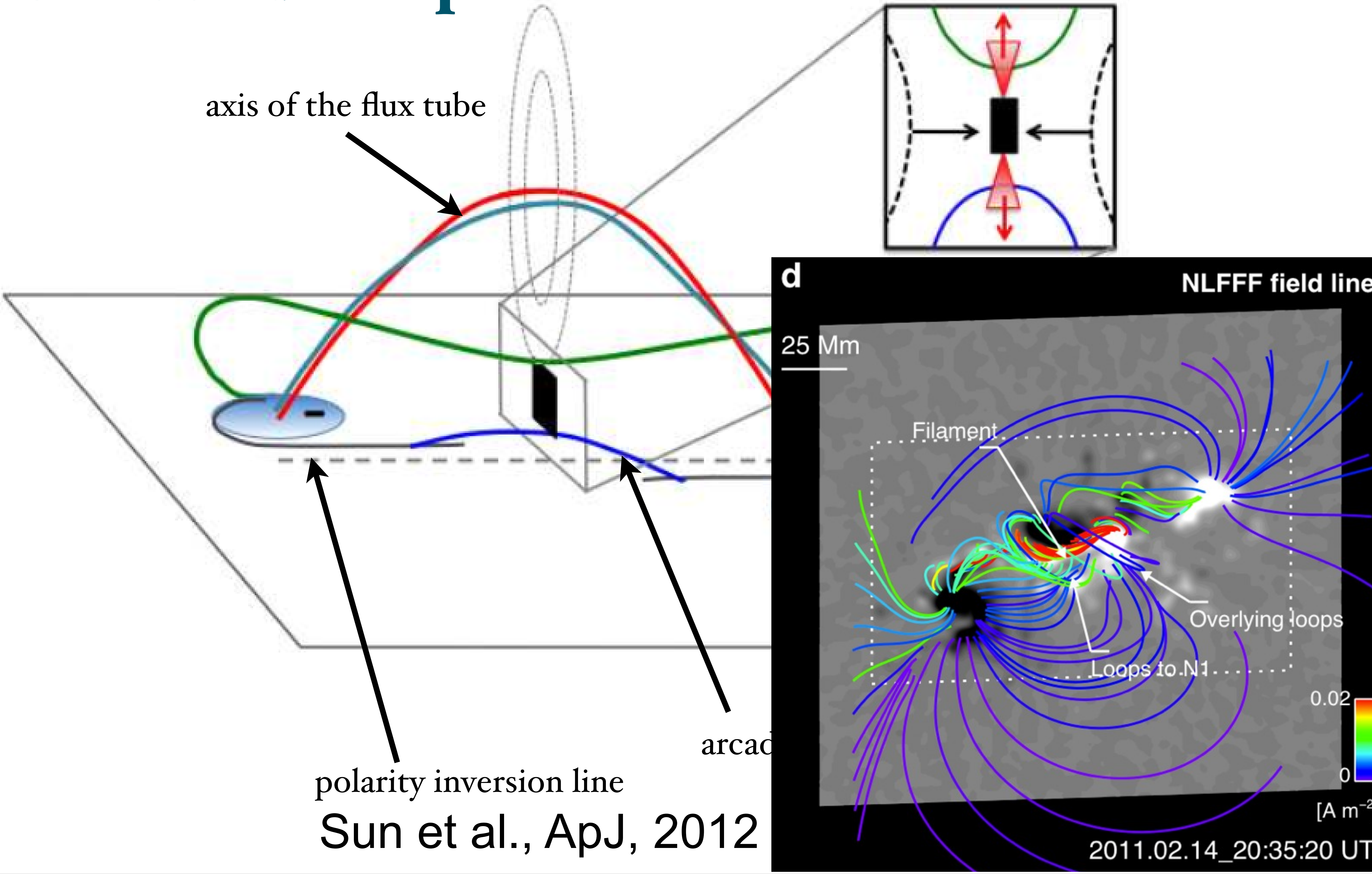

Sun et al., ApJ, 2012

Feb15 flare: HXR emission

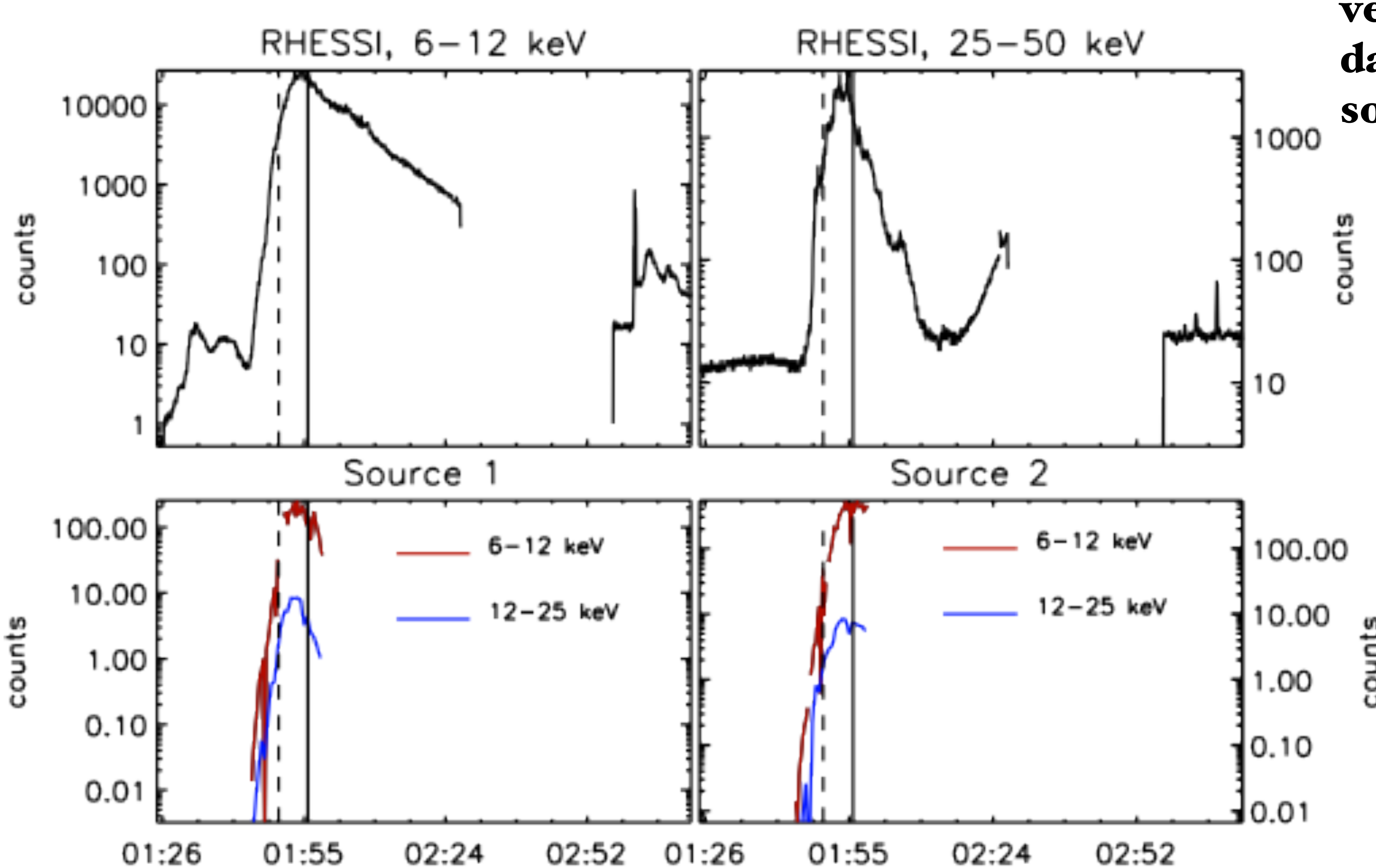

vertical lines
dashed: 01:50UT
solid: 01:56 UT

Feb15 flare: HXR emission

vertical lines
dashed: 01:50UT
solid: 01:56 UT

Feb15 flare: HXR emission

Alvarado-Gomez et al, 2012

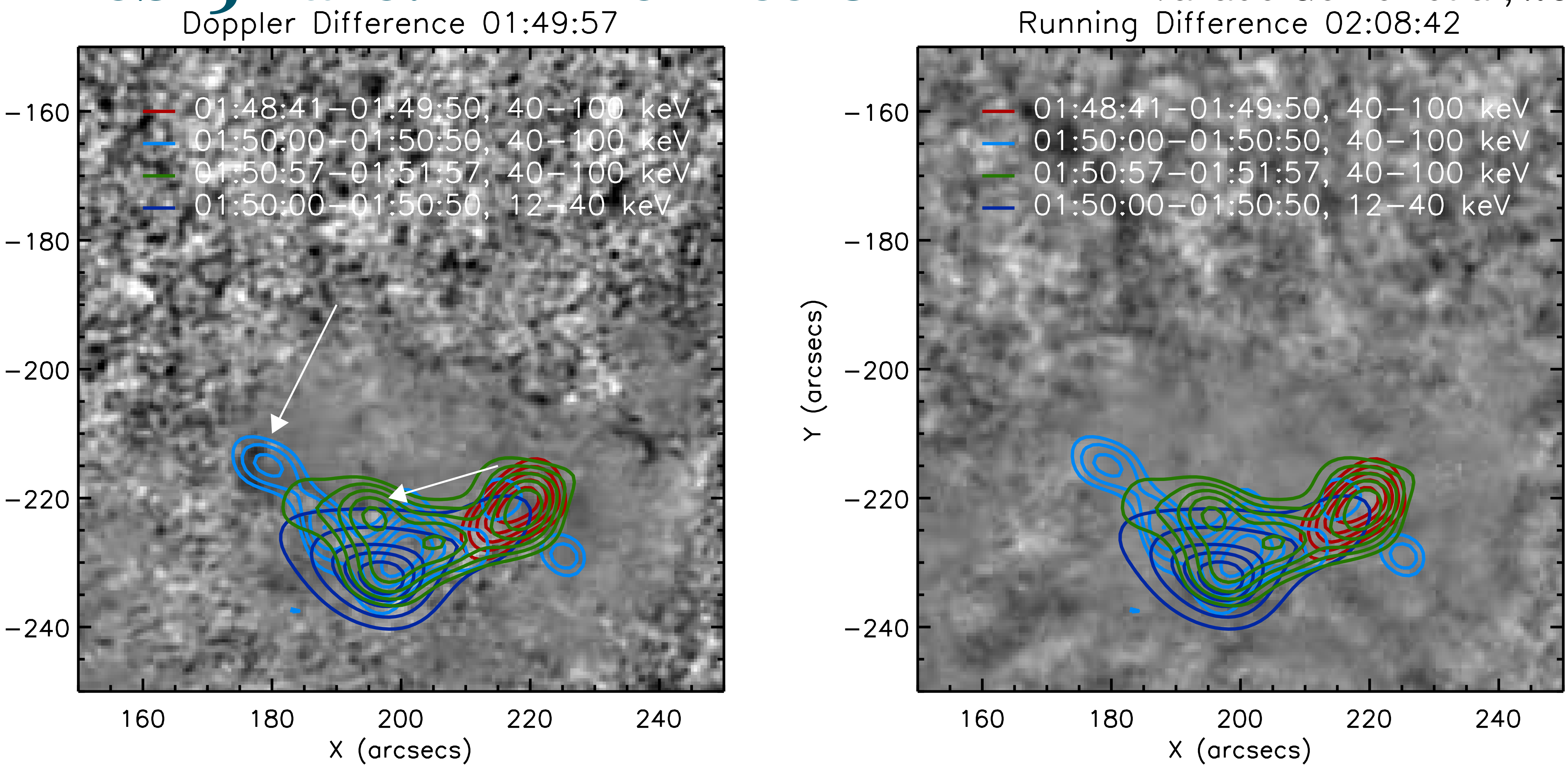

Feb15 flare: HXR emission

Alvarado-Gomez et al, 2012

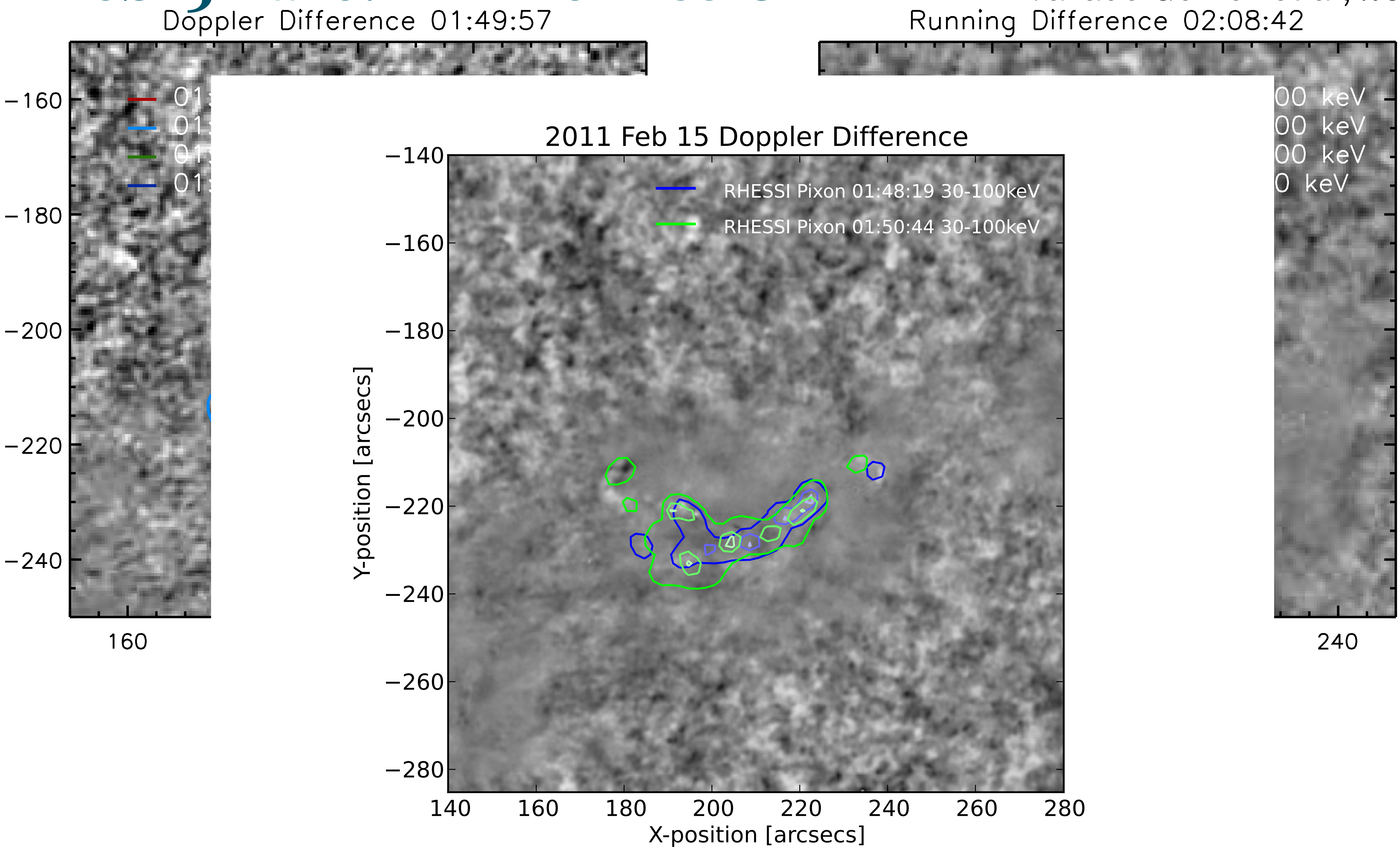

February quake: Variations at TD sources

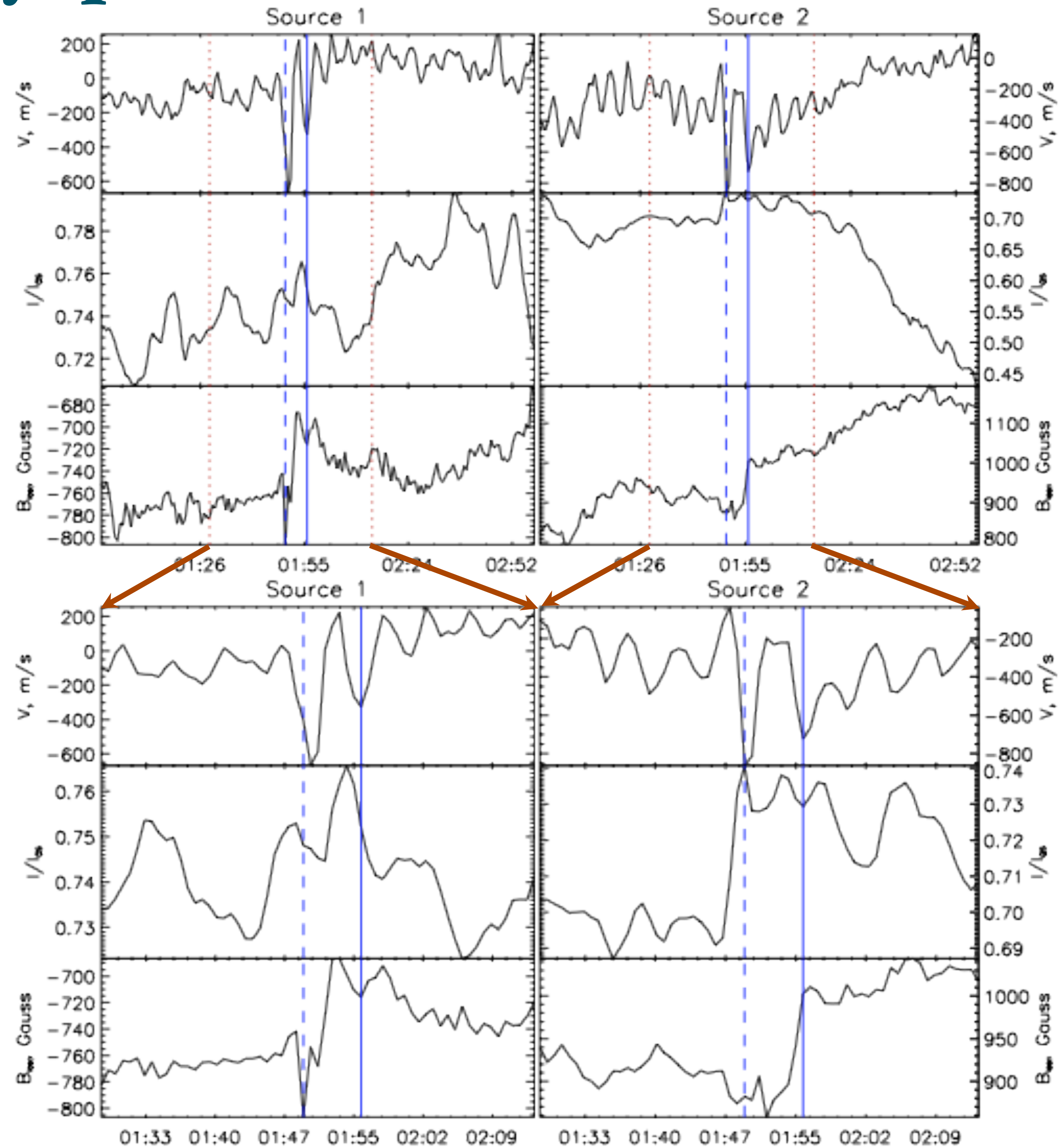

vertical lines,
dashed: 01:50UT
solid: 01:56 UT

February quake: Variations at TD sources

February quake: Variations at TD sources

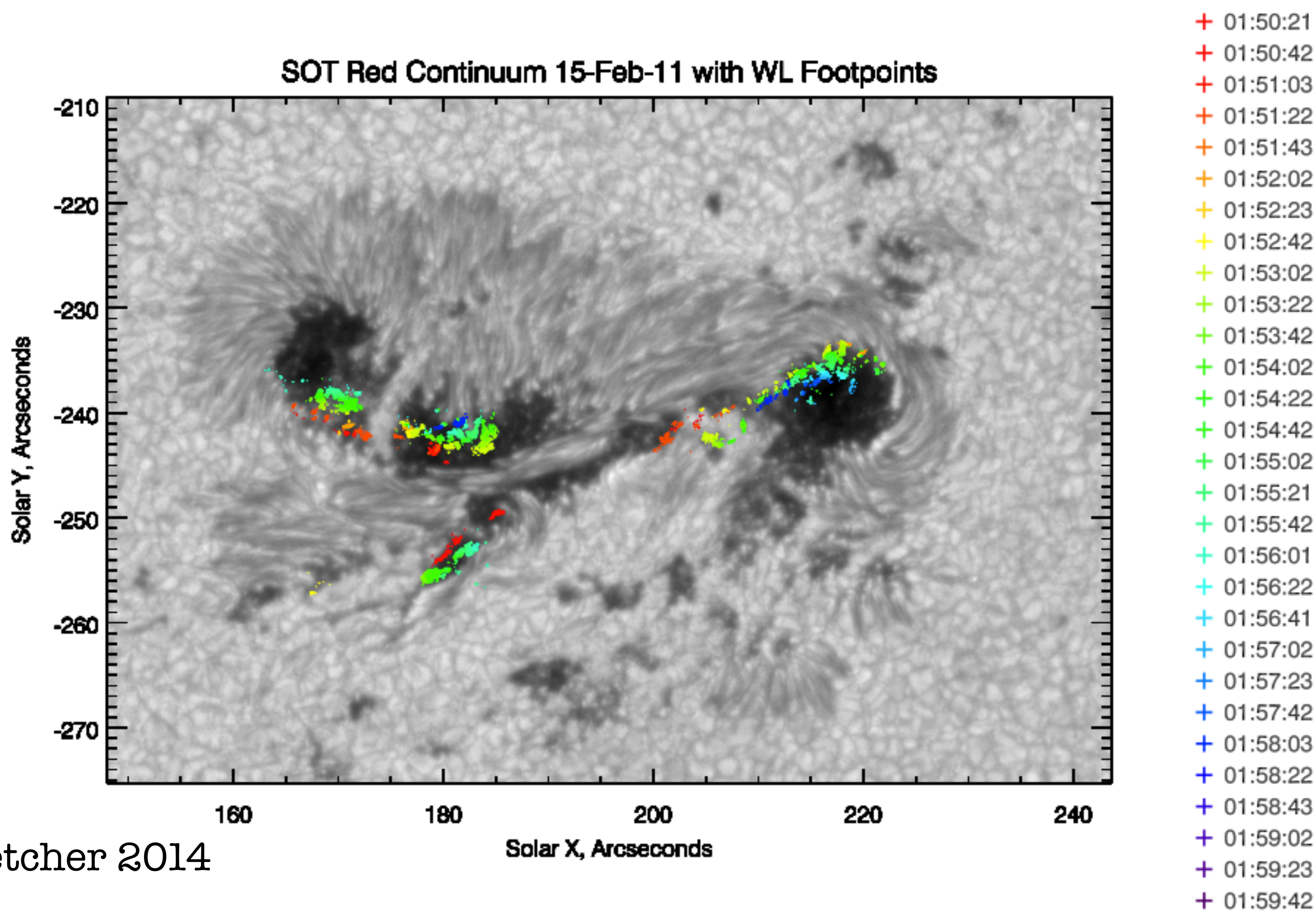

Kerr & Fletcher 2014

FIG. 4.— *White light flare footpoints overlaid on a red continuum image.*

velocity transients at SQ sources

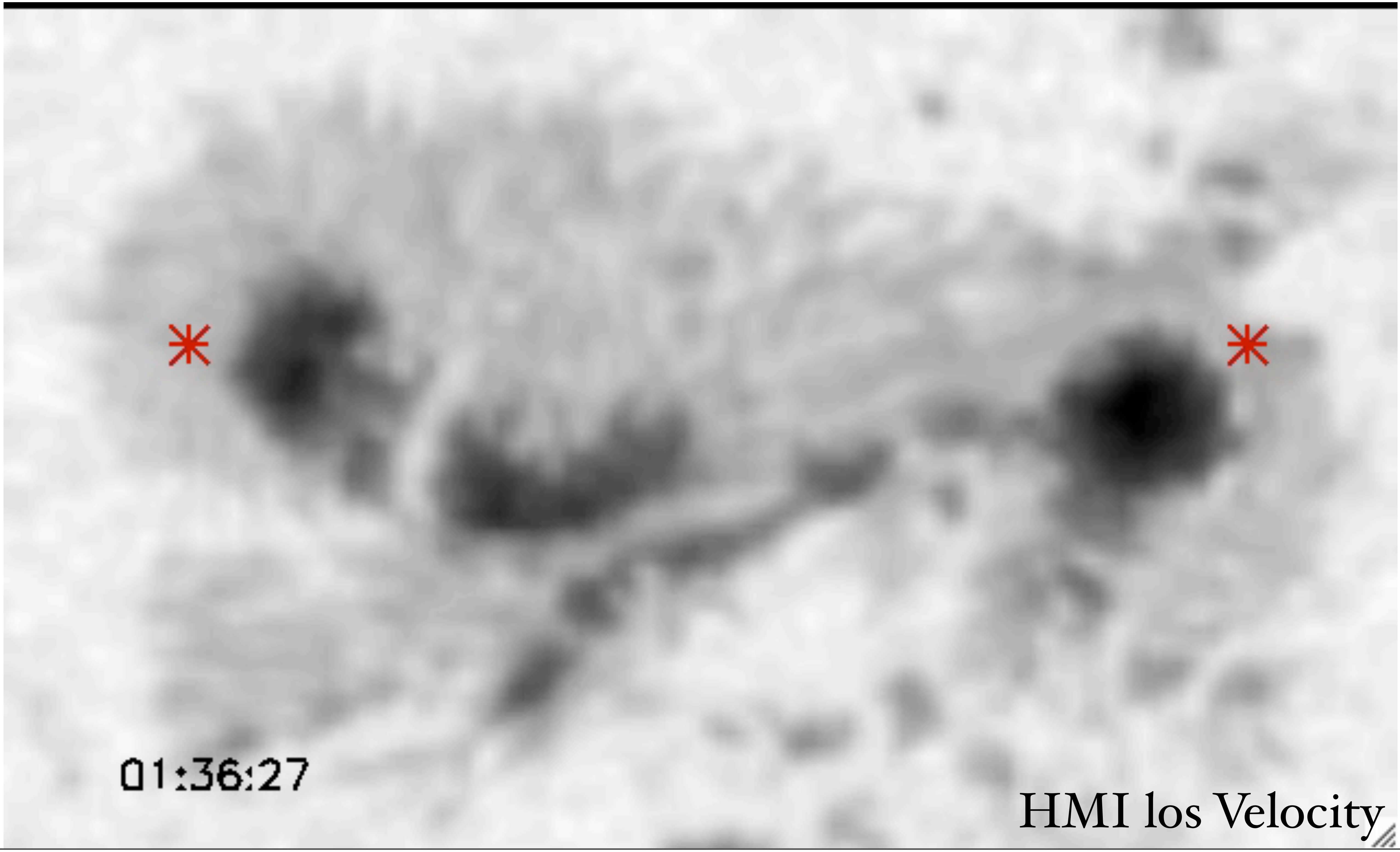

velocity transients at SQ sources

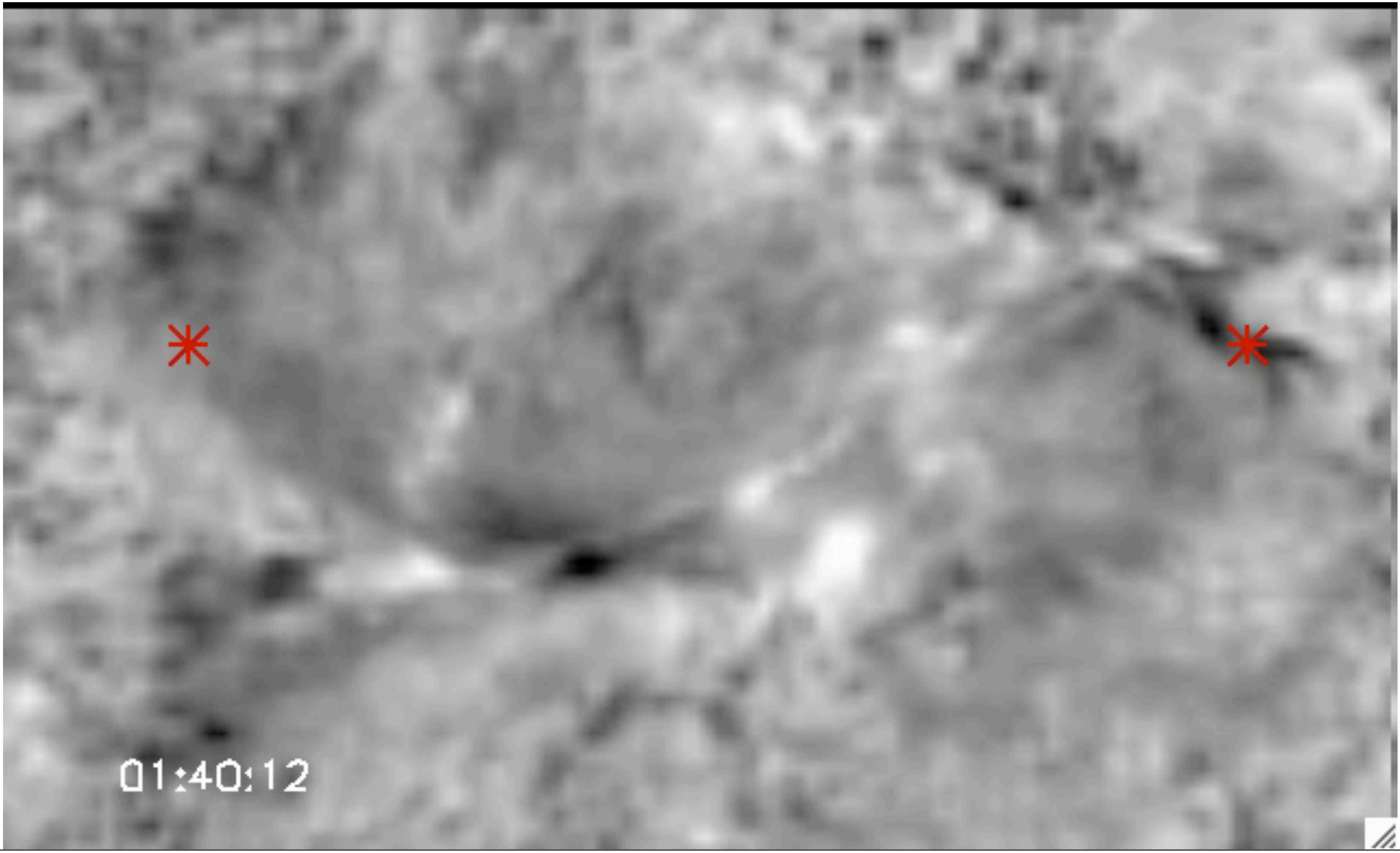

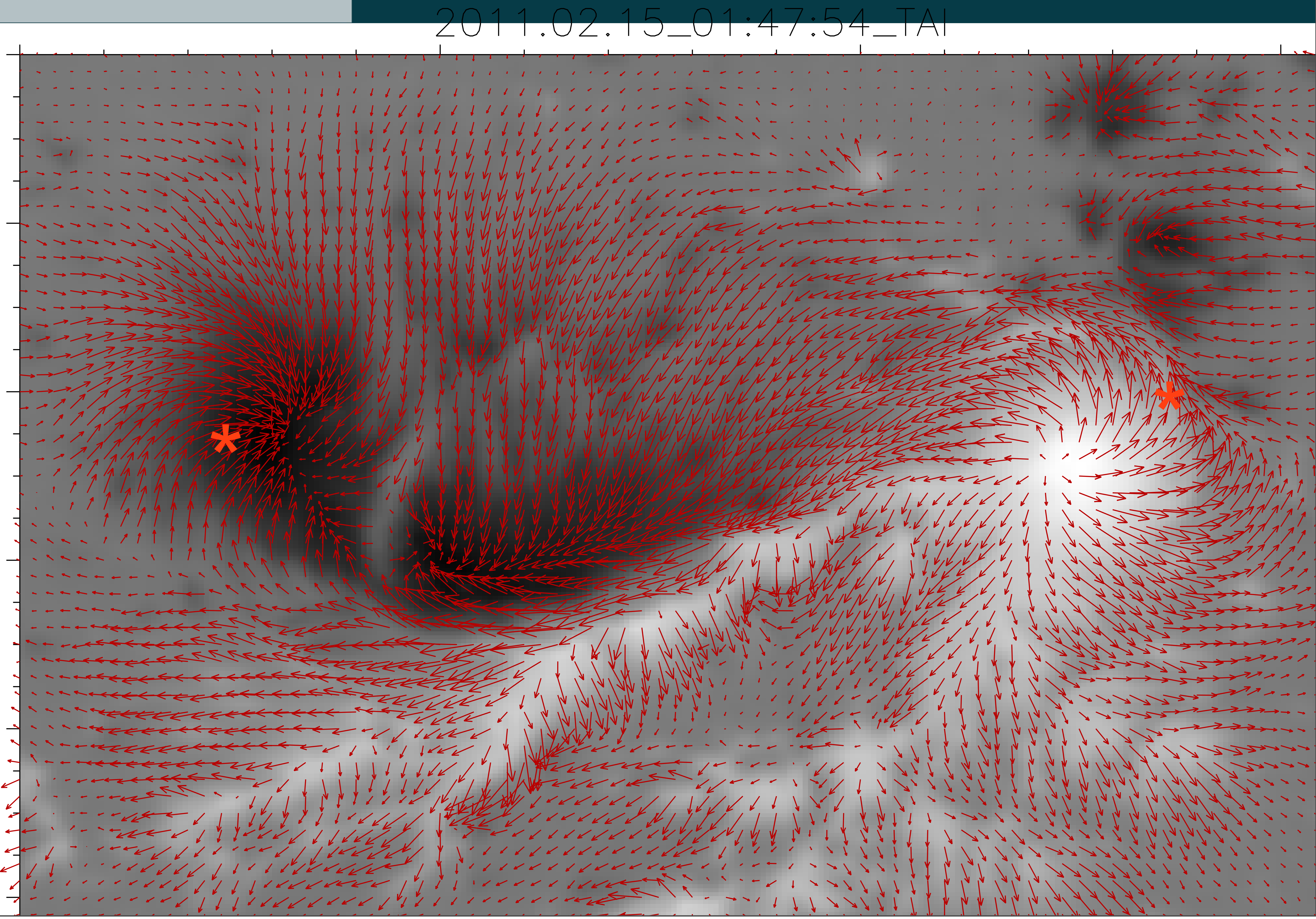
2011.02.15_01:47:54_TAI

February 15, 2011 - directional egression

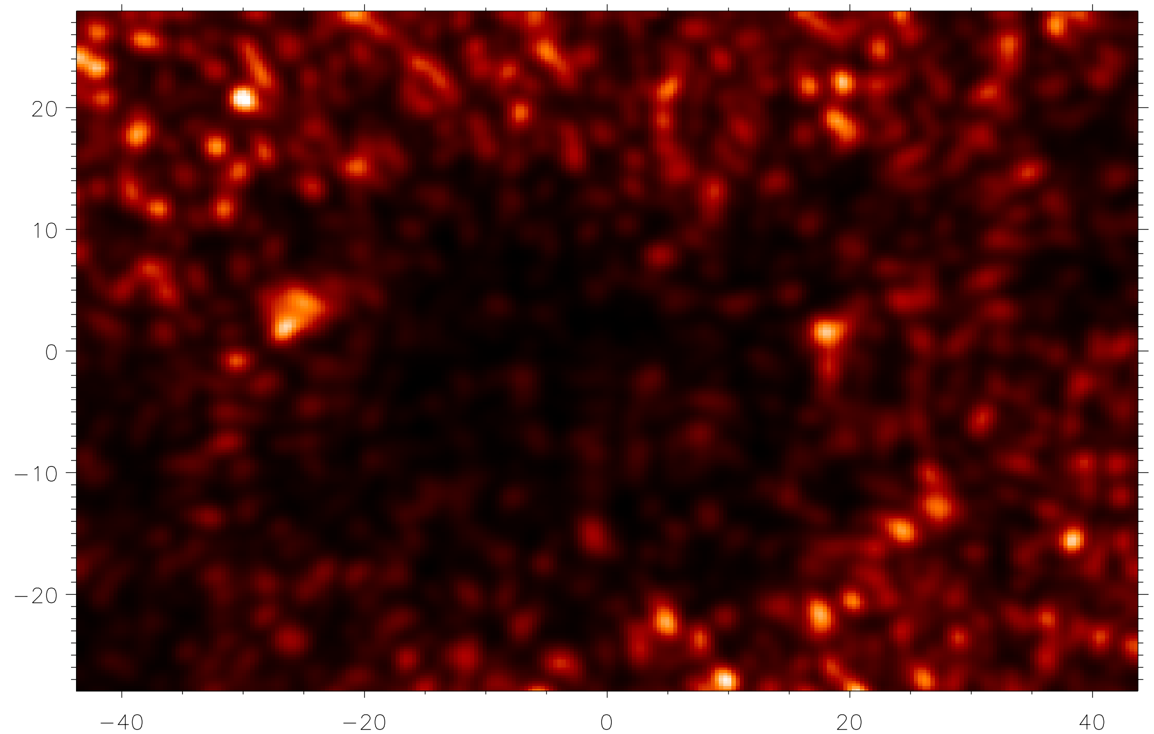

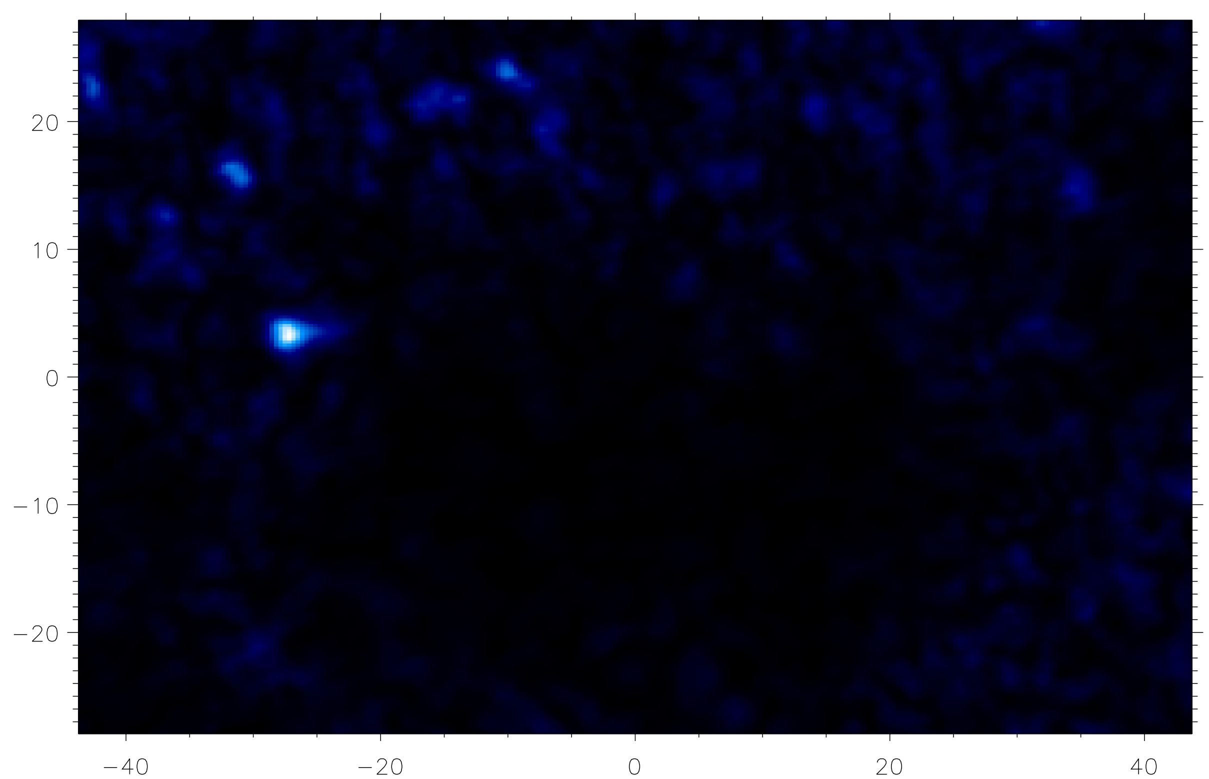

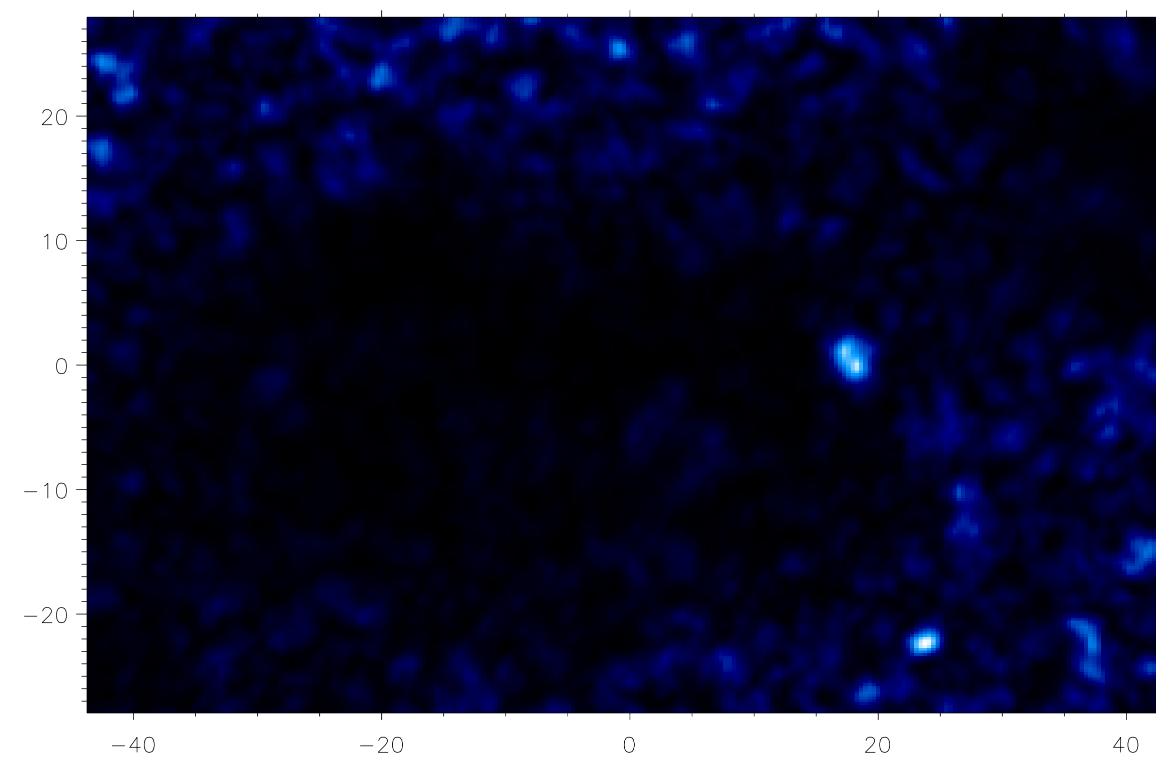

February 15, 2011 - directional egression

February 15, 2011 - directional egression

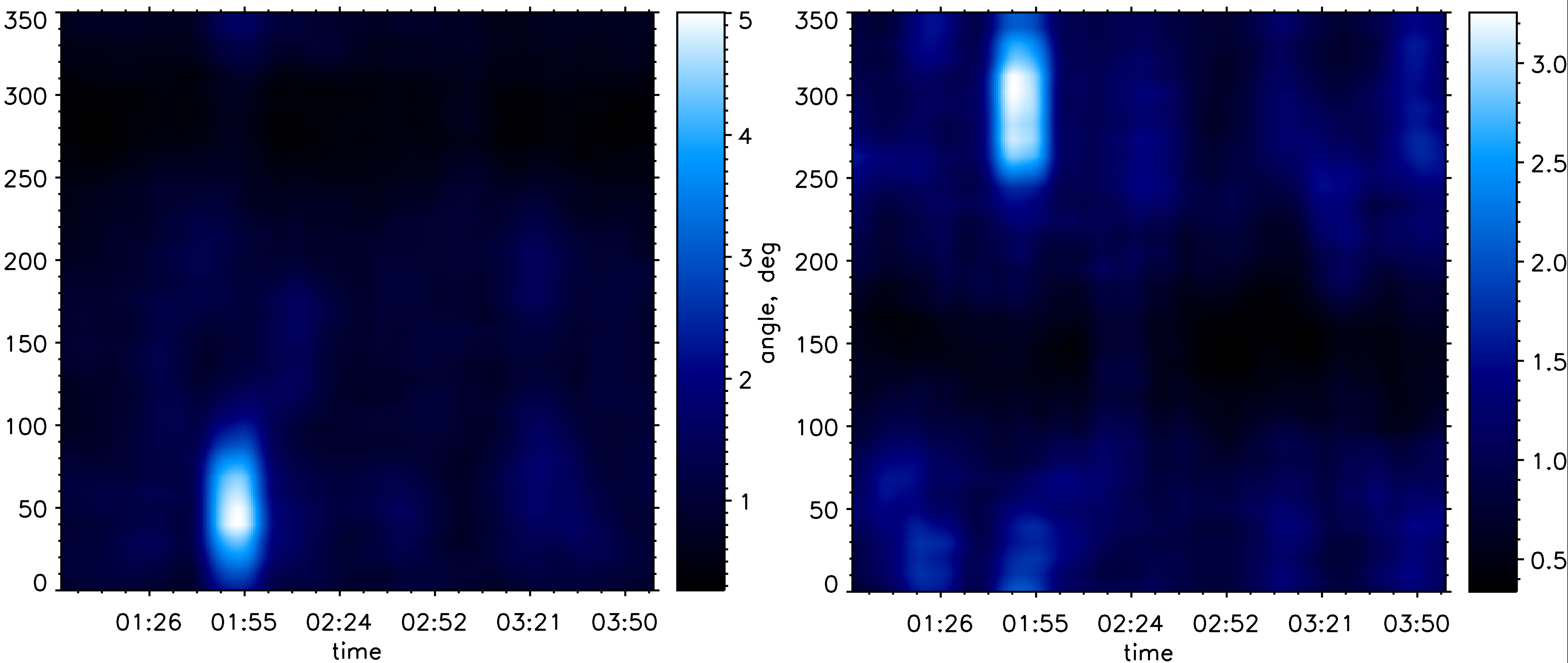

February 15, 2011 - directional egression

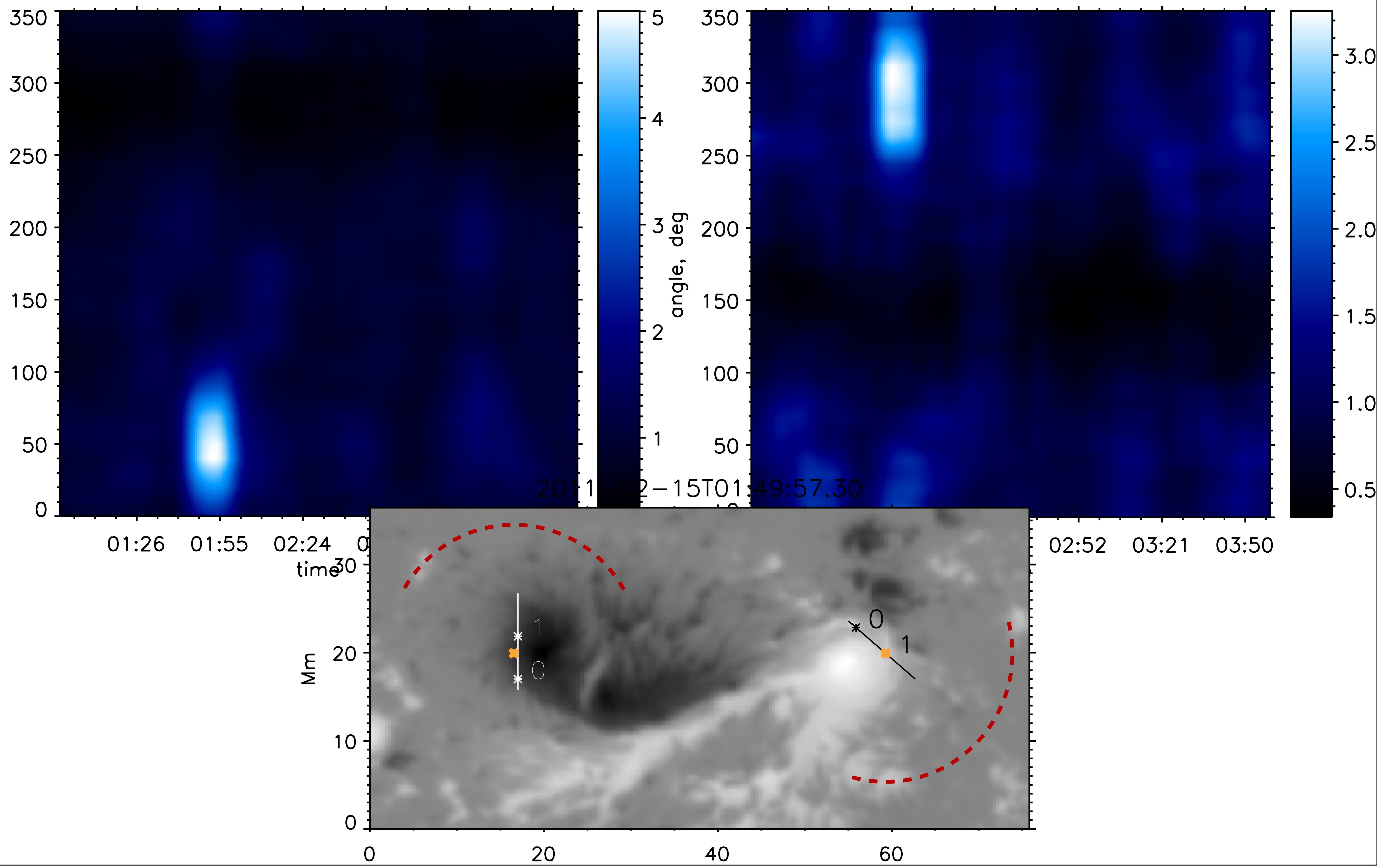

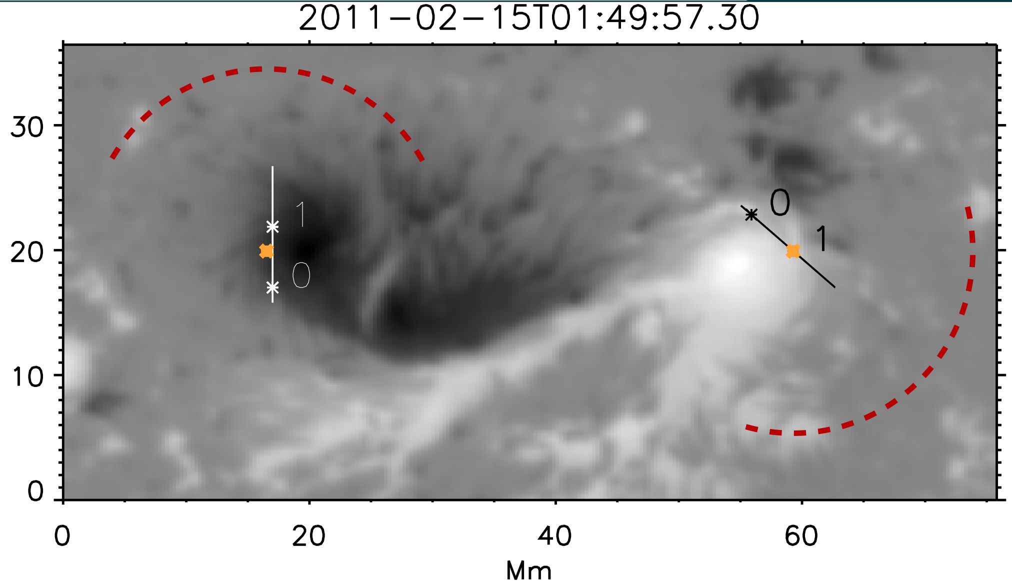

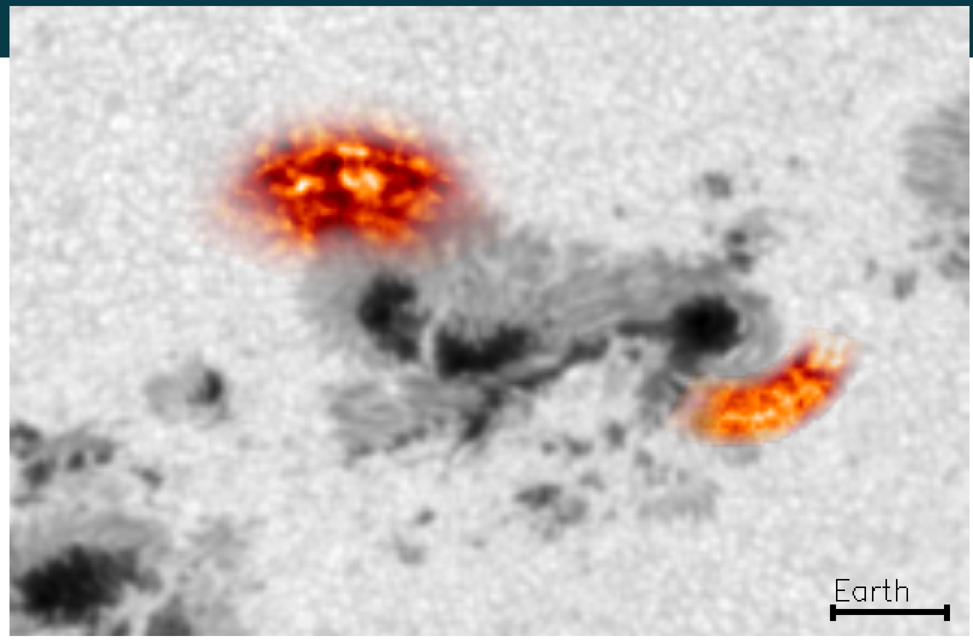

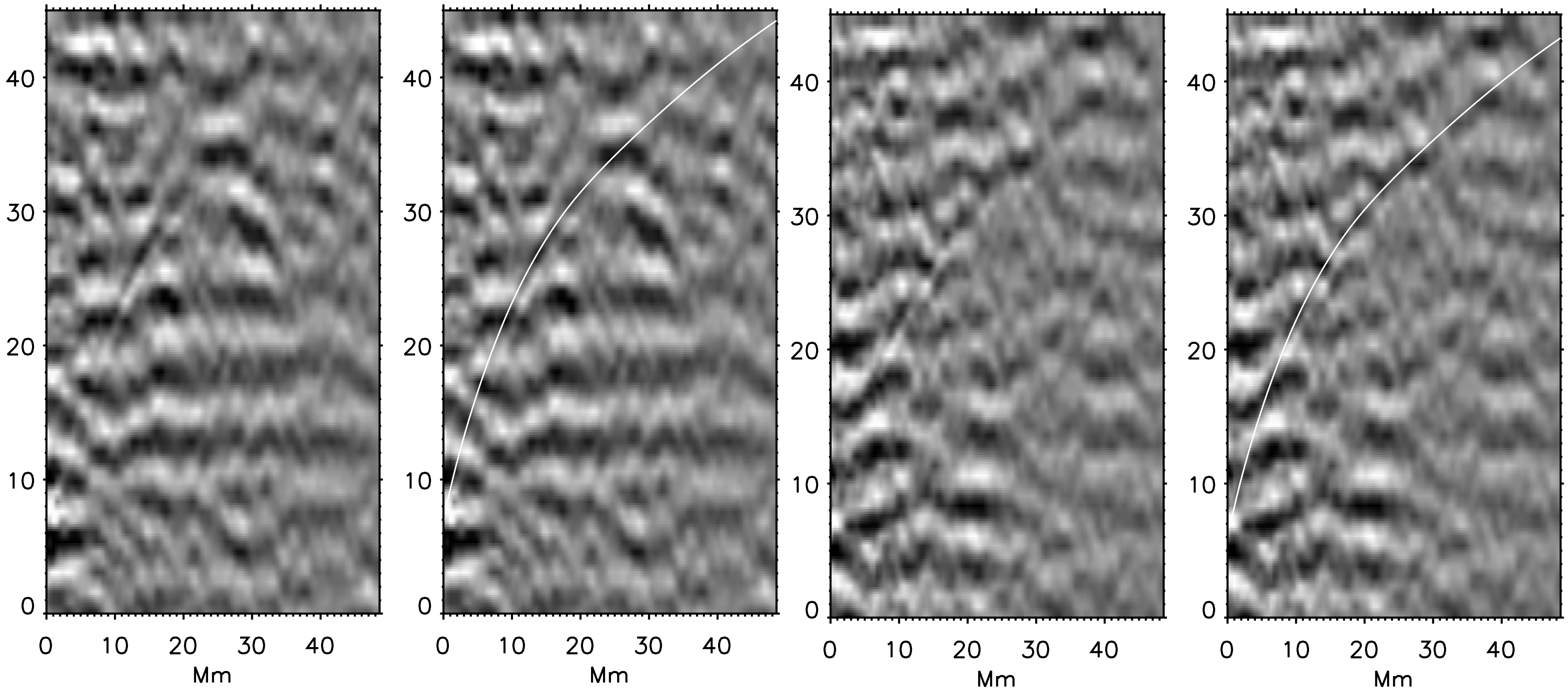

Estimated quake start-times:
S1: 01:50:15 \pm 45s
S2: 01:49:30 \pm 45s

Zharkov et al., SolPhys 2013

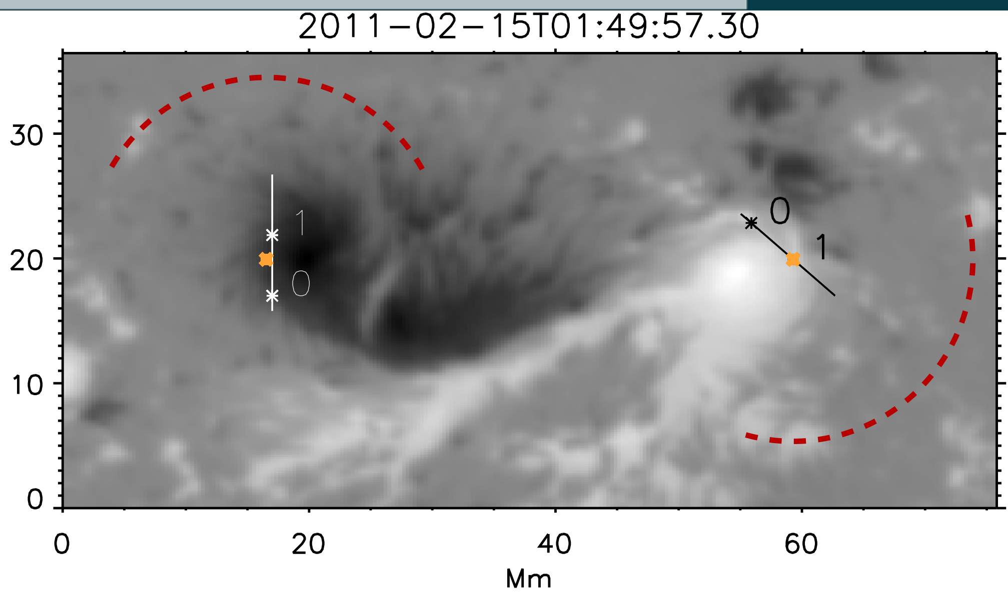

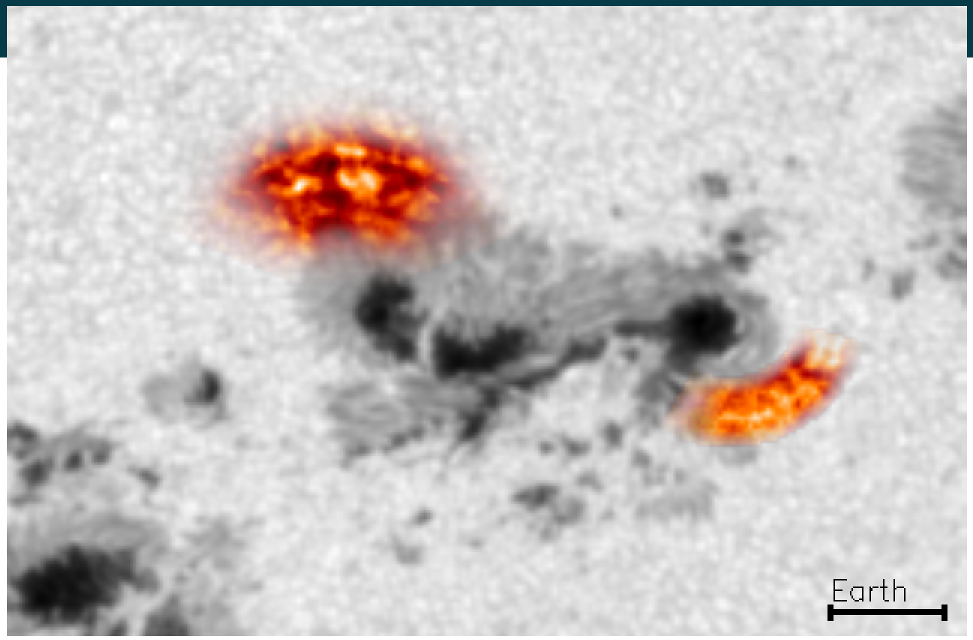

Zharkov et al., SolPhys 2013

Estimated quake start-times:
S1: 01:50:15 \pm 45s
S2: 01:49:30 \pm 45s

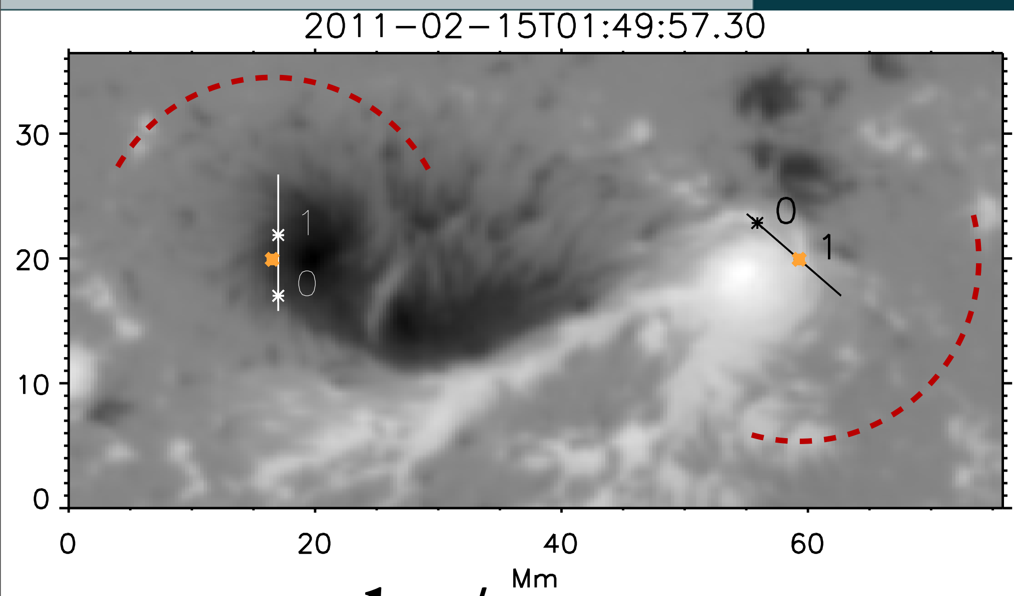

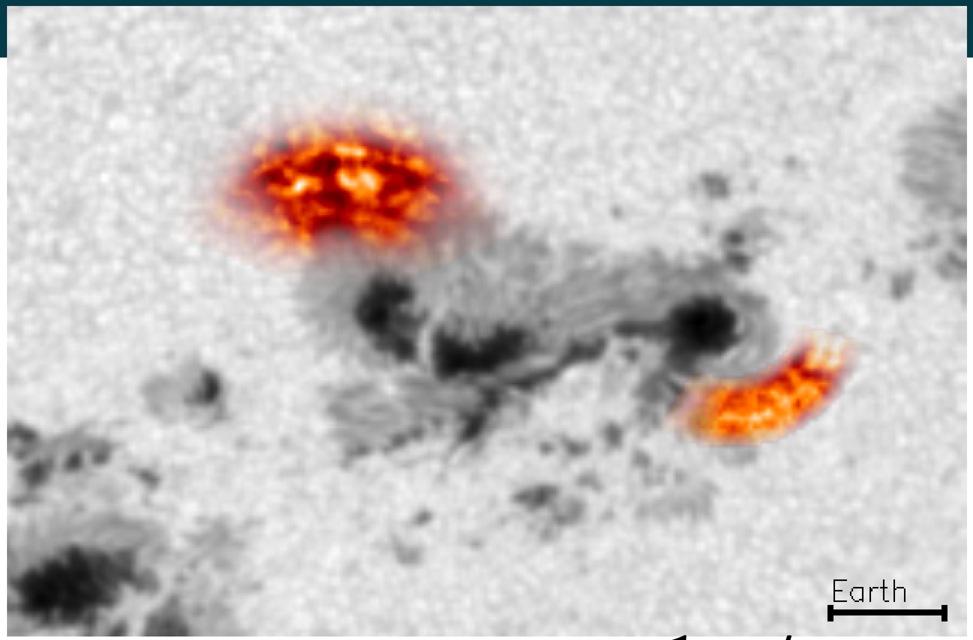

13 - 25 km/s

14 - 22 km/s

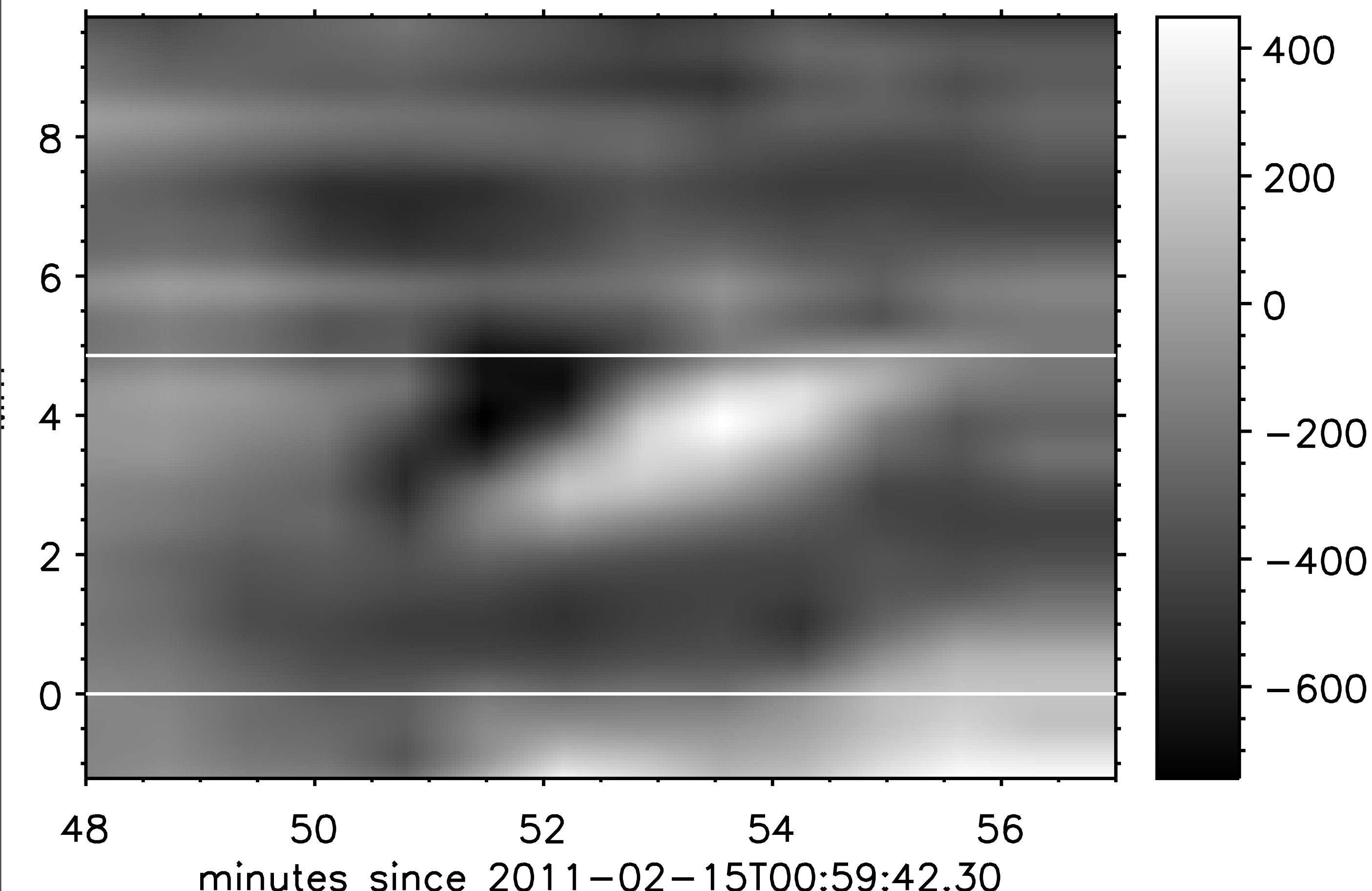

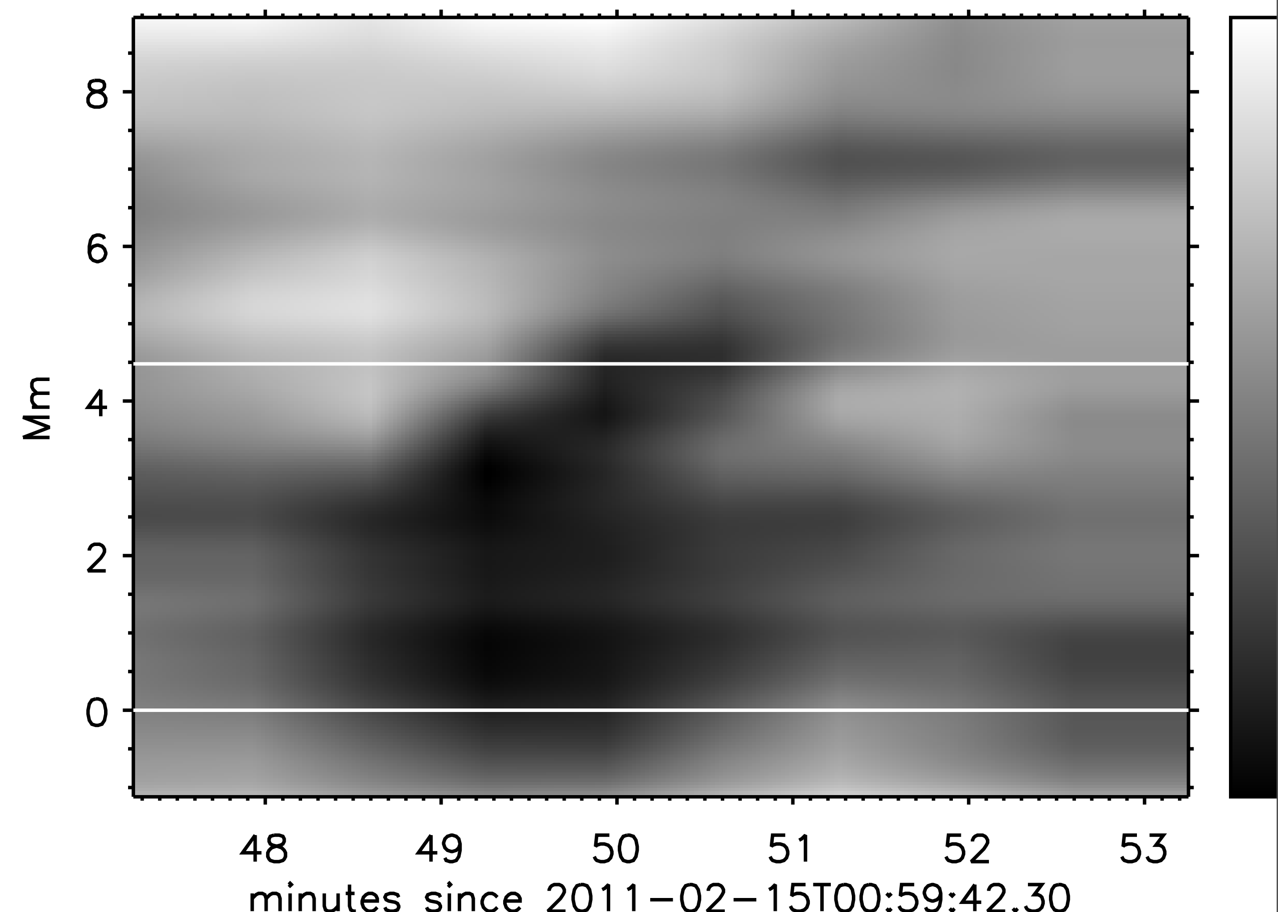

Estimated quake start-times:
S1: 01:50:15 \pm 45s
S2: 01:49:30 \pm 45s

Zharkov et al., SolPhys 2013

moving source

initial conditions can incorporate moving spherical source:

$$\mathbf{x}_s = \mathbf{x}_s(t)$$

$$\mathbf{v} = \frac{d\mathbf{x}_s}{dt}$$

$$\omega_0 = \omega_f + \mathbf{k}_0 \cdot \mathbf{v}$$

moving source

initial conditions can incorporate moving spherical source:

$$\mathbf{x}_s = \mathbf{x}_s(t)$$

$$\mathbf{v} = \frac{d\mathbf{x}_s}{dt}$$

$$\omega_0 = \omega_f + \mathbf{k}_0 \cdot \mathbf{v}$$

supersonic source?

$\varphi_0(\theta, \phi, t_0) = 0$. This corresponds to the wave-field on initial surface simply written as $\Psi_0 = A_0(\theta, \phi, t_0)$, meaning that the pressure perturbation, $\rho^{\frac{1}{2}}\delta p$, is varying slowly on the initial surface. As in previous Section 5.2, $\frac{\partial \varphi_0}{\partial \theta} = 0$, $k_{z0} = k_{h0} \tan\theta$, system (3.4) leads to the following solution:

$$\begin{cases} k_0^2 = \dfrac{\omega_{ac}^2}{v^2\cos^2\gamma - c^2}, & (5.4) \\ \omega_0 = \mathbf{k}_0.\mathbf{v} = k_0 v \cos\gamma, & (5.5) \\ k_{h0} = k_0\cos\theta, \quad k_{z0} = k_0 \sin\theta, & (5.6) \end{cases}$$

where $\mathbf{k}_0$ is the wavevector, $\mathbf{v}$ is source velocity, $v = |\mathbf{v}|$, and γ is the angle between the two vectors. From the above it follows that non-evanescent acoustic waves ($k_0^2 > 0$) are generated if and only if the source moves with supersonic speed $v^2 > c^2$. Moreover, let us rewrite (5.5) as

$$\omega_0 = \omega_{ac}\frac{\cos\gamma}{\sqrt{\cos^2\gamma - \frac{c^2}{v^2}}}, \qquad (5.7)$$

supersonic source 2d

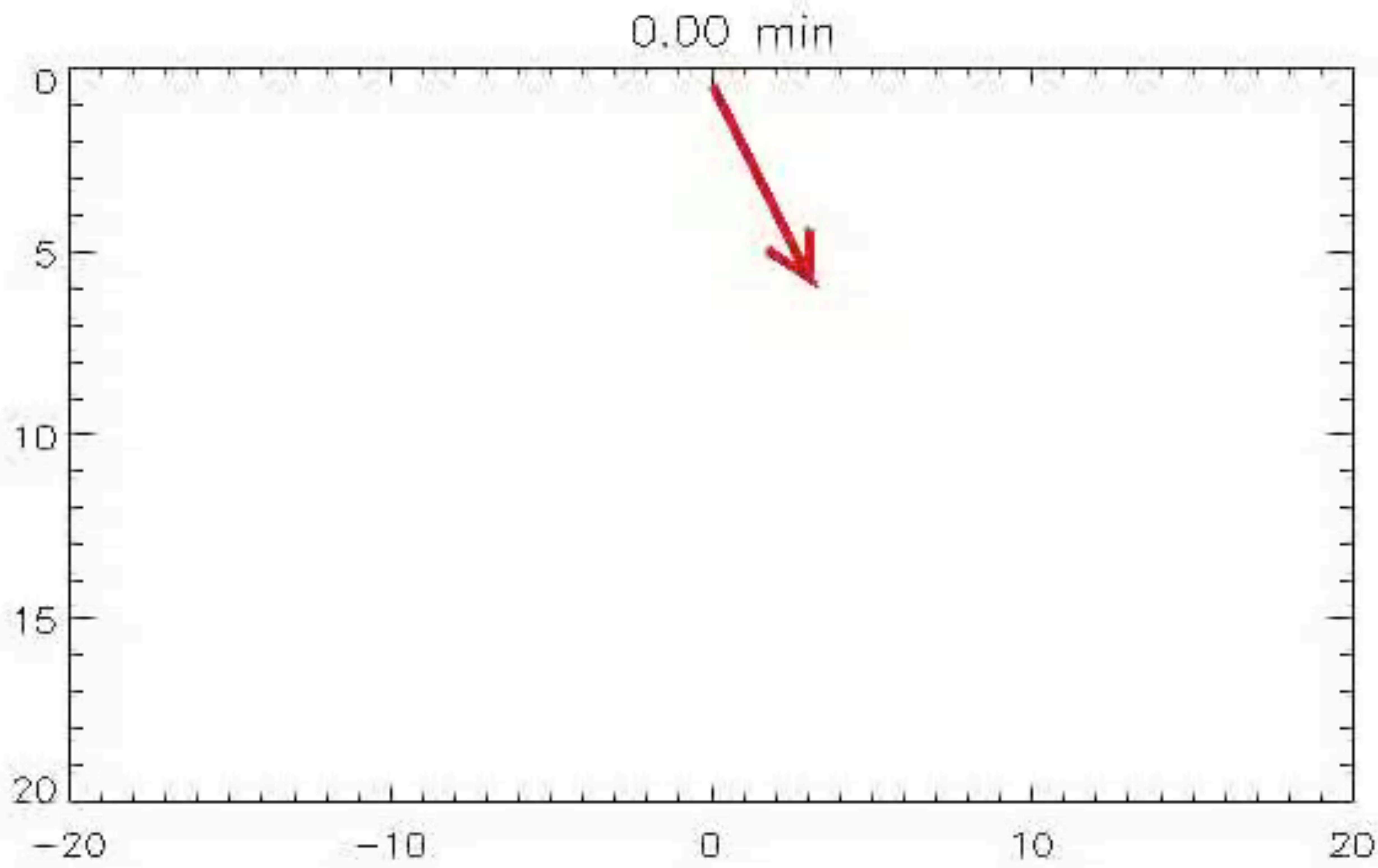

NOAA 11158, los magnetic field, SDO/HMI

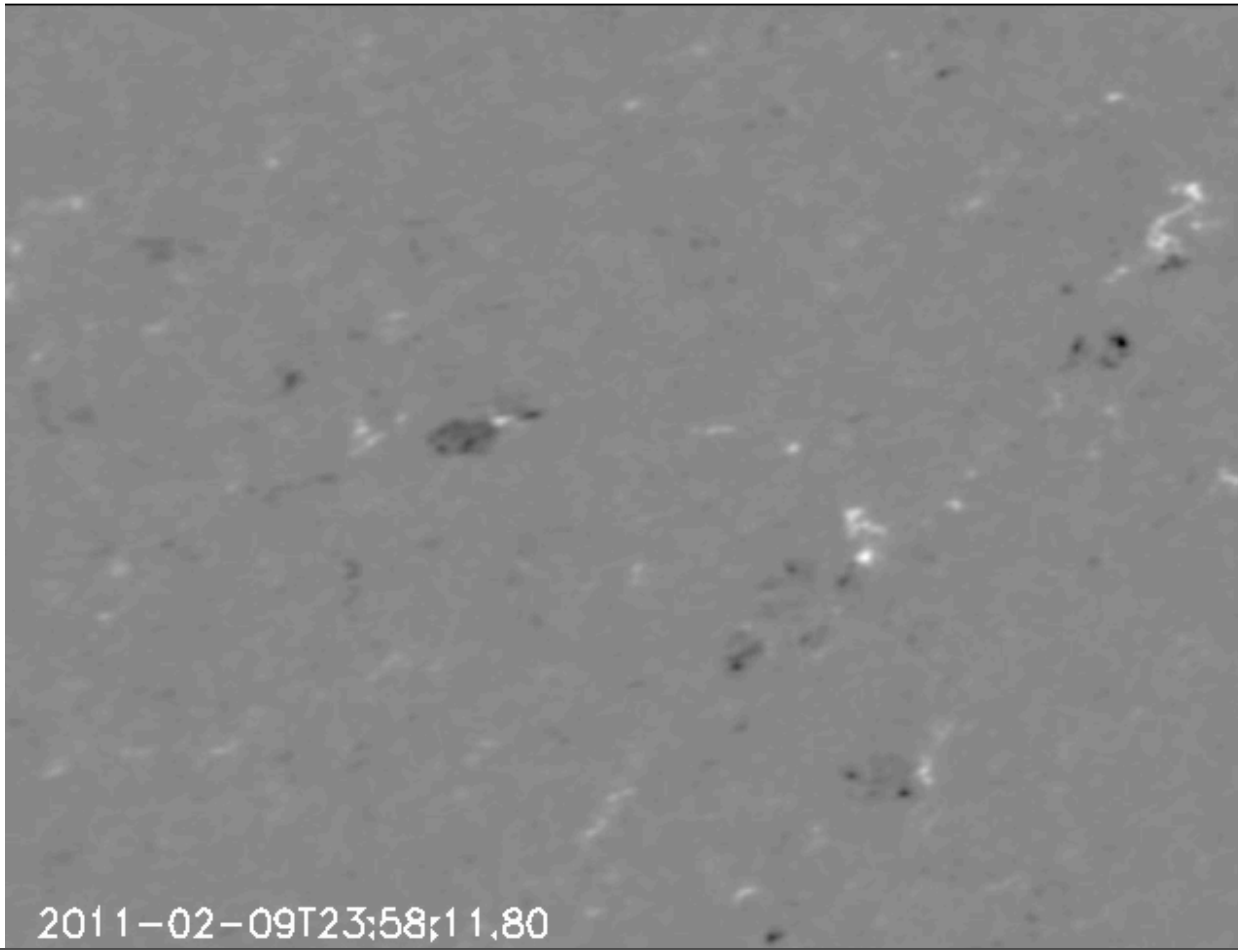

NOAA11158: M6.6 Feb 13, 17:38

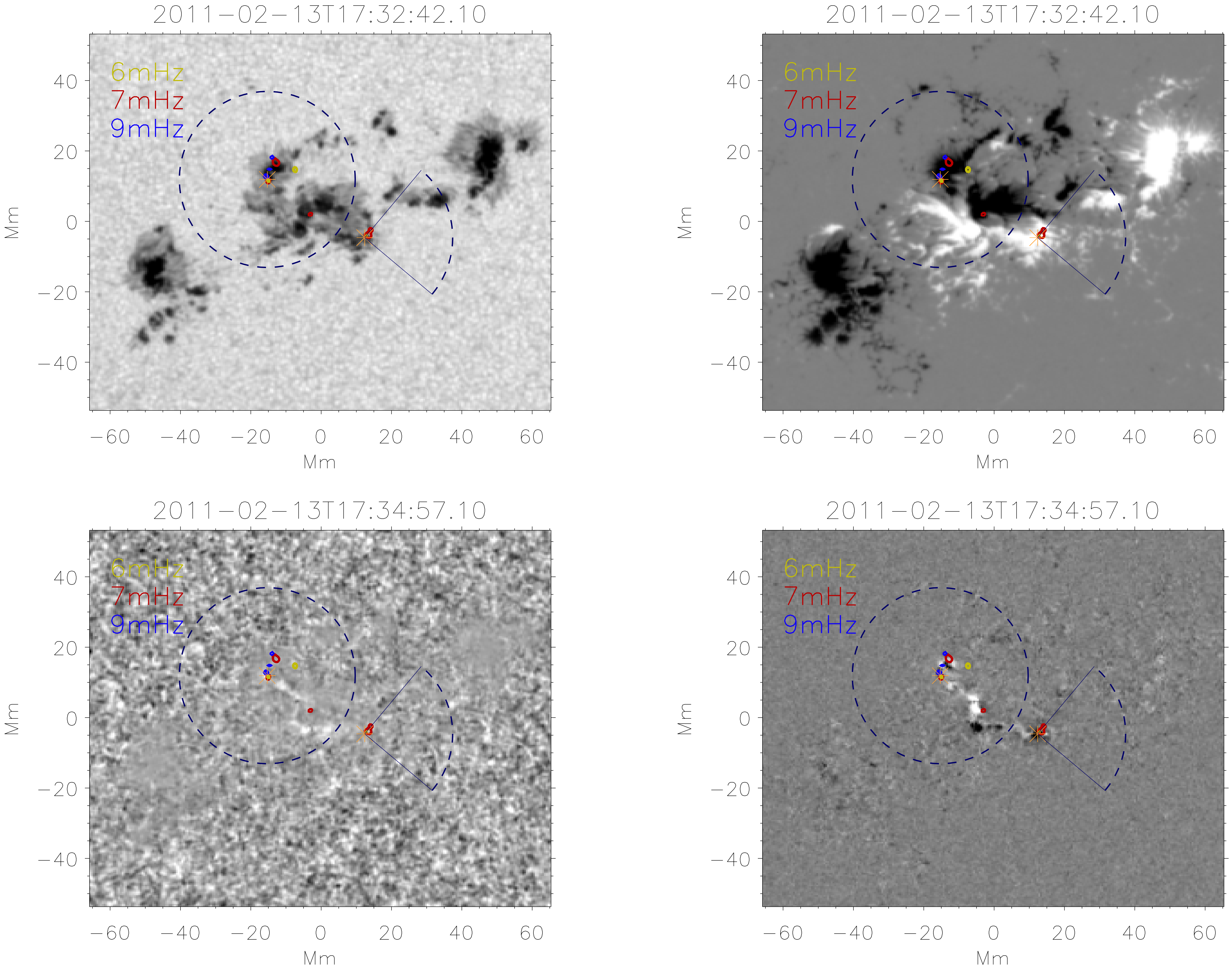

NOAA11158: M6.6 Feb 13, 17:38

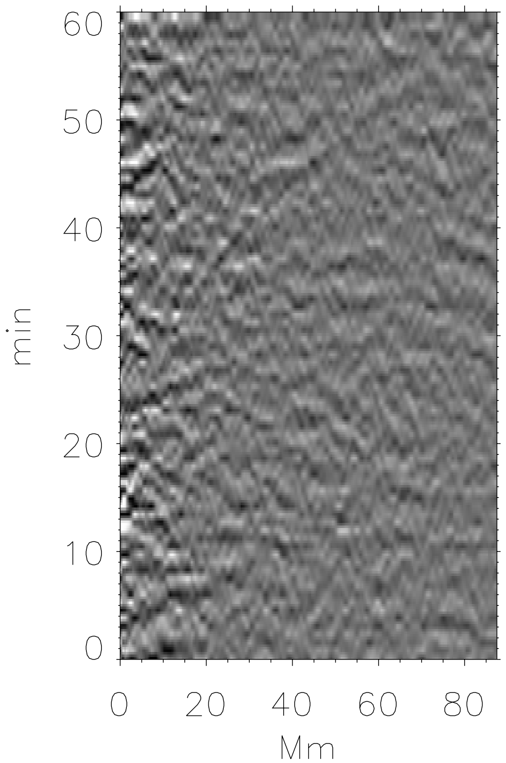

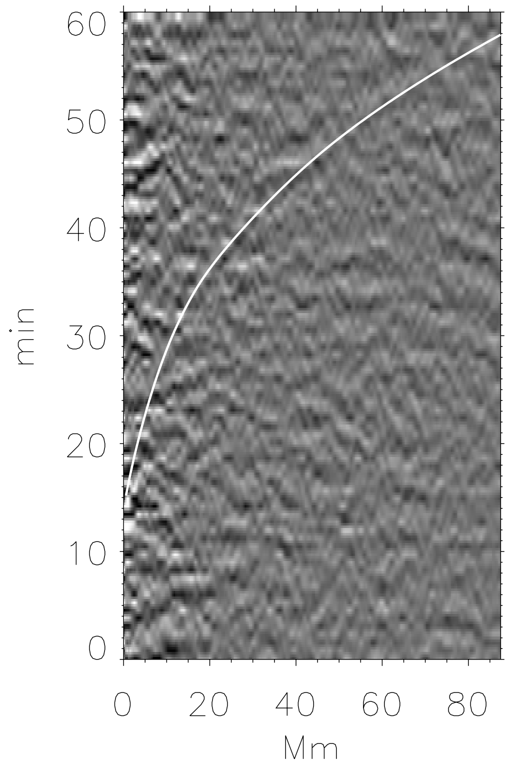

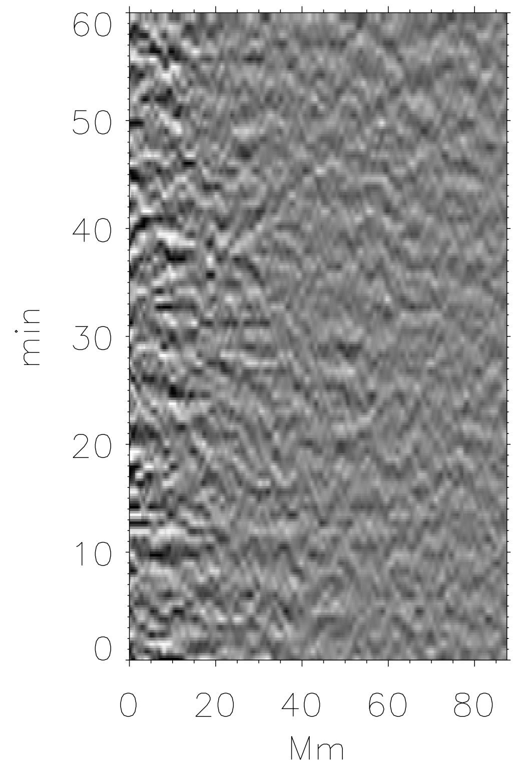

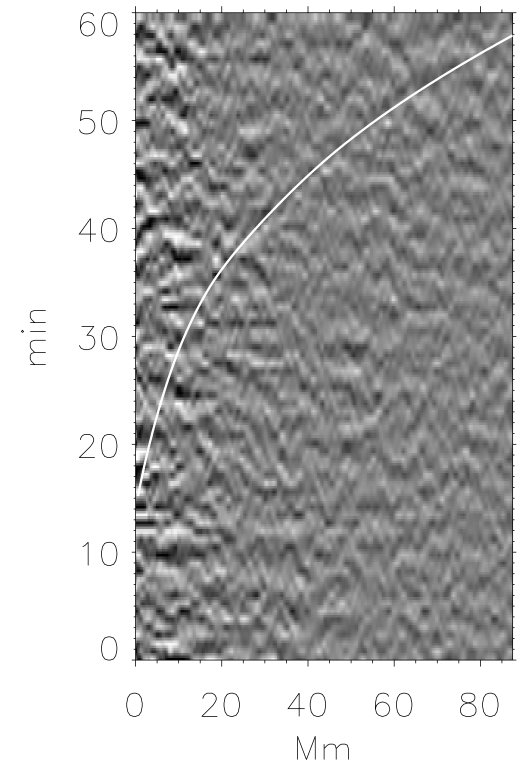

NOAA11515: July 6, C9.2 19:24

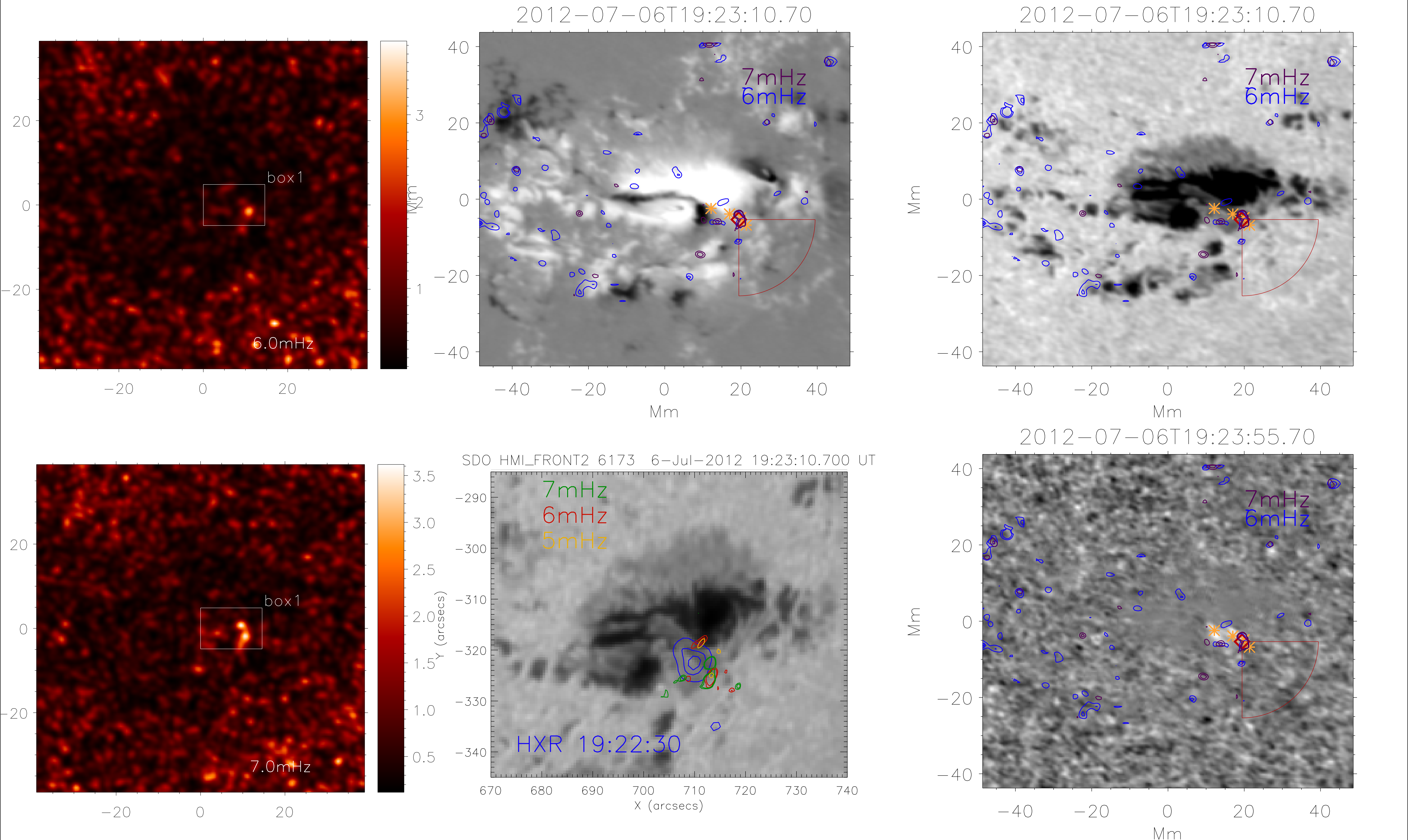

NOAA11515: July 6, C9.2 19:24

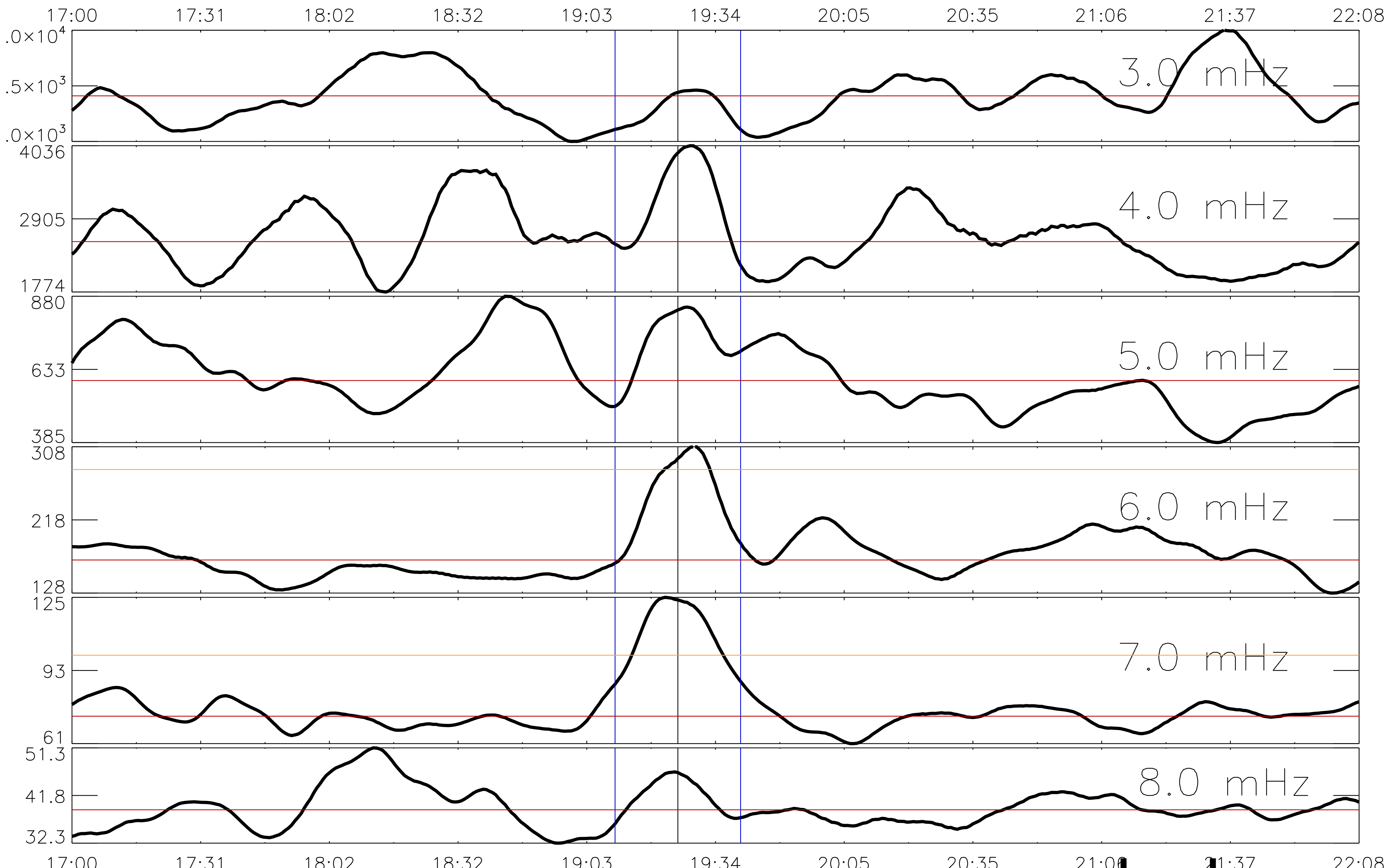

zharkov et al 2014

NOAA11515: July 6, C9.2 19:24

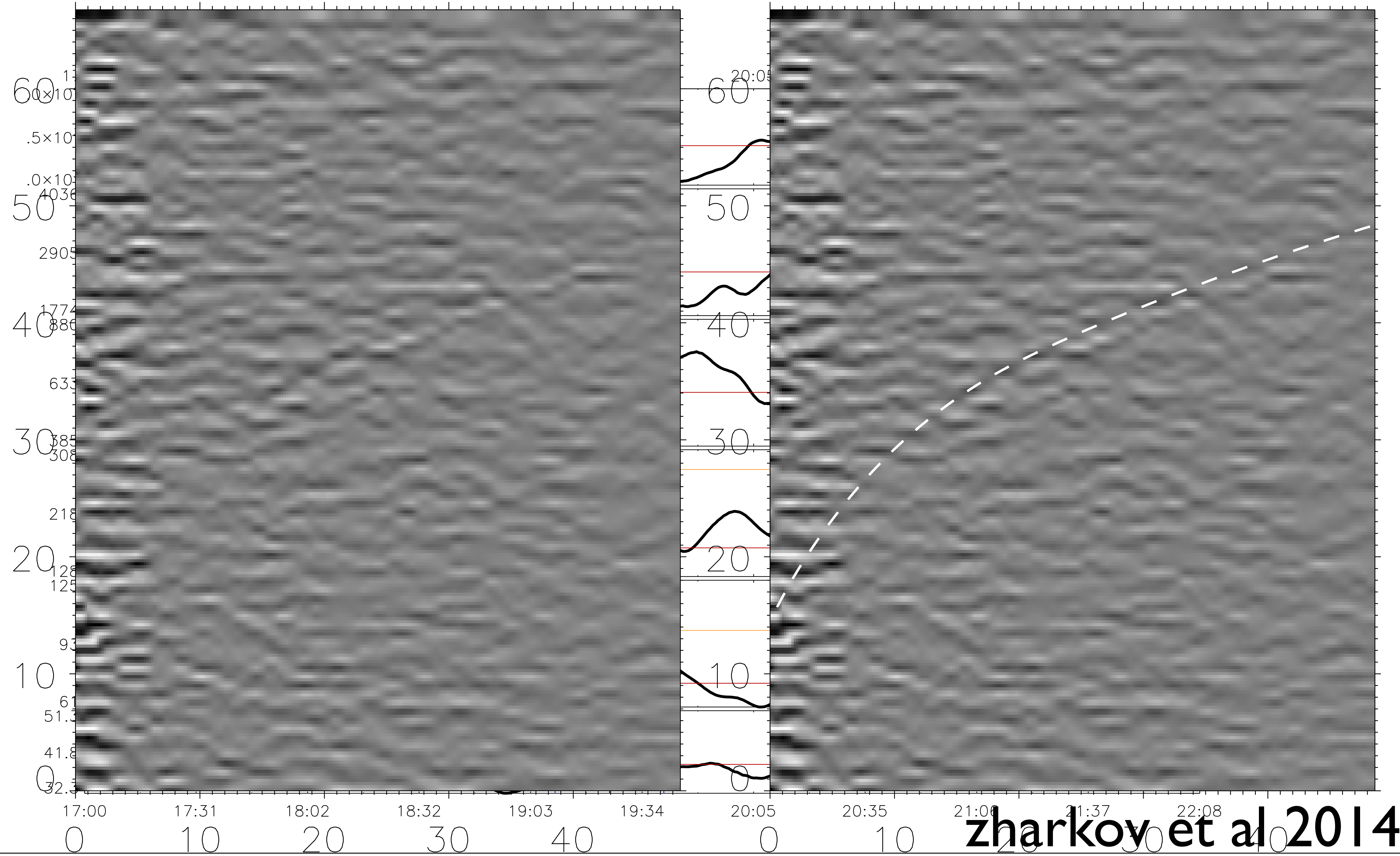

zharkov et al 2014

NOAA11515: July 6, C9.2 19:24

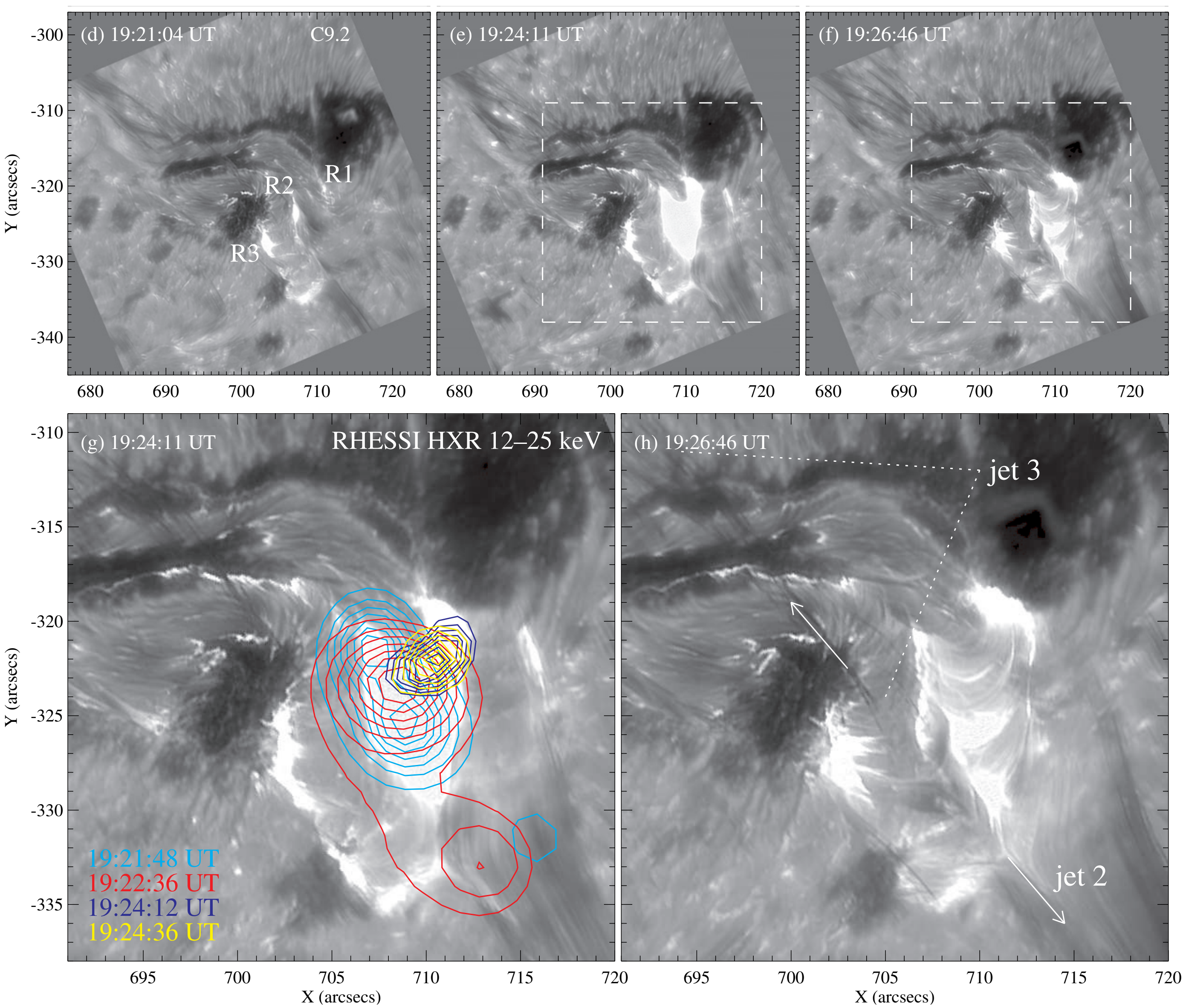

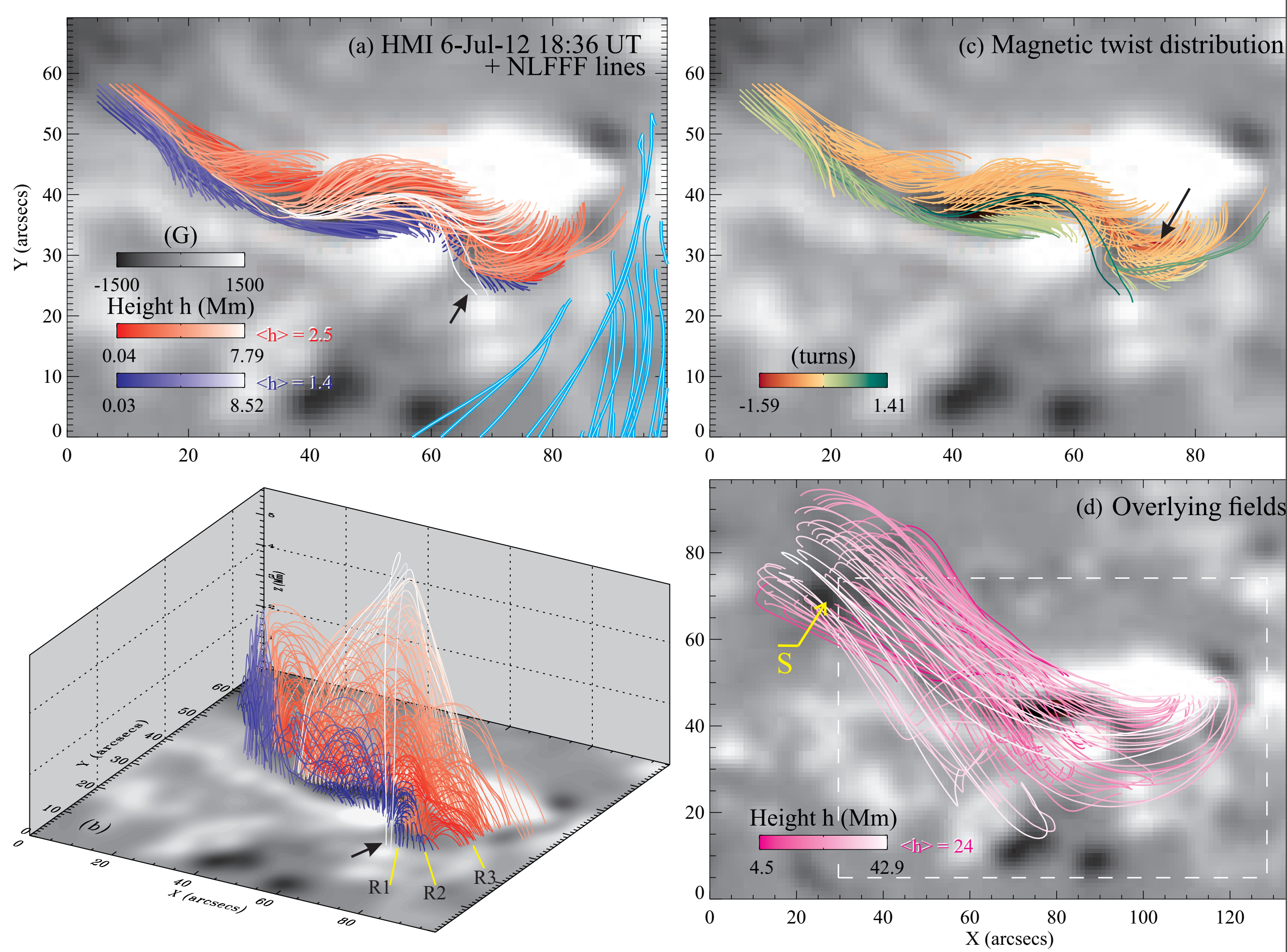

Wang et al, 2014

Conclusions

- Sunquakes provide another method to probe energy release during eruption.
- February 15, 2011 quakes only had weak associated white-light emission and weak HXR, ruling out backwarming scenario - but the analysis still on-going
- February 15, 2011: strong downflows and supersonic transients are seen at both locations;
- But backwarming scenario (WL&HXR emission at quake location) is still seen most often - different mechanisms for different quakes?
- Ripples carry information about the source, not just subsurface properties - leading to development of flare seismology
- Intriguing indications that flux rope eruption and sun-quakes may be connected => significant energy deposition could occur before the main particle acceleration.
- Improved methods of detection and better data coverage lead to discovery of new events - but many fall into grey area, more work!
- HMI data is great - now we have the opportunity to study sunquakes systematically, building up statistics